

POLITECNICO DI TORINO

Collegio di Ingegneria Chimica e dei Materiali

**Corso di Laurea Magistrale
in Ingegneria Chimica e dei Processi Sostenibili**

Tesi di Laurea Magistrale

**Preparation of micron-sized eccentric silica
core-polystyrene shell fluorescent particles
as probes for dynamic motion of colloids**



Relatore

prof. Roberto Pisano

Candidato

Lorenzo Stratta

Ottobre 2018

On the way, Govinda said: "Oh Siddhartha, you have learned more from the Samanas than I knew. [...] Truly, if you had stayed there, you would soon have learned to walk on water."

"I do not seek to walk on water," said Siddhartha.

Hermann Hesse

Index

Sommario	i
S.1. Definizione di colloide	i
S.2. Sintesi di nano- e micro- particelle: stato dell'arte	i
S.2.1. Sintesi di particelle di silice	iii
S.2.2. Incorporazione di un colorante fluorescente nelle particelle di silice	iii
S.2.3. Produzione di particelle non sferiche	vi
S.2.4. Incorporazione di un colorante nel guscio polimerico	v
S.3. Scopo del lavoro	vi
S.4. Metodi	vii
S.4.1. Reagenti	vii
S.4.2. Produzione del nucleo di silice	vii
S.4.3. Rivestimento in PBMA	viii
S.4.4. Sintesi dello shell polimerico esterno	ix
S.4.5. Caratterizzazione e strumentazione	ix
S.5. Risultati	x
S.5.1. Sintesi delle particelle di silice	x
S.5.1.1. Ritardo nell'iniezione del colorante	x
S.5.1.2. Eventuale rivestimento di pura silice	x
S.5.1.3. Concentrazione di ammoniaca	x
S.5.1.4. Concentrazione di acqua e TEOS	x
S.5.1.5. Confronto con particelle di pura silice	xi
S.5.1.6. Fluorescenza dell'RITC	xii
S.5.2. Rivestimento in PBMA	xii
S.5.3. Sintesi dello shell polimerico	xii
S.5.3.1. Rivestimento in PBMA	xii
S.5.3.2. Tempo di reazione e concentrazione di stirene	xiii
S.5.3.3. Presenza di un elettrolita	xiii
S.5.3.4. Velocità di miscelazione	xiii
S.5.3.5. Concentrazione dei nuclei	xiv
S.5.3.6. Fluorescenza del pirene	xiv
S.6. Conclusioni	xv
1. Introduction	1
1.1. A definition of colloids	1
1.2. State of the art	3
1.2.1. Silica cores	3
1.2.2. Incorporation of a fluorescent dye in silica particles	3
1.2.3. Production of nonspherical particles	5
1.2.4. Incorporation of a fluorescent dye in the polystyrene shell	8
1.3. Motivation of this thesis	9
2. Methods	11
2.1. Reactants	11
2.2. Experimental procedures	11
2.2.1. Cores	11
2.2.2. PBMA coating	17
2.2.3. Shells	21
2.3. Characterisation and instrumentations	28
3. Results and discussions	29
3.1. Cores particles	29
3.1.1. Injection delay	29
3.1.2. Eventual silica coating	32
3.1.3. Ammonia concentration	33
3.1.4. Water and TEOS concentration	35

3.1.5.Reproducibility	39
3.1.6.Reference with pure silica	41
3.1.7.Fluorescence of RITC	43
3.2. PBMA coating	44
3.3. Shells	45
3.3.1.PBMA coating	45
3.3.2.Reaction time and styrene concentration	46
3.3.3.Electrolyte	52
3.3.4.Mixing rate	54
3.3.5.Core particles concentration	56
3.3.6.Fluorescence of pyrene	58
4. Conclusions	61
5. Bibliography	63

Sommario

I sistemi colloidali sono presenti in un'ampia gamma di fenomeni artificiali e naturali e di conseguenza hanno un incredibile numero di applicazioni sia nell'ambito industriale che nella vita di tutti i giorni. Per esempio processi come la catalisi eterogenea, lo scambio ionico, la purificazione di acqua e gas, le polimerizzazioni in emulsione, la cromatografia e così via, dipendono fortemente dai colloidali^[1]

In questo lavoro di tesi è stato sviluppato un metodo innovativo per la produzione di particelle colloidali con una particolare struttura "core-shell eccentrica", incorporanti due diversi coloranti fluorescenti, al fine che le stesse potessero essere usate come sonde per lo studio della fluidodinamica rotazionale dei colloidali. Lo studio è nato da una proposta di collaborazione tra il laboratorio della Tohoku University a cui fa capo il professor Daisuke Nagao e alcuni ricercatori dell'ETH di Zurigo interessati allo studio della fluidodinamica rotazionale dei colloidali nei loro diversi stati di aggregazione.

S.1 Definizione di colloide

Ovunque, nel mondo che ci circonda, è possibile trovare sistemi con particolari caratteristiche che possono essere chiamati "colloidali". Per essere definito "colloidale", un sistema deve essere innanzitutto composto di due fasi, A e B, immiscibili tra di loro. Un'ulteriore condizione è che la fase A sia finemente dispersa nella fase B e quindi "*la sostanza A è chiamata fase dispersa e la sostanza B, mezzo di dispersione*".^[2] Sfortunatamente questa non è una definizione esaustiva perché non dà informazioni a proposito di "quanto" debba essere "fine" la dispersione e per questo è necessario introdurre alcune altre considerazioni.

La prima è necessaria per distinguere un sistema colloidale da una comune soluzione ed è che le particelle della fase dispersa siano abbastanza grandi da "vedere" le molecole della fase disperdente come una fase continua e non come un gruppo di molecole individuali.

La seconda dà, invece, informazioni a proposito della dimensione massima che le particelle possono raggiungere. Per essere considerate colloidali, le particelle che compongono il sistema devono essere piccole abbastanza da muoversi seguendo il moto Browniano. Il moto Browniano, anche chiamato "moto termico", è un moto irregolare dovuto alle interazioni tra le particelle colloidali e le vibrazioni caotiche delle molecole che compongono il mezzo disperdente. Risulta quindi abbastanza difficile definire esattamente cosa sia e cosa non sia un colloide. In ogni caso è comunque possibile definire un ordine di grandezza per queste particelle. Dalla prima considerazione la dimensione minima "*dovrebbe essere almeno dieci volte più grande delle molecole di solvente*"^[3], quindi circa 1 nm. La dimensione massima invece la si può intuire dalla seconda considerazione in quanto "*il moto termico è rilevante solo quando lo spostamento termico è una frazione misurabile della dimensione lineare delle particelle durante un intervallo di tempo sperimentale tipico*", quindi tra 1 μm ^[2] e 10 μm ^[3].

I sistemi colloidali possono essere la combinazione di qualunque fase, solida, liquida o gassosa, ad eccezione, ovviamente della combinazione gas-gas. Alcuni colloidali molto comuni sono: fumo (solido in gas), nebbia (liquido in gas), vernice (solido in liquido), latte e maionese (liquido in liquido), schiuma da barba (gas in liquido), alcune leghe (solido in solido) e la schiuma isolante (gas in solido)^[2].

Può essere sorprendente realizzare che solo agli inizi del ventesimo secolo una prima teoria del moto Browniano fu proposta e verificata rispettivamente da Albert Einstein e Jean Perrin^[4]. Grandi sforzi

sono stati fatti durante gli ultimi decenni per rappresentare analiticamente questi sistemi e molti passi avanti sono stati fatti, ma rimangono tuttavia ancora molte domande a cui dare risposta.

Il problema più grosso incontrato nell'analisi di questi sistemi è la preparazione di particelle molto ben caratterizzate. La possibilità di avere a disposizione particelle con dimensioni, forme e interazioni definite in maniera univoca è essenziale per il confronto tra la teoria e le simulazioni. La definizione di modelli analitici per sistemi altamente polidispersi non solo è difficile dal punto di vista matematico, ma è un problema anche per via del relativamente limitato numero di particelle che possono essere simulate con un computer rispetto a quelle che comporrebbero realmente un esperimento classico^[4].

Considerate queste circostanze, il progetto di questa tesi è nato grazie alla collaborazione tra l'ETH di Zurigo (Svizzera) e la Tohoku University (Giappone). I ricercatori dell'ETH di Zurigo erano interessati allo studio della fluidodinamica rotazionale di particelle colloidali nei pressi della temperatura di transizione vetrosa.

Una singola particella sferica dispersa in un fluido, in uno spazio tridimensionale, ha 6 gradi di libertà, 3 traslazionali e 3 rotazionali, su rispettivi assi. Sebbene sia abbastanza facile osservare una traslazione, è quasi impossibile fare lo stesso con una rotazione a causa dell'intrinseca simmetria rotazionale tipica di una sfera perfetta. Per questa ragione era di fondamentale importanza creare un particolare tipo di particelle che potessero eliminare la simmetria fonte di problemi, mantenendo la struttura sferica esterna per non modificare la fluidodinamica del sistema.

La richiesta commissionata era di produrre particelle eccentriche di tipo "core-shell" con nucleo in silice e guscio in polistirene, come in Figura S.1., incorporanti due diversi coloranti fluorescenti nel nucleo e nel guscio rispettivamente, con dimensioni abbastanza precise. Il guscio avrebbe dovuto avere un diametro di circa 1,4 μm e il nucleo di circa 400 nm.

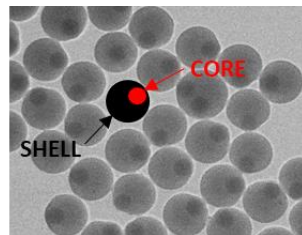


Figura S.1. Rappresentazione schematica di particelle eccentriche core-shell.

Avendo a disposizione queste particelle diventa quindi possibile misurare la dinamica rotazionale di sfere colloidali usando un microscopio confocale, come riportato da Liu e Böker^[5]. Il metodo consiste, sostanzialmente, nel riconoscimento di un asse ottico definito da \mathbf{u} che connetta il centro dello shell al centro del core. Seguendo come il vettore evolve nel tempo è possibile determinare come la particella abbia ruotato, come descritto in Figura S.2. .

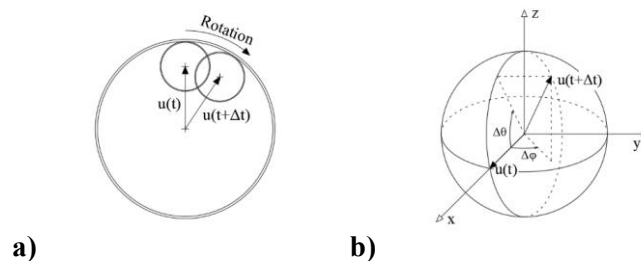


Figura S.2. Rappresentazione schematica del vettore u (a) e di un possibile set di coordinate per le particelle colloidali (b). Figura modificata da [5].

S.2 Sintesi di nano- e micro- particelle: Stato dell'arte

S.2.1 Sintesi di particelle di silice

La produzione di particelle colloidali di silice è stata studiata approfonditamente verso la fine del ventesimo secolo da Stöber *et al.*^[6], i quali proposero un metodo per produrre particelle colloidali monodisperse tramite una reazione di idrolisi di alchilsilicati e la successiva idrolisi dei relativi acidi silicici in soluzione alcolica. Il diametro delle particelle prodotte con questo metodo può variare dagli 0,05 μm fino ai 2 μm . Il sistema è composto da almeno quattro composti con relativi compiti: alcol puro (o una miscela alcolica) come solvente, alchil silicati come fonte di silicio, acqua come iniziatore e ammoniaca come catalizzatore morfologico per la produzione di particelle sferiche. Ogni parametro del processo è stato studiato sistematicamente e ad oggi è possibile controllare con grande precisione il diametro delle particelle modificando le concentrazioni iniziali dei reagenti.

Sebbene Stöber *et al.*^[6] descrissero il processo di sintesi secondo un punto di vista puramente qualitativo, un gran numero di articoli scientifici analizzano il processo anche secondo un punto di vista matematico e cinetico, uno dei quali è lo studio di Chen *et al.*^[7] che descrive in maniera dettagliata tutti i parametri cinetici e le equazioni che governano le reazioni aventi luogo durante la sintesi.

S.2.2 Incorporazione di un colorante fluorescente nelle particelle di silice.

Una procedura generale per incorporare un colorante fluorescente in particelle colloidali di silice è stata proposta da van Blaaderen e Vrij^[8] nel 1992 e successivamente da Verhaegh e van Blaaderen^[9] nel 1994. Nei loro studi descrissero come fosse possibile incorporare un colorante, il rhodamine isotiocianato (RITC), dentro la struttura della silice utilizzando un agente di accoppiamento, il (3-aminopropil)trirossisilano (APTES). Grazie a questo metodo la composizione delle sfere di silice può essere controllata al punto che il colorante può essere posizionato sulla superficie, distribuito nell'intero volume di un core interno o in una sottile corona circolare all'interno delle particelle come descritto in Figura S.3.

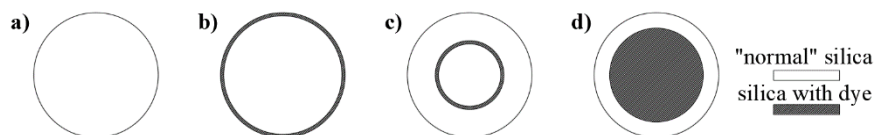


Figura S.3. Rappresentazione schematica della possibile incorporazione di un colorante in una particella di silice. Particella senza colorante (a), con colorante sulla superficie (b), in una corona circolare dentro alla particella (c) o distribuito nel volume di un core interno (d). Figura modificata da [8].

Sebbene questo processo sia generico e ben sviluppato, si concentra solo sul come introdurre il colorante dentro alle particelle e non da informazioni dettagliate su come controllare il diametro delle particelle, argomento che quindi è stato analizzato all'interno di questa tesi.

S.2.3 Produzione di particelle non sferiche

Normalmente, quando si realizzano polimerizzazioni successive, ci si aspetterebbe che gli strati più esterni crescessero uniformemente sopra i nuclei di partenza generando particelle concentriche e sferiche. Sebbene ciò accada quando vi è una grossa affinità tra nuclei e gusci, come succede ad esempio nel caso di particelle di silicio, il risultato non è scontato quando si lavora con polimerizzazioni organiche.

Nel 1990, Sheu *et al.* pubblicarono due lavori complementari^{[10][11]} in cui descrissero in dettaglio come produrre particelle colloidali non sferiche tramite polimerizzazioni successive e proposero un metodo accurato per descrivere le cause e i meccanismi del processo. In questo studio vennero usati nuclei monodispersi di polistirene reticolato e la successiva polimerizzazione ottenuta usando miscele di stirene-divinilbenzene(DVB). La non-sfericità delle particelle è dovuta alla separazione di fase tra matrici polimeriche più o meno reticolate e il meccanismo di tale processo è descritto in Figura S.4.

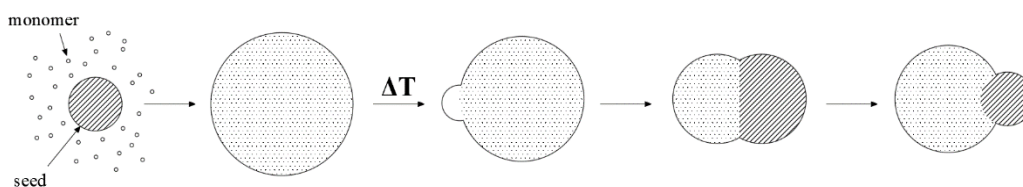


Figura S.4. Rappresentazione schematica del meccanismo di adsorbimento del monomero e successiva separazione di fase.

Sfortunatamente questo metodo non può essere applicato direttamente alla produzione delle particelle richieste dai ricercatori dell'ETH di Zurigo per due motivi. Il primo è che questo metodo è applicabile solamente su nuclei a matrice polimerica in quanto il monomero della seconda polimerizzazione deve poter essere adsorbito nella particella, cosa che risulta impossibile quando si ha a che fare con particelle di silice. Il secondo è che la forma deve rimanere sferica, mentre il metodo di Sheu *et al.*^{[10][11]} si basa esclusivamente sulla produzione di particelle non-sferiche.

Per questo motivo, sebbene mantenendo alcuni concetti teorici, è necessario modificare e adattare il processo per nuclei inorganici e differenti morfologie. Questo adattamento è stato sviluppato da Nagao *et al.*^[12] nell'articolo in cui descrissero come produrre particelle polimeriche anisotropiche a forma di “pupazzo di neve” contenenti nuclei di silice. In questo processo l'agente di accoppiamento 3-metacrilossipropiltrimetossisilano (MPTMS) venne usato per l'ibridizzazione tra nuclei inorganici e gusci organici. La produzione di queste particolari particelle deriva da una doppia polimerizzazione in cui le superfici dei nuclei di silice vengono dapprima modificate dall'MPTMS e successivamente la prima polimerizzazione ricopre le particelle di un sottile strato di poli-metilmetacrilato (PMMA) stabilizzato con il sodio *p*-stirensolfonato (NaSS). La seconda polimerizzazione è fatta quindi utilizzando le particelle prodotte durante la prima reazione e lo stirene come monomero. Il risultato è una particella anisotropica come mostrato in Figura S.5.

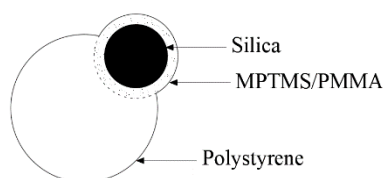


Figura S.5. Rappresentazione schematica di una particella con morfologia a “pupazzo di neve”.

In questo processo, il primo strato polimerico serve ad adsorbire lo stirene della seconda polimerizzazione e ad indurre la successiva separazione di fase durante la seconda polimerizzazione. Sebbene il processo sia ora applicabile a nuclei silicici la morfologia finale delle particelle non è ancora sferica e per risolvere questo problema esistono diversi modi. In questa tesi si è deciso di agire su una delle forze spingenti che inducono la separazione di fase, la tensione superficiale. Nello specifico, è verosimile assumere che la separazione di fase sia tanto più accentuata quanto più è grande la repulsione tra il primo e il secondo guscio polimerico. Per questo motivo, usando un monomero come il butilmetacrilato (BMA) per il primo strato, che è più compatibile con lo stirene del guscio, si dovrebbe ottenere una minore separazione di fase e quindi particelle eccentriche ma sferiche. Questa assunzione è stata testata e verificata all'interno di questa tesi.

S.2.4 Incorporazione di un colorante nel guscio polimerico

Uno dei primi aspetti che bisogna prendere in considerazione quando si decide di inserire un colorante nelle particelle eccentriche è la scelta del colorante in quanto la morfologia delle particelle stesse dipende strettamente dalle interazioni che intercorrono tra nuclei e gusci e l'inserimento di un composto estraneo nel sistema può portare ad una modifica degli equilibri che garantiscono la più o meno eccentricità delle particelle. Inoltre, il colorante da inserire nei gusci deve essere sufficientemente diverso da quello inserito nei nuclei in modo da poterli distinguere efficacemente al microscopio confocale. Infine, il colorante non solo deve poter essere incorporato, ma non deve neanche desorbire dopo la reazione per non perdere intensità luminosa.

Per questi motivi un candidato perfetto è il pirene. La sua struttura molecolare non differisce di molto da quella dello stirene, non andando a modificare quindi le interazioni tra il primo guscio polimerico e il secondo, le sue lunghezze d'onda di eccitazione e di emissione differiscono ampiamente da quelle dell'RITC usato per i nuclei rendendoli ben distinguibili, ed è praticamente insolubile in acqua, solvente

utilizzato durante la polimerizzazione del guscio esterno, rendendo quasi impossibile il desorbimento dalle particelle formate.

L'utilizzo del pirene per colorare particelle di polistirene è stato studiato approfonditamente da Tamai *et al.*^[13] e da Kalyanasundaram e Tomas^[14].

S.3 Scopo del lavoro

L'obiettivo di questa tesi è stato quello di produrre le particelle richieste dai ricercatori dell'ETH di Zurigo e, possibilmente, di creare una semplice ed efficiente procedura che potesse essere replicata con sufficiente precisione da ottenere buone sonde sperimentali.

Nello specifico la richiesta era di produrre particelle eccentriche con un nucleo di silice di 400 nm e un guscio di polistirene con un diametro di 1,4 μm . Inoltre era essenziale incorporare due diversi coloranti fluorescenti in ciascuno di essi in modo da permetterne l'osservazione al microscopio confocale.

Le particelle sono composte di tre parti: il nucleo di silice, il primo strato polimerico che serve a collegare il nucleo al guscio e a garantire l'eccentricità nella particella e il guscio di polistirene.

La prima parte del lavoro si è focalizzata sulla produzione dei nuclei fluorescenti. La sintesi di particelle di silice è molto ben conosciuta, ma l'introduzione di un colorante fluorescente cambia il sistema reattivo e, per questo motivo, è stato necessario studiare in che modo il processo cambi e se sia possibile controllarlo.

Il primo strato polimerico, prodotto usando il BMA, è stato analizzato per determinare la sua necessità ed efficacia nella produzione di particelle eccentriche.

Infine il guscio polimerico è stato studiato. Non solo è stato necessario verificare che fosse possibile produrre il tipo di particelle eccentriche richieste, ma è stato importante definire in che misura sia possibile avere un controllo sul processo e sul diametro finale. Per questo motivo uno studio su quali fossero i parametri limitanti del processo è stato fatto e l'introduzione del secondo colorante è stata analizzata per valutare la sua compatibilità con il sistema.

S.4 Metodi

S.4.1 Reagenti

Etanolo (99.5%), ammoniaca (NH_3) (25% soluzione acquosa), tetraetil ortosilicato (TEOS), persolfato di potassio (KPS), sodio *p*-stirenesolfonato (NaSS), NaCl e pirene sono stati ottenuti da Wako Pure Chemical Industry (Japan) e usati come ricevuti. Stirene (con 0.003% *p*-*t*-butilcatecol come stabilizzatore) e butil metacrilato (BMA) (con 0.01% Idrochinone come stabilizzatore) sono stati ottenuti da Wako Pure Chemicals Industry (Japan) e usati dopo la rimozione dell'inibitore. (3-aminopropil) trietossisilano (APTES) è stato ottenuto da Shinetsu (Japan) e usato come ricevuto. 3-metacrilossipropil trimetossisilano (MPTMS) è stato ottenuto da JNC Corporation (Japan) e usato come ricevuto. Rodamine B isotiocianato (RITC) è stato ottenuto da Aldrich (U.S.A.) e usato come ricevuto. L'acqua è stata deionizzata e distillata fino ad ottenere una resistenza elettrica superiore a $18 \text{ M}\Omega\cdot\text{cm}$.

S.4.2 Produzione del nucleo di silice

La produzione dei nuclei di silice con il colorante RITC è stata effettuata tramite un metodo Stöber modificato come descritto in Figura S.6.

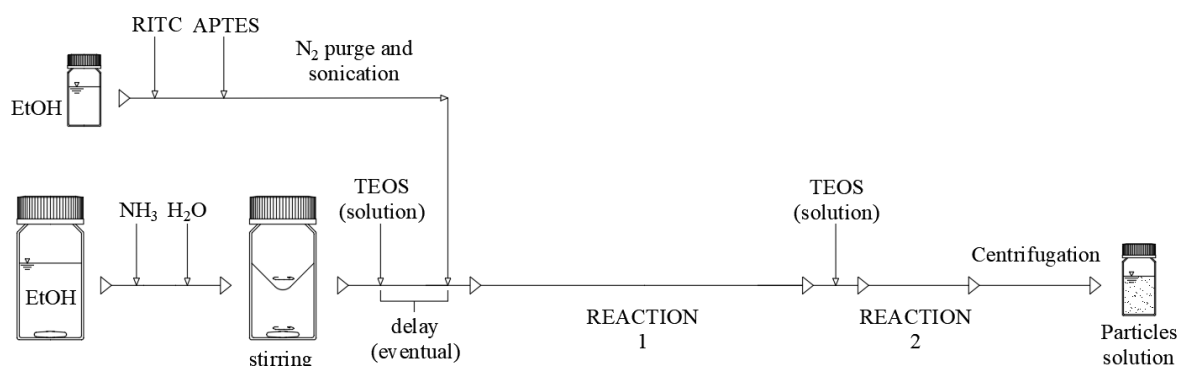


Figura S.6. Schema di processo per la produzione dei nuclei fluorescenti.

Uno studio sistematico è stato effettuato per valutare in quale misura l'introduzione del colorante fluorescente influisce sulla produzione dei nuclei e se fosse possibile controllare il diametro delle particelle. I seguenti parametri sono stati analizzati:

- Eventuale **ritardo** tra l'iniezione della soluzione contenente il TEOS e quella contenente il colorante.
- Presenza di un eventuale **rivestimento di pura silice** sulle particelle.
- Concentrazione di **ammoniaca**.
- Concentrazione di **acqua**.
- Concentrazione di **TEOS**.
- Presenza del **colorante fluorescente**.

S.4.3 Rivestimento in PBMA

Il rivestimento con il PBMA è necessario per indurre l'eccentricità tra i nuclei di silice e i gusci di polistirene in maniera controllata. Il grado di eccentricità dipende dall'interazione reciproca tra nuclei, gusci e solvente in cui avviene la reazione e in base ai materiali utilizzati si possono avere diverse morfologie come descritto in Figura S.7.

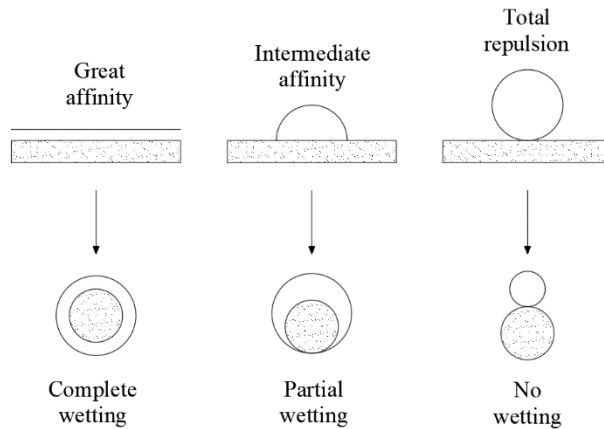


Figura S.7. Descrizione schematica del processo che causa l'eccentricità nelle particelle.

Siccome la silice dei nuclei è estremamente idrofila e il polistirene dei gusci è estremamente idrofobico, non è possibile collegare direttamente la silice al polistirene in quanto il risultato non sarebbe una particella sferica. Per questo motivo è necessario utilizzare un materiale con caratteristiche intermedie tra la silice e il polistirene che mantenga una certa repulsione tra nucleo e guscio ma che la riduca rispetto alla condizione iniziale. Il PBMA assolve perfettamente a questo compito essendo un polimero con una catena idrocarburica idrofobica ed un gruppo polare, quindi idrofilico. Il processo è descritto in Figura S.8.

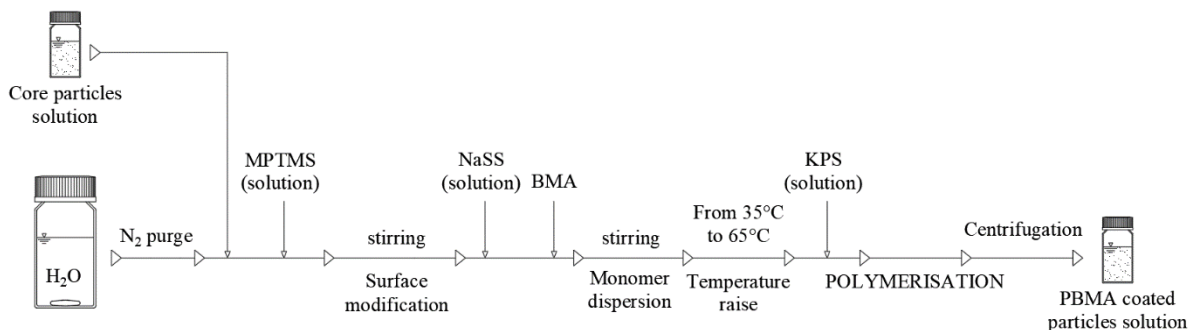


Figura S.8. Schema di processo per la produzione del primo rivestimento polimerico.

S.4.4 Sintesi dello shell polimerico esterno

Una volta rivestiti i nuclei con il PBMA è possibile effettuare l'ultima polimerizzazione per produrre i gusci eccentrici. Lo scopo di questa parte è stata quella di valutare quali parametri avessero un'influenza sul processo e in quale misura fosse possibile agire su di essi per controllare il diametro finale delle particelle. Uno schema del processo è descritto in Figura S.9.

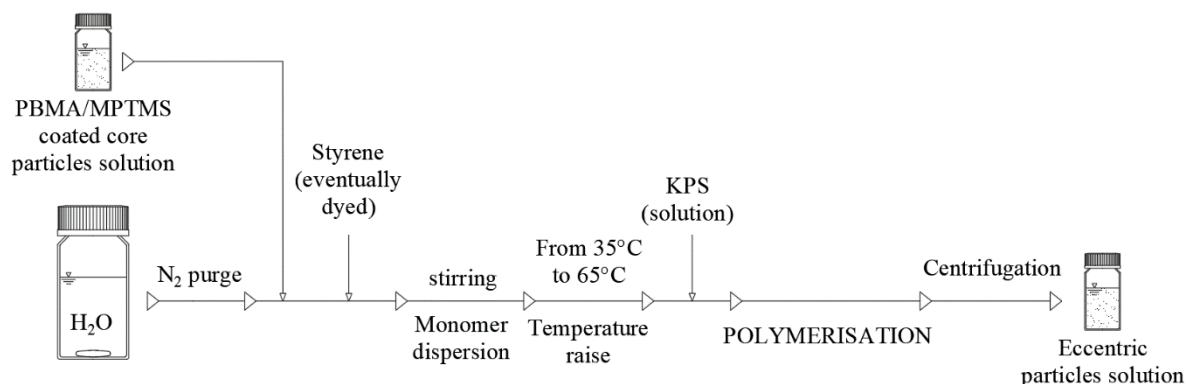


Figura S.9. schema di processo per la produzione dei gusci in polistirene.

Sono stati analizzati i seguenti parametri:

- Presenza dello **strato in PBMA**.
- Concentrazione di **stirene**.
- **Tempo** di reazione.
- Presenza di un **elettrolita**.
- Velocità di **miscelazione**.
- Concentrazione dei **nuclei**.

S.4.5 Caratterizzazione e strumentazione

Le particelle sono state osservate ed analizzate utilizzando un microscopio a trasmissione elettronica (FE-STEM, modello HD-2700 Type B della Hitachi, Giappone).

Il potenziale ζ è stato misurato usando una macchina per l' Electrophoretic Light Scattering (ELS, modello ELSZ-2 della Otsuka Electronics Co., Giappone).

Le osservazioni della fluorescenza sono state fatte con un microscopio confocale modello C2si della Nikon, Giappone, con una lampada UV Spectroline (modello ENF-240 C/J, U.S.A.) e con un fluorometro (modello F700 della Hitachi, Giappone).

S.5 Risultati

S.5.1 Sintesi delle particelle di silice

S.5.1.1 Ritardo nell'iniezione del colorante

L'introduzione del colorante fluorescente nei nuclei di silice riduce la loro stabilità in quanto, essendo l'RITC una molecola non carica elettricamente, riduce il potenziale ζ delle particelle. Di conseguenza, un eventuale ritardo nell'iniezione della soluzione contenente il colorante rispetto all'iniezione del TEOS e quindi all'inizio della reazione di idrolisi del silicato, determina uno spostamento dell'instabilità in fasi diverse della nucleazione e dell'accrescimento dei nuclei. Dai risultati ottenuti a tempi di iniezione del colorante diversi si può vedere come il diametro medio delle particelle non venga modificato sostanzialmente mentre il coefficiente di variazione, o polidispersità, aumenti in maniera significativa e proporzionale al ritardo. Per questo motivo si è deciso di ridurre al minimo il tempo intercorso tra le due iniezioni di reagenti al fine di ridurre il più possibile la polidispersità del sistema.

S.5.1.2 Eventuale rivestimento di pura silice

Come già anticipato, l'introduzione del colorante RITC nelle particelle di silice ne riduce fortemente la stabilità in quanto il colorante va a ricoprire la superficie delle particelle di molecole non cariche elettricamente che ne riducono quindi il potenziale ζ . Questa affermazione è verificata dal confronto dei valori di potenziale ottenibili per particelle di pura silice, circa -55 mV, e quelli di particelle colorate e prodotte in un singolo step reattivo, circa -25 mV. Per ovviare al problema e riportare i valori di potenziale ζ a quelli assimilabili a particelle di pura silice, e quindi stabili, è possibile rivestire i nuclei con strati non contenenti il colorante fluorescente. La superficie delle particelle risulterà essere quindi composta da sola silice e di conseguenza il potenziale ζ non sarà più influenzato dalla presenza del colorante. Dai risultati ottenuti è possibile vedere che un solo rivestimento in pura silice è sufficiente a riportare i valori di potenziale a livelli ottimali e che rivestimenti successivi non portano ad un effettivo miglioramento della stabilità.

S.5.1.3 Concentrazione di ammoniaca

Il diametro medio delle particelle, almeno alle basse concentrazioni in esame, risulta essere direttamente proporzionale alla concentrazione di ammoniaca ed è, a tutti gli effetti, un possibile modo per controllare il diametro. Sfortunatamente però, con l'aumento della concentrazione di ammoniaca nel reattore, anche la polidispersità aumenta e lo fa con un andamento esponenziale.

S.5.1.4 Concentrazioni di acqua e TEOS

Sebbene la concentrazione di TEOS non incida in alcun modo né sul diametro, né sulla polidispersità delle particelle, la concentrazione di acqua risulta essere uno dei fattori dominanti del processo, tramite il quale è possibile controllare il diametro dei nuclei. L'andamento, visibile in Figura S.10, è molto simile a quello già descritto da Stöber *et al.*^[6]. A basse concentrazioni di $[H_2O]$ il diametro aumenta in maniera quasi proporzionale all'acqua, fino a che non raggiunge un massimo, approssimativamente attorno alle 8,5 mol/l, dopo il quale ricomincia a diminuire. Nella zona di concentrazioni di acqua compresa tra 3 M e 7 M, la curva dei diametri è abbastanza lineare da permettere un buon controllo del diametro tramite una semplice interpolazione.

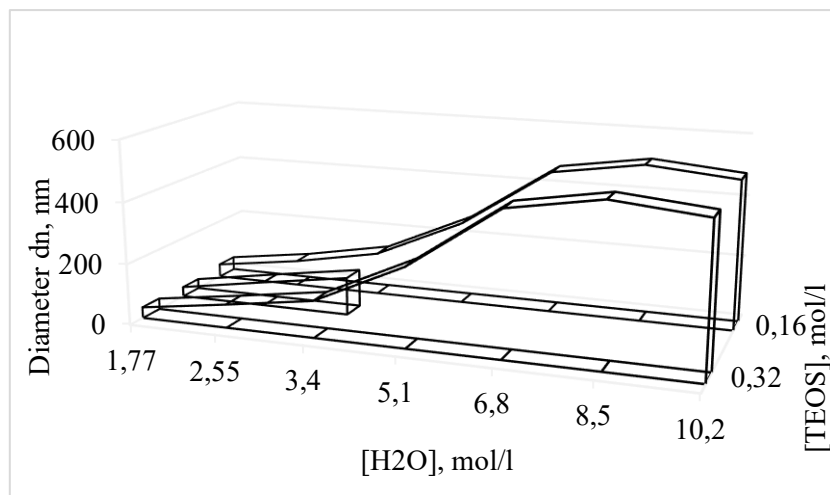


Figura S.10. Diagramma a tre assi che mostra l'andamento del diametro rispetto alle concentrazioni di acqua e TEOS.

S.5.1.5 Confronto con particelle di pura silice

Dal confronto tra particelle prodotte con e senza l'utilizzo del colorante fluorescente è possibile notare, in Figura S.11, come, sebbene l'andamento del diametro nei confronti della concentrazione di acqua sia molto simile nei due casi, il diametro delle particelle contenenti l'RITC risulti essere sempre maggiore a quello delle particelle di pura silice. Questa differenza è verosimilmente dovuta all'instabilità e alla relativa aggregazione tra particelle causata dal colorante. Siccome la fase di nucleazione è ristretta ad un limitato, molto corto, periodo di tempo successivo all'inizio della reazione, assunzione verosimile dati i bassi valori di polidispersità, il numero totale di nuclei risulterà essere minore nel caso in cui l'RITC sia presente nel reattore. Un numero minore di nuclei in accrescimento, con la stessa quantità di silicio convertita in silice, significa sostanzialmente un maggior volume per particella e quindi un maggior diametro. Un ulteriore fattore che spiega parte della differenza di diametro tra i due casi è il volume occupato dalle molecole di RITC nella struttura della silice. Il colorante ha, ovviamente, un suo volume, che andrà ad aggiungersi a quello della silice e, di conseguenza, il volume delle singole particelle risulterebbe aumentato anche se il numero totale delle stesse non cambiasse.

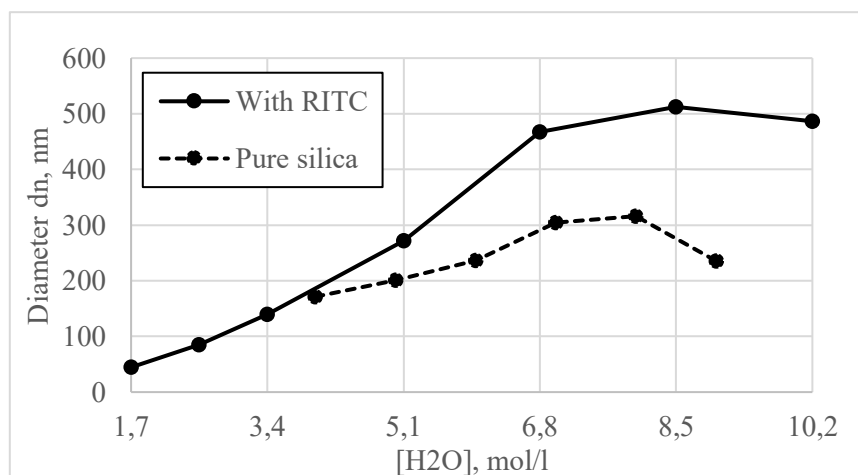


Figura S.11. Confronto tra i risultati ottenuti nel caso di particelle di pura silice (linea tratteggiata) e particelle contenenti il colorante fluorescente (linea continua).

S.5.1.6 Fluorescenza dell'RITC

Una volta pronte, le particelle sono state osservate al microscopio confocale utilizzando un laser con lunghezza d'onda di 561 nm. La fluorescenza risulta essere molto forte e persistente e rende possibile il riconoscimento agevole delle singole particelle.

S.5.2 Rivestimento in PBMA

In Figura S.12 è possibile vedere il rivestimento in PBMA dei nuclei. Questo strato, seppur molto sottile, è sufficiente a garantire una copertura omogenea delle particelle e di conseguenza a modificarne la superficie affinché la tensione superficiale tra nuclei e gusci sia tale da produrre l'eccentricità voluta.

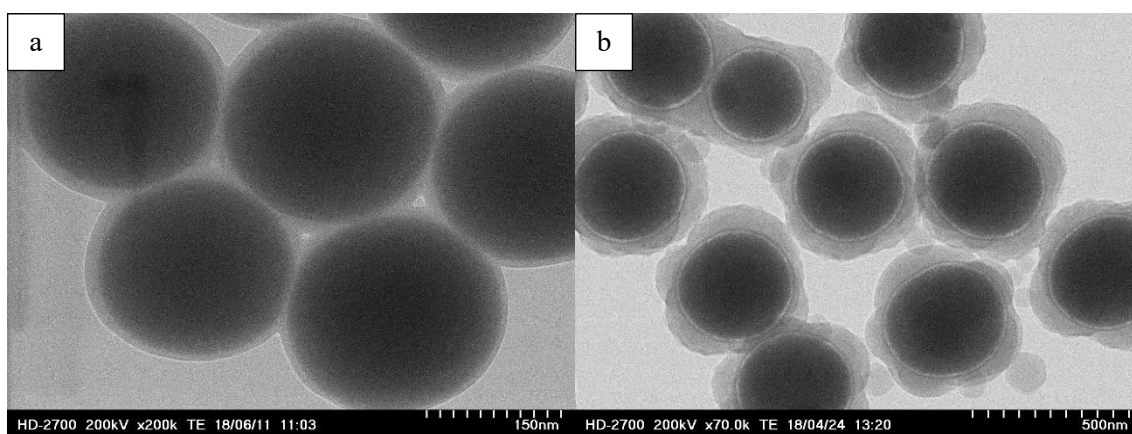


Figura S.12. Immagini ottenute al microscopio elettronico che mostrano il sottile strato di PBMA sui soli nuclei (a) e tra nuclei e gusci (b).

S.5.3 Sintesi dello shell polimerico

S.5.3.1 Rivestimento in PBMA

Sebbene, come già detto, il rivestimento in PBMA sia molto sottile, la sua presenza è indispensabile per l'ottenimento delle particelle desiderate. Come è possibile vedere in Figura S.13, gusci cresciuti su nuclei non preventivamente rivestiti di PBMA crescono, a parità di ogni altra condizione sperimentale, con una morfologia a lobi, mentre, in presenza del PBMA, eccentrici e sferici. Questa differenza è dovuta alla maggiore repulsione che intercorre tra la silice ed il polistirene e che porta alla formazione di forme irregolari al fine di ridurre l'energia libera del sistema.

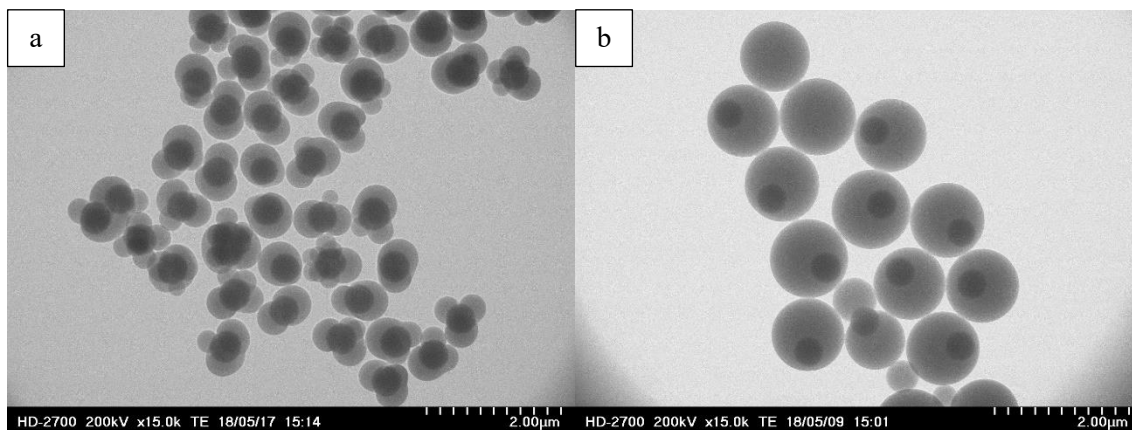


Figura S.13. Immagini ottenute al microscopio elettronico che mostrano la differente morfologia dei gusci cresciuti su nuclei non modificati con il PBMA (a) e con il rivestimento in PBMA (b).

S.5.3.2 Tempo di reazione e concentrazione di stirene

Sia lunghi tempi di reazione che alte concentrazioni di stirene producono gusci spessi, ma il diametro raggiunge un massimo superati certi valori. Quando il tempo di reazione e la concentrazione crescono oltre le 15 ore e 0,2 mol/l rispettivamente, non si osserva più un incremento nel diametro delle particelle. Questo, probabilmente, è dovuto alla massiccia produzione di particelle secondarie che condiziona fortemente il processo intero.

S.5.3.3 Presenza di un elettrolita

La presenza di un elettrolita nel reattore diminuisce la permittività della soluzione riducendo di conseguenza anche la stabilità delle particelle. In queste condizioni le particelle secondarie tendono ad aggregarsi tra di loro o con le particelle eccentriche, riducendo il numero totale di particelle che concorre allo sfruttamento del monomero e quindi aumentandone il diametro. Sfortunatamente però, l'aggregazione non avviene solo tra le particelle secondarie ma anche tra nuclei di particelle eccentriche in accrescimento. Questo causa l'inglobamento di nuclei multipli in una singola particella, caratteristica che peggiora la qualità del prodotto finale rendendo più complicata la definizione di un asse ottico in fase di tracciamento delle rotazioni al microscopio confocale.

S.5.3.4 Velocità di miscelazione

In ogni reazione il trasporto di massa e la fluidodinamica del sistema sono parametri fondamentali che devono essere considerati. In questo studio l'unico modo per avere un controllo su questi due aspetti è stata la velocità di rotazione dell'ancoretta magnetica posizionata nel reattore. Come possibile vedere schematicamente in Figura S.14, la velocità di miscelazione ha effetti sia sul diametro delle particelle che sulla loro morfologia. A basse velocità di rotazione dell'ancoretta magnetica, la diffusione dello stirene tra la fase oleosa e quella acquosa è troppo lenta per produrre una conversione significativa del monomero e un grosso diametro delle particelle. Quando la velocità di miscelazione viene aumentata il trasporto di massa migliora e di conseguenza anche la velocità di reazione, la conversione e il diametro delle particelle. Sfortunatamente però, quando la velocità di miscelazione aumenta troppo, il vortice generato dall'ancoretta magnetica raggiunge l'ancoretta stessa, le tre fasi presenti nel reattore, fase acquosa, fase oleosa e fase gassosa, vengono miscelate profondamente. In queste condizioni, i nuclei rivestiti di PBMA, avendo caratteristiche intermedie tra l'idrofilico e l'idrofobico, si posizionano a

cavallo della superficie di separazione di fase. Così facendo i gusci polistirenici crescono all'esterno dei nuclei, producendo una morfologia molto simile a quella di particelle a "pupazzo di neve". Ovviamente, siccome l'obiettivo primario di questo studio è quello di produrre particelle sferiche, questa condizione rappresenta un limite oltre il quale non è possibile lavorare a meno di non cambiare la strumentazione di processo.

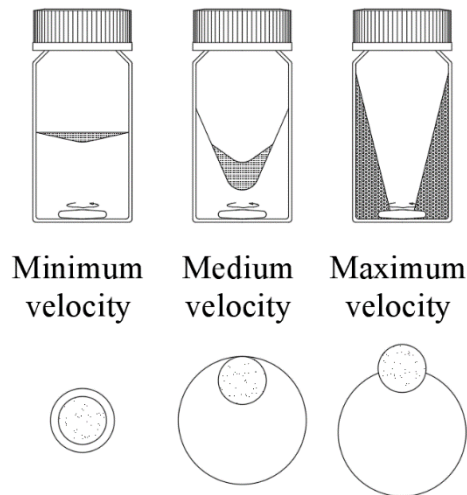


Figura S.14. Confronto tra condizioni fluidodinamiche nel reattore e morfologie delle particelle.

S.5.3.5 Concentrazione dei nuclei

Siccome la concentrazione dei nuclei è decisamente inferiore a quella delle particelle secondarie che si formano durante la polimerizzazione, una modifica nella concentrazione dei nuclei, almeno per quanto riguarda i valori relativamente bassi utilizzati in questo studio, non influenza in alcun modo riconoscibile il diametro finale delle particelle eccentriche.

S.5.3.6 Fluorescenza del pirene

Sebbene non sia stato possibile osservare direttamente la fluorescenza del pirene introdotto nei gusci al microscopio confocale non avendo a disposizione un laser a lunghezza d'onda appropriata, è stato possibile verificarne la presenza nelle particelle in due modi. Una prima osservazione, macroscopica e generale, è stata fatta posizionando una soluzione contenente particelle in cui era stato introdotto il pirene sotto ad una lampada ad ultravioletti e confrontandola con soluzioni di particelle simili ma senza colorante. Infine una verifica più precisa e dettagliata è stata fatta con il fluorometro ed analizzando lo spettro di emissione del campione di particelle irraggiate con un fascio luminoso a lunghezza d'onda di 350 nm. Il confronto tra i picchi dello spettro con i valori riscontrabili in letteratura^[14], ha determinato in maniera univoca la presenza del pirene dentro ai gusci di polistirene.

Un'ultima conferma è infine arrivata dall'analisi fatta dai ricercatori dell'ETH di Zurigo che, con il loro microscopio confocale, sono stati in grado di osservare contemporaneamente entrambe le fluorescenze dell'RITC e del pirene confermando la buona riuscita del progetto.

S.6 Conclusioni

Questa tesi si è concentrata sullo sviluppo di una procedura per la produzione di particelle core-shell eccentriche che incorporino due coloranti fluorescenti rispettivamente nel nucleo e nel guscio affinché possano essere usate come sonde nello studio della scienza dei colloidi.

L'obiettivo è stato raggiunto e i ricercatori dell'ETH di Zurigo che hanno commissionato la ricerca ne hanno confermato la buona riuscita. Sono stati inoltre in grado di osservare, anche se solo in maniera preliminare, le rotazioni delle particelle tramite il microscopio confocale.

Nonostante con questo studio si sia trovata una nuova procedura per creare questo tipo di particelle, esistono ancora molte domande rimaste insolte e molti sforzi devono essere fatti per migliorare la tecnica. La procedura per produrre i nuclei di silice/RITC è sufficientemente ben definita e precisa, ma è limitata alla produzione di particelle con diametro inferiore a 550 nm. Per questo motivo è importante determinare altre soluzioni per incrementare ulteriormente il diametro come polimerizzazioni successive o l'utilizzo di diversi reagenti come alcoli o silicati superiori in peso molecolare. Per quanto riguarda il rivestimento in PBMA sarebbe interessante valutare se e come lo spessore dello stesso possa influire sulla forma e dimensione dei gusci di polistirene e se polimeri diversi possano portare a risultati migliori. Nel processo della produzione dei gusci di polistirene, invece, grossi sforzi dovrebbero essere fatti per migliorare la riproducibilità del sistema reattivo e per controllare in maniera più precisa il diametro delle particelle. Ad esempio parametri come la temperatura di reazione, la concentrazione di iniziatore e l'introduzione di nuovi reagenti stabilizzanti nel sistema dovrebbero essere valutati.

L'applicazione diretta di queste particelle è, come già detto quando la ricerca è stata introdotta, lo studio della dinamica rotazionale di sfere colloidali in diversi stati di aggregazione ma, in buona sostanza, queste particelle sono delle ottime sonde per lo studio di qualunque tipo di aspetto riguardante la fluidodinamica dei colloidi. Inoltre la possibilità di disporre di sonde monodisperse che emettono una fluorescenza, come nel caso dei nuclei di silice/RITC, è di grande valore nella produzione di materiali funzionalizzati e del loro studio.

1 Introduction

Colloidal systems are present in a wide range of natural and artificial phenomena and consequently have an incredible number of applications in both industrial and every-day life. For example, processes as heterogeneous catalysis, ions exchange, water and gases clarification, lubrication, emulsion polymerisation, food processing, chromatography and so on, heavily rely on the colloids ^[1].

1.1 A definition of colloids

Everywhere in the world we live in it is possible to find systems with peculiar characteristics that can be called “colloids”.

To be defined as “colloidal”, a system has to be, in first instance, composed of two phases, A and B, immiscible one another.

A further condition is that the phase A should be finely dispersed into the phase B and “*substance A is then called the disperse phase and substance B, the dispersion medium*”^[2].

Unfortunately this is not an exhaustive definition because it does not give any information about “how fine” the dispersion should be and thus we need to introduce another couple of considerations.

The first one is required to distinguish a colloidal system from a common solution and it is “*that the structure of the solvent on the molecular length scale enters the interaction of the colloidal particle with the solvent molecules only in an averaged way*”^[3]. This means that the particles of the disperse phase cannot be too small and that they should be big enough to “see” the solvent as a continuous phase and not as a group of individual molecules.

The second one gives, on the other hand, some information about the maximum dimension of the units of the phase A. To be considered as a colloid, the particles that compose the system should be small enough to behave following the Brownian motion. The Brownian motion, also called “thermal motion”, is an irregular motion determined by the interaction between the colloidal particles and the chaotic vibration of the molecules composing the dispersion medium.

It is quite easy to see from the latter two how difficult could be to exactly determine what is a colloid and what is not.

However, it is still possible to define a scale order for these particles. From the first consideration the minimum size of the colloidal particle “*should be at least about ten times the linear dimension of a solvent molecule*”^[3], so around 1 nm. The upper limit comes instead from the second one since “*thermal motion is relevant only when thermal displacements are a sizable fraction of the linear dimension of the particle during typical experimental time range*” so around 1 μm ^[2] to 10 μm ^[3].

Colloidal systems could be the combination of any kind of phase, solid, liquid or gas, except, of course, for the gas-gas combination. Some of the most common colloids are: smoke (solid in gas), fog (liquid in gas), paint (solid in liquid), milk and mayonnaise (liquid in liquid), shave foam (gas in liquid), some alloys (solid in solid) and the insulating foam (gas in solid)^[2].

It can be surprising to realise that only in the beginning of the 20th century a first theory for the Brownian motion was proposed and effectively verified by Albert Einstein and Jean Perrin respectively ^[4].

Big efforts were made during the last decades to define analytical representations of these systems and numerous and essential steps forward were achieved, but still many questions remain unsolved.

The biggest problem encountered in the analysis of such kind of phenomena is the preparation of well-characterized particles. The availability of colloids with uniquely defined size, shape and interactions is crucial for the comparison between theories and simulations and thus for the validation of the firsts. The definition of analytical models for highly polydispersed systems is not only challenging under a

mathematical point of view, but it is also difficult because of the relatively small number of particles that can be simulated with a computer compared to the effective number that typically characterize bulk samples [4].

Considering these circumstances, the project of this thesis was born under the collaboration between the ETH of Zurich (Swiss) and the Tohoku University (Japan).

More specifically, the researchers from the ETH of Zurich were interested in the study of the rotational behaviour that colloidal particles have in proximity of their glass transition.

A single spherical particle in a fluid medium, in a 3-dimensional space, has 6 degree of freedom, 3 translational and 3 rotational, on respective axis. Although it is quite easy to observe a translation, it is almost impossible to do the same with a rotation due to the intrinsic rotational symmetry of a perfect sphere. For this reason, it was of crucial importance to create a particular kind of particles that could overcome the problematic symmetry, but keeping the outer spherical structure in order to maintain unaltered the fluid dynamic of the system.

The request commissioned was to produce eccentric silica core-polystyrene shell particles (as in Figure 1.1), incorporating two different fluorescent dyes respectively, with rather specific inner and outer diameters. The shell diameter was approximately 1.4 μm and the cores diameter approximately 400 nm.

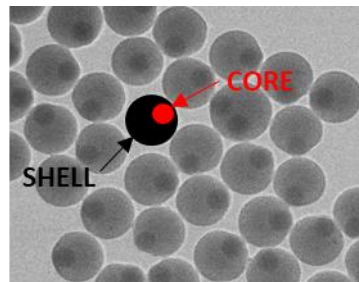


Figure 1.1. A schematic representation of an eccentric core-shell particle.

Having these particular particles, it becomes possible to measure both the translational and rotational dynamic of colloidal spheres using a confocal microscopy, as reported by Liu and Böker[5].

This method consists, basically, in the recognition of an optical axis defined by \mathbf{u} that connects the centre of the shell to the centre of the core. By following how this vector evolves during time it is possible to determine how the particle rotate as described in Figure 1.2 .

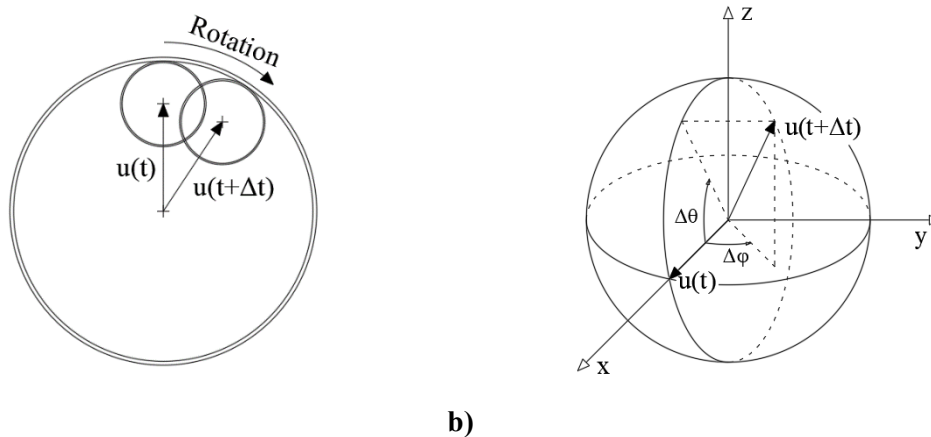


Figure 1.2. A schematic representation of vector \mathbf{u} (a) and a possible set of coordinates for the colloidal particles (b). Figure modified from [5].

1.2 State of the Art

1.2.1 Silica cores

For what that concern the production of the silica-cores without the incorporation of any kind of dye the process is very well known and understood. The first analysis of this process was made by Stöber *et al.*^[6] in 1968 and since that moment this particular procedure was intensively used all over the world. In their research Stöber *et al.* designed an easy way to produce monodispersed silica particles with diameters that could range from 0.05 μm up to 2 μm . In this system the particles were grown as a consequence of the hydrolysis of alkyl silicates and subsequent condensation of the silicic acid in an alcoholic solution. The reaction system was composed of at least four components with specific tasks: pure alcohol (or an alcoholic mixture) as the solvent, alkyl silicate as the silicon source, water as the initiator, and ammonia as the morphological catalyist that cause the formation of spherical particles.

The influence of all the components of the system in the diameter outcome was analysed systematically and described in detail.

It is reported that the particles diameter increases changing the solvent composition going from pure methanol to pure *n*-butanol and that this is due to a slower reaction rate in the higher alcohols. The size distribution, however, resulted wider in higher alcohols, but could be narrowed by mixing different solvents.

Similarly, the reaction rates became slower and the particles diameters bigger changing the alkyl silicates from tetramethyl ester up to tetrapentyl ester. It is reported, for example, that with a ethanol-ethyl ester system it is not possible to produce particles larger than 1 μm in a single step.

The effect of the concentrations of all the reactants over the particles diameter was also analysed.

Even though a change in the concentration of the ester did not produce any change in the diameter, both water and ammonia had a strong influence on it.

The condensation rate depends mostly on the concentration of water and the diameter increases almost linearly with the water content reaching a maximum over around 5 to 6 mol/l. Exceeding this optimum, though, the trend is reversed.

The ammonia was found to be a morphological catalyist since in the absence of it the silica flocculated and only irregularly shaped particles or no sphere at all were found in the system. However the content of ammonia have a role also on the dimension of the particles and in this study it was found that at higher concentration the final diameter increased reaching a maximum when the solution was saturated with ammonia.

It is important to notice that even if in their work Stöber *et al.* described the synthesis process only under a qualitative point of view, numerous works describe the process also under a mathematical and chemical perspective. One in particular is the study of Chen *et al.*^[7] that gives information on all the kinetics parameters of the reactions involved in the formation of the particles and provide simple equations that describe the evolution of the system.

1.2.2 Incorporation of a fluorescent dye in silica particles.

A general procedure to incorporate a fluorescent dye in silica particles was proposed by van Blaaderen and Vrij^[8] in 1992. They described how to incorporate a dye or a fluorophore into the silica structure using a silane coupling agent, the (3-aminopropyl)triethoxysilane (APTES). Thanks to this method the composition of the silica spheres can be controlled in such a way that the dye can be placed on the surface, in a thin shell inside the particles, distributed through the volume of an inner core or in a combination of the three as described in Figure 1.3.

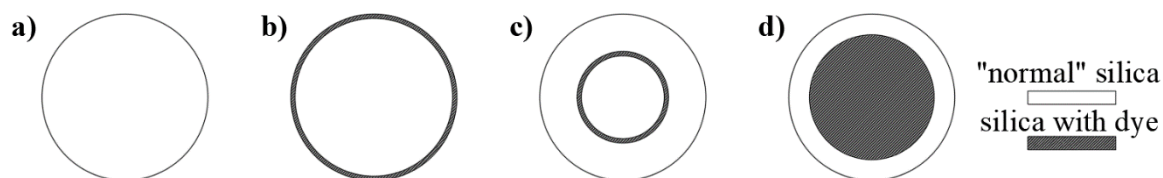


Figure 1.3. Schematic representation of the possible incorporation of a dye in a silica particle. A particle without the dye (a), with the dye on the surface (b), in a thin shell inside the particle (c) or distributed in the volume of an inner core (d). Figure modified from [8].

In this particular work the fluorophore was chosen to be the fluorescein isothiocyanate (FITC).

They proved effectively that the dye did not adsorb in the silica particles without an external help trying to add free dye in an alcoholic solution with silica particles and then centrifugating the system. As expected the fluorophore was all washed out during the centrifugation and the particles did not exhibit any fluorescence in a further examination.

For this reason they modified the fluorophore molecule with the already said APTES by an addition reaction between the amine group of the coupling agent and the thioisocyanate group of the dye and added this new compound to the reactive system. After the modification, the fluorescent molecule has three siloxane groups that can react with those of the TEOS and therefore the dye is easily incorporated in the silica matrix of the particles. With this procedure, not only it is possible to introduce a dye in the particles but, since it is covalently bound to the silica, it is also impossible to remove it.

Although this process is generic and well developed, it focuses only on how to introduce the fluorophore inside the particles and does not give detailed information on how to control the diameter, topic that will therefore be discussed in this thesis.

Subsequently, Verhaegh and van Blaaderen^[9], in 1994, produced monodispersed silica spheres with a total diameter of 400nm and an inner core of 200nm labeled with the fluorescent dye rhodamine isothiocyanate (RITC) and analysed the fluorescent properties, the dye concentration in the particles and its bleachability. They also discussed about the possibilities and limitations in using a confocal microscopy to study individual fluorescent particles in the bulk of concentrated model dispersions.

In this work the dye RITC was used because of its higher resistance to photo-bleaching, the tendency of a fluorescent compound to lose its fluorescence if hit by a strong light. Again, it was stated that the RITC does not adsorb in the silica particles and then the modification of the dye was performed in the same way as for the FITC.

The inner core was prepared injecting the colour solution into a reaction system based on the Stöber process and then the pure-silica shell was grown on the cores injecting some fresh TEOS and water in the reactor without changing the reaction solution. This decision was taken since the core particles are not as stable as normal-silica ones because they present on the surface some dye molecules that, being charge-neutral, decrease the absolute value of the particles' ζ -potential. Therefore they would not resist a centrifugation to remove the coloured reactive solution without self-aggregating in the process. However it was stated that the dye remained in the solution did not interfere in the growth step and that the particles had fluorescent core only. Considering that the RITC does not adsorb on silica, the small amount of dye that did not react with the APTES, and therefore did not enter into the core, had no way to be included in the growth mechanism and for this reason it is easy to understand why the missing change of the reaction solution did not cause any trouble. At this point, however, the surface of the particles is made of pure silica and therefore the stability is as high as of an only-silica particle.

The molar ratio between TEOS and RITC was chosen to be 580:1. It is known that the fluorescence intensity increases with the dye concentration in the silica matrix almost linearly until it reaches a certain concentration. From this concentration the slope of the curve decreases and could also change sign due to a phenomenon called "self-quenching" that basically consists in an extra transition of the excited

electrons that reaches the ground state and therefore do not emit photons. In their work Verhaegh and van Blaaderen analysed the fluorescence dependence over the RITC concentration in the silica cores and established that the above mentioned limiting concentration is located somewhere between the molar ratio of TEOS:RITC of 450:1 and 700:1.

1.2.3 Production of nonspherical particles.

Normally, when performing a seeded growth reaction, one would expect the outer shell to grow uniformly over the seed particles generating spherical concentric particles. Even though this happens when the core and the shell are highly compatible as in the process described to coat a fluorescent silica particle with other pure silica, something different could happen when working with organic polymerisations.

In 1990, Sheu *et al.* published two complementary works^{[10][11]} in which they described in detail how to produce nonspherical latex particles by seeded emulsion polymerisation and proposed an accurate method to describe the causes and the mechanism of such process. In these works the odd shape of the particles is considered as the direct consequence of the phase separation between more or less crosslinked polymeric matrices.

Both of the articles focused on the emulsion polymerisation of styrene-divinylbenzene (DVB) mixtures over monodispersed crosslinked polystyrene seeds.

In the first work^[10] it is described the thermodynamic principle on which the production of nonspherical particles is based and the mechanism of the phase separation. The concentration of DVB needed in the seeds to have a crosslinked reticulum and how time influences the phase separation are also described in this work.

On the other hand, in the second article^[11] many processistic parameters that could influence the particles' morphology were analysed. In particular: monomer/polymer ratio, degree of crosslinking in both the seeds and the protuberances, the polymerisation temperature and the size of the seed particles. An attempt in subsequent polymerisation was also described.

The phase separation is a consequence of the initial swelling of the crosslinked seed particles with the monomer and a further shrinkage due to thermodynamic factors like the temperature and the surface tension between the phases.

A thermodynamic study was reported as follows.

For a system composed of crosslinked polymer particles, monomer and an aqueous phase, at the equilibrium, the chemical potential of the monomer in the polymer ($\Delta\bar{G}_{m,p}$) should be equal to the chemical potential of the monomer in the aqueous phase ($\Delta\bar{G}_{m,a}$):

$$\Delta\bar{G}_{m,p} = \Delta\bar{G}_{m,a} \quad (1.1)$$

However, for monomers that are scarcely soluble in water as the styrene is, it is often possible to neglect the second term so that eq. (1.1) becomes:

$$\Delta\bar{G}_{m,p} = 0 \quad (1.2)$$

The chemical potential of the monomer in the polymer can be divided into three terms: one due to the monomer-polymer mixing forces ($\Delta\bar{G}_m$), one due to the polymer elastic-retractive forces ($\Delta\bar{G}_{el}$) and one due to the particle-water interfacial tension forces ($\Delta\bar{G}_t$).

$$\Delta\bar{G}_{m,p} = \Delta\bar{G}_m + \Delta\bar{G}_{el} + \Delta\bar{G}_t = 0 \quad (1.3)$$

The mixing term, $\Delta\bar{G}_m$, describe the partial molar free-energy change of the chemical potential in relation of the absorption of the monomer and is negative since the monomer is highly soluble in the polymer, leading to a promotion of the particle expansion. The elastic free-energy change, $\Delta\bar{G}_{el}$, is an entropy term that describe how the entropy of the polymer network change when the particle swell. Considering that the number of polymer chains remains constant during the absorption process, it is

easy to understand that the entropy of the network will decrease since the volume of the particle will increase and thus the polymer chains will have to dispose in a more-linear configuration to occupy all the volume and the crosslinked chains will have to stretch. This term is therefore positive and oppose to a further swell. The last term, $\Delta\bar{G}_t$, related to the surface tension and caused by the increment in the contact area of the particle with the aqueous solution is, again, always positive since a certain work has to be provided to the system to “create” new surface and, again, it opposes to the swelling.

Swelling of the particles, then, takes place when the sum of these three terms is negative and stop when it reaches the equilibrium at $\Delta\bar{G}_{m,p} = 0$. If something in the system changes in a way that leads to a positive value of $\Delta\bar{G}_{m,p}$ (as, for example, an increment in temperature) phase separation will occur until the equilibrium is reached again.

The mechanism that leads to the phase separation was described schematically as in Figure 1.4.

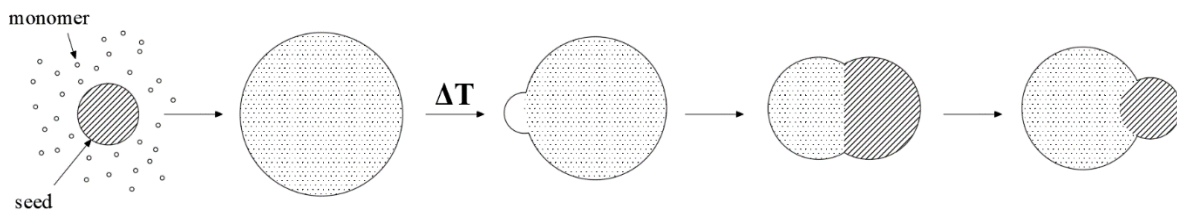


Figure 1.4. Schematic representation of the mechanism of of the phase separation.

In the initial stage the crosslinked seed particle and the monomer in the aqueous solution coexist.

In the second stage the seed particle starts to swell absorbing the monomer at room temperature until it reaches the equilibrium chemical potential as previously described.

Then the temperature is increased and the chemical potential exceed zero so that the phase separation start in an attempt to reach again the equilibrium. In this stage the monomer is extruded out of the polymer reticulum and form a new phase domain.

Subsequently the polymerisation in the new domain starts as well as new monomer migrate from the seed particle and the aqueous solution into the growing bulge. This stage will continue until the chemical potential in the protuberance will be equal to the chemical potential in the seed domain.

At the end of the polymerisation the nonspherical particle is formed and the two domains are easily distinguishible.

In addition to the thermodynamic analysis, Sheu *et al.*^[10] in this work determined also some quantitative parameters that were needed for the process.

In first instance they evaluated which was the minimum DVB concentration that was needed in the production of the seed particles to generate a crosslinked reticulum and established that it was 0.03% DVB/Styrene.

This value was of incredible importance when the effect of the crosslinked network on the phase separation was tested. In fact, they showed that in particles prepared with a DVB concentration lower than the minimum needed for the formation of a crosslinked reticulum the phase separation did not occur at all and the shape remained perfectly spherical. Increasing the DVB concentration, on the other hand, increased the degree of phase separation and with very highly crosslinked networks the production of multiple phases domains occurred. With this information it was cleared out that the crosslinking degree have a major influence in the swelling/shrinking process.

With experiments on the kinetics of the phase separation they also pointed out that the new domain grows by absorption of monomer from the seed domain, which contract as a result, in perfect accordance with the mechanism proposed.

As already announced, in the second work^[11], all the possible combinations of the variables in the system were analysed and described in detail so that now it is possible to control directly the morphology of the particles and obtain the desired shape and dimension.

Unfortunately, this method cannot be applied directly to the production of the particles requested by the researchers from the ETH of Zurich for two reasons.

The first one is that this method can be applied only on polymeric networks because one of the fundamental requirements is that the monomer for the polymerisation should absorb into the particles and this is not possible when using silica spheres.

The second is that this time the shape should remain spherical to maintain the fluid dynamic of the particles and the method of Sheu *et al.* is strictly based on a non-spherical morphology.

For these reasons, even though maintaining the theoretical concepts, it is necessary to modify and adapt the method for inorganic seeds and different morphologies.

This adaptation was well developed by Nagao *et al.*^[12] in the article in which they described the synthesis of anisotropic snowman-shaped polymer particles containing silica spheres.

In this work a silane coupling agent, the 3-methacryloxypropyltrimethoxysilane (MPTMS), was used for the hybridization between inorganic and organic materials. This compound is provided with three siloxane groups that link with the silica surface of the seed particles and a vinyl group that can be introduced into the polymeric chain during the polymerisation. Moreover, thanks to its four functional groups the MPTMS is also a crosslinking agent during the polymerisation.

The synthesis of the snowman particles comes from a two-steps soap-free emulsion polymerisation. In the first step silica spheres prepared with the Stöber method are used as seeds, the surface is modified with the MPTMS and the first polymerisation is performed using methylmethacrylate (MMA) as the monomer in the presence of the sodium *p*-styrenesulfonate (NaSS) as ionic co-monomer to improve the stability of the system. During this step, a uniform layer of crosslinked poly-methylmethacrylate (PMMA) is formed around the silica particles. The second polymerisation is then performed using these particles as seeds and the styrene as a monomer. The result is an anisotropic particle as in Figure 1.5.

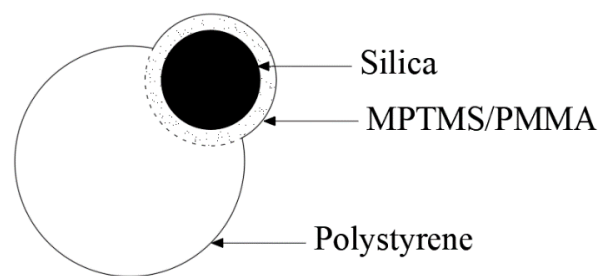


Figure 1.5. Schematic representation of a “snowman particle” with its components distinction.

In this process, the first coating with the MPTMS/PMMA is essential because it provides a crosslinked polymeric network that should swell with the styrene monomer and then shrink inducing the phase separation. It was also pointed out how the concentration of the MPTMS, and thus the crosslinking degree, have a major importance in the acentric degree of the particle. In other words, the more crosslinked is the MPTMS/PMMA shell, the more extruded will be the polystyrene bulge, as one could expect from the previously described study of Sheu *et al.*

As already said another problem that was necessary to eliminate was the non-sphericity of the particles. To overcome this, there are multiple choices that could be taken referring to the thermodynamic analysis made by Sheu *et al.* The phase separation occurs in accordance to the sum of three different terms inside the particle as in equation 1.3 and thus, controlling these three mechanisms, it should be possible to

control the morphology of the particle. In this thesis, it was chosen to control the term related to the surface tension. In specific, it is reasonable to assume that the phase separation occurs with a higher strength the more the two polymer in the first and second coating are incompatible. So this means, by contrary, that if a monomer with a higher affinity with polystyrene is used for the first polymerisation, it is reasonable to expect that the protrusion is lower and eventually it would lead to an eccentricity that is limited only to the inside of the particle and leave the outside spherical. This assumption was effectively tested using the butylmethacrylate (BMA) that has a higher molecular weight and therefore is more compatible with the polystyrene. Not only this new monomer was tested, but it also resulted to be effective in the production of the required eccentric particles subject of this thesis as will be described in the next chapters.

Another possibility that is important to be mentioned is the utilisation of two subsequent polymerisation steps of the styrene monomer. In this case, the controlling factor will be the crosslinking degree of the first shell and with an accurate choice of the concentrations, it is possible to produce almost the same particles as using the BMA.

1.2.4 Incorporation of a fluorescent dye in the polystyrene shell.

The first aspect that has to be considered is the choice of the fluorescent dye. As already described, the process that leads to the formation of the eccentric particles depends strongly on the composition of the reactive system and the introduction of a stranger compound could potentially change irreversibly the morphology of the particles. Moreover, the colour have to be incorporated into the polystyrene matrix and, possibly, it should remain inside the shell and not desorb after the reaction. Last but not least the new colour must be sensibly different from the one inserted in the silica cores so that the two domains could be easily recognised in a confocal microscope. For these reasons, the fluorophore pyrene was a perfect candidate.

Its excitation wavelength is around 350nm and the emission peaks are located between 375nm and 400nm^[13], considerably distant from those of the RITC which excitation maximum is positioned around 555nm and emits around 600nm^[9].

Pyrene is an organic compound composed of four benzene groups and therefore it is highly soluble both in the styrene monomer, and in the polystyrene polymer. Since its structure is very similar to that of the styrene monomer it will increase the hydrophobicity of the oily phase only slightly during the secondary polymerisation so that the surface tension between the MPTMS/PBMA particles and the styrene will not change enough to give substantial modification during the phase separation. Moreover pyrene is almost not soluble in water so that its desorption after the reaction could be neglected in first instance. Still it will be necessary to test and certify all these assumptions for this specific case of study.

The incorporation of pyrene in polystyrene particles has already been performed before by Tamai *et al.*^[13]. Polystyrene/pyrene fluorescent particles were synthesized by miniemulsion polymerisation adding pyrene dissolved in styrene monomer into an aqueous solution with a surfactant. After the reaction the particles showed fluorescence emissions as expected. The concentration of the fluorophore was chosen to be 2mol% vs. styrene.

In this article the presence of the pyrene molecules into the polymeric matrix is confirmed analysing its emission spectra. Its spectra shows two distinctive peaks, located at 376nm (I_1) and 388nm (I_3). The intensity ratio I_1/I_3 ranges from 1.87 when pyrene is dissolved in water to 0.6 when dissolved in aliphatic hydrocarbon solvents. The value measured in the experiment reported in this article is equal to 0.9^[14] that is exactly the same as the one characteristic for pyrene in polystyrene so it was possible to assume that the dye was successfully incorporated into the polymeric particles.

A general big problem of pyrene is that it is easily quenched by the molecular oxygen resulting in a low fluorescent intensity under air, so Tamai *et al.*^[13] also discussed this aspect. They measured the emission intensity of pyrene dissolved in cyclohexane under air and under nitrogen and repeated the measurements for the pyrene incorporated in the polystyrene particles. The intensity ratio I_{air}/I_{N_2} was then calculated and evaluated in <0.1 and 0.94 respectively. This result indicates that, unlike in the

hydrocarbon solution, almost no fluorescence quench takes place in the particles and that, therefore, the incorporation of the fluorophore into polymeric particles will protect it from the undesirable interaction with the oxygen in the air.

1.3 Motivation of this thesis

The objective of this thesis was to produce the particles requested by the researchers of the ETH of Zurich and to, possibly, create a simple, efficient procedure that can be replicated with sufficient precision to give good experimental probes.

In specific, the request was to produce eccentric particles with a silica core with a diameter around 400 nm and an eccentric polystyrene shell with a diameter around 1.4 μm . Moreover, it was essential to incorporate two different fluorescent dyes in each one to allow their observation under a confocal microscope.

The particles are composed of three main parts: the silica core, the first thin polymer layer that is required to link the core to the shell and to guarantee the eccentricity in the particle and the polystyrene shell.

The first part of the work is focused on the production of the fluorescent cores. The synthesis of silica particles is very well known, but the introduction of a fluorescent dye changes the reactive system. For this reason, a detailed study on this process was made and the possibility of a control over the diameter was analysed. The influence of the main reaction parameters on the process was studied and a comparison between pure-silica particles and RITC-dyed particles was made to determine in which measure the introduction of a fluorescent dye affects the synthesis.

The first polymer coating, performed using the monomer butylmethacrylate (BMA), was analysed to determine its necessity and effectiveness in producing eccentric particles.

At last, the polymer shell was studied. Not only it was necessary to define the possibility to produce eccentric particles, but it was important to define in which measure it is possible to have any kind of control over this system. For this reason, a systematic study was made to determine the limiting parameters in the process and to optimize the synthesis to obtain particles in the requested diameter. Finally, the introduction of a second fluorescent dye in the shell was performed and its fluorescent characteristics were analysed to determine its compatibility with the dye in the core.

The following chapters are organised as follows.

A first chapter aims to define the methods and procedures used in this work. All the experiments are explained in detail and the choices made during the work are described. In the following chapter all the results are explicated and a description of the mechanisms is given and in the last chapter summarize the conclusions obtained during this work.

2 Methods

2.1 Reactants

Ethanol (99.5%), ammonia (NH₃) (25% aqueous solution), tetraethyl orthosilicate (TEOS), potassium persulfate (KPS), sodium *p*-styrenesulfonate (NaSS), NaCl and pyrene were purchased from Wako Pure Chemical Industry (Japan) and used as received. Styrene (with 0.003% *p*-*t*-butylcatechol stabilizer) and butyl methacrylate (BMA) (with 0.01% Hydroquinone stabilizer) were purchased from Wako Pure Chemicals Industry (Japan) and used after inhibitor removal. (3-aminopropyl) triethoxysilane (APTES) was purchased from Shinetsu (Japan) and used as received. 3-methacryloxypropyl trimethoxysilane (MPTMS) was purchased from JNC Corporation (Japan) and used as received. Rhodamine B isothiocyanate (RITC) was purchased from Aldrich (U.S.A.) and used as received. Water was deionized and distilled to have an electric resistance higher than 18 MΩ·cm,

2.2 Experimental procedures

2.2.1 Core particles

The goal of this part was the production of 400 nm silica/RITC core particles and, possibly, an analysis on if and how it is possible to control the particles' diameter.

A modified Stöber method was used to produce the fluorescent silica core particles. The process consists in:

1. *Preparation of the dye solution.* The dye RITC is dissolved into ethanol and the coupling agent APTES is added to perform the modification of the dye molecules. The solution is kept under nitrogen to reduce the possible interaction with the atmospheric oxygen and it is put in the sonicator for at least half an hour to guarantee a perfect mixing.
2. *Preparation of the reactive solution.* A mixture of ethanol, ammonia (in aqueous solution) and the eventual additional water is prepared in the reactor and the system is placed in a liquid isothermal bath at room temperature. Mixing is provided by a magnetic stir bar placed inside the reactor and kept in movement by the magnetic stirrer under the isothermal bath.
3. *Reaction.* A solution of TEOS dissolved in ethanol and the solution containing the dye are added into the reactor subsequently. The reaction will then proceed for five hours (reaction time 1 in Table 2.1) to reach complete conversion.
4. *Addition of a stabilizing silica layer.* An additional solution of TEOS dissolved in ethanol is added to the reactor and the reaction will proceed for one hour (reaction time 2 in Table 2.1).
5. *Centrifugation.* A series of centrifugations and redispersions are performed until the supernatant is clear and all the unreacted dye is washed away.

The schematic process is described in Figure 2.1 and the main parameters are shown in Table 2.1.

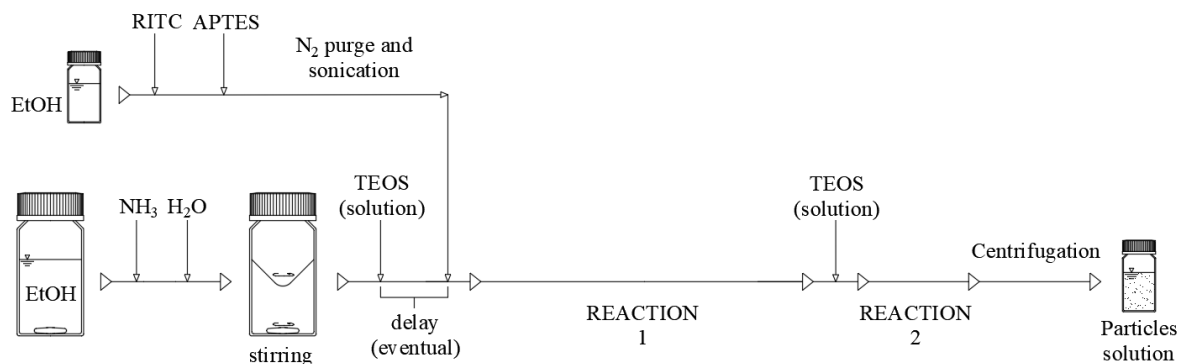


Figure 2.1. A scheme of reaction process.

Table 2.1. Main reaction parameters.

Parameter	Value	Unit
Reaction volume	30	ml
Reaction temperature	35	°C
Reaction time 1	5	h
Reaction time 2	1	h

An intensive and systematic study was made to analyse how the introduction of the fluorescent dye modify the process and how it is possible to control the diameter of the particles. All the following parameters were analysed:

- Eventual **delay** between the injections of the TEOS solution in the reactor and the dye solution.
- Presence of additional **only-silica layers** on the particles.
- **Ammonia** concentration.
- **Water** concentration.
- **TEOS** concentration.

The solution containing the dye was prepared always with the same concentrations, as described in Table 2.2. The quantity of RITC was chosen to be 0.01 mmol so that the molar ratio TEOS:RITC was close to the range 450:1 to 700:1 for all the experiments. This ratio is the one that gives the maximum fluorescence intensity as described by Verhaegh and van Blaaderen^[9]. The APTES was added in the quantity of 0.023 mmol so that it could be in large excess respect to the RITC (2.3 times greater) and, therefore, maximize the conversion of the dye in the coupling reaction and maximize the incorporation of the dye in the silica lattice.

Table 2.2. Composition of the solution containing the fluorescent dye. The values in bold are those that were decided a priori and the others were calculated starting from those. Concentrations refer to the reaction volume.

Component	Volume, ml	Weight, mg	Moles, mmol	Concentration, mmol/l
EtOH	0.5	399.00	8.661	288.69
RITC	-	5.36	0.010	0.33
APTES	0.0054	5.09	0.023	0.77

The solvent was always ethanol and it was calculated so that the total volume would sum up to the reaction volume of 30 ml. When the TEOS was added to the reactor to begin the reaction it was always dissolved in 5 ml of ethanol.

When an additional only-silica layer was grown over the coloured particles, the TEOS required was dissolved in 1 ml and 0.7 ml respectively for the first and the second layer. These quantities are summed up in Table 2.3.

Table 2.3. Composition of TEOS solutions.

Destination	Ethanol, ml	TEOS, ml
Main body	5	variable
First layer	1	0.2
Second layer	0.7	0.3

The experiments proceeded as follows:

Experiments from **I to V** were made to analyse how an eventual **delay** in the injection of the solution containing the fluorescent dye, respect to the injection of the TEOS solution, could modify the product. The delay was fixed in five equidistant values, from 6 min to 10 min. The concentrations of the reactive components were those of a typical Stöber experiment ($[\text{TEOS}] = 0.16 \text{ M}$, $[\text{H}_2\text{O}] = 2.87 \text{ M}$, $[\text{NH}_3] = 1.00 \text{ M}$, as shown in Table 2.4) and were equal for all the five samples so that no other parameter could influence the results. The particles were coated with two additional only-silica layers.

Table 2.4. Experimental conditions of samples I to V. The values in bold are those that were object of investigation.

Run	$[\text{NH}_3]$, mol/l	$[\text{H}_2\text{O}]$, mol/l	$[\text{TEOS}]$, mol/l	RITC Injection delay, min	Number of layers, -
I	1	2.87	0.16	6	2
II	1	2.87	0.16	7	2
III	1	2.87	0.16	8	2
IV	1	2.87	0.16	9	2
V	1	2.87	0.16	10	2

Experiments from **VI to IX** focused on the influence of the **ammonia** concentration. Four values were tested: 0.6 M, 0.8 M, 1.0 M and 1.2 M as shown in Table 2.5. The delay between the injection of the TEOS solution and the RITC/APTES solution was fixed to 1 min. The TEOS concentration remained unchanged and equal to 0.16 M. The water concentration was raised to 3.4 M and kept constant for the four runs. This decision was a consequence of the fact that the ammonia is available in aqueous solution at 25% in weight ($w_{\text{NH}_3}/w_{\text{H}_2\text{O}}$) and, therefore, 3.4 M is the minimum, unavoidable, water concentration that will be present in the system if ammonia is present at a concentration of 1.2 M. Two only-silica layers were grown on the fluorescent particles.

Table 2.5. Experimental conditions of samples VI to IX. The values in bold are those that were object of investigation.

Run	[NH₃], mol/l	[H₂O], mol/l	[TEOS], mol/l	RITC Injection delay, min	Number of layers, -
VI	0.6	3.4	0.16	1	2
VII	0.8	3.4	0.16	1	2
VIII	1.0	3.4	0.16	1	2
IX	1.2	3.4	0.16	1	2

The sets of experiments **1 to 8** and **18 to 25** were performed to define how both the **water** concentration and the **TEOS** concentration affect the diameter of the particles. The concentration of ammonia was fixed to be equal to 0.6 M. Water concentration and TEOS concentration are shown in Table 2.6. One only-silica layer was grown on the particles. The dye solution and the TEOS solution were injected subsequently.

Table 2.6. Experimental conditions of samples 1 to 8 and 18 to 25. The values in bold are those that were object of investigation.

Run	[NH ₃], mol/l	[H ₂ O], mol/l	[TEOS], mol/l	RITC Injection delay, min	Number of layers, -
1	0.6	1.7	0.32	-	1
2	0.6	1.7	0.24	-	1
3	0.6	1.7	0.16	-	1
4	0.6	2.55	0.32	-	1
5	0.6	2.55	0.24	-	1
6	0.6	2.55	0.16	-	1
7	0.6	3.4	0.32	-	1
8	0.6	3.4	0.24	-	1
18	0.6	5.1	0.16	-	1
19	0.6	5.1	0.32	-	1
20	0.6	6.8	0.16	-	1
21	0.6	6.8	0.32	-	1
22	0.6	8.5	0.16	-	1
23	0.6	8.5	0.32	-	1
24	0.6	10.2	0.16	-	1
25	0.6	10.2	0.32	-	1

Experiments **26**, **27**, **30** and **31** were prepared **without additional only-silica layers** for a better comprehension on the effective influence of the coating on the particles' stability. Ammonia concentration was 0.6 M and TEOS concentration 0.16 M. Water concentration was equal to 6.2 M and 6.3 M for runs 26-27 and 30-31 respectively. These value where calculated by interpolation in the curve "diameter/[H₂O]" obtained from the set of experiments 18-25 to have a diameter close to 400 nm. The dye solution and the TEOS solution were injected subsequently. Reaction conditions are summarized in Table 2.7.

Table 2.7. Experimental conditions of samples 26, 27, 30 and 31. The values in bold are those that were object of investigation.

Run	[NH ₃], mol/l	[H ₂ O], mol/l	[TEOS], mol/l	RITC Injection delay, min	Number of layers, -
26	0.6	6.2	0.16	-	0
27	0.6	6.2	0.16	-	0
30	0.6	6.3	0.16	-	0
31	0.6	6.3	0.16	-	0

Experiment **64** was made to test the **reproducibility** of the process and its receipt was used as seed solution for the polymer coating in the following steps. All the concentrations are summarized in Table 2.8. One only-silica layer was grown on the particles. The dye solution and the TEOS solution were injected subsequently.

Table 2.8. Experimental conditions of sample 64.

Run	[NH₃], mol/l	[H₂O], mol/l	[TEOS], mol/l	RITC Injection delay, min	Number of layers, -
64	0.6	6.2	0.18	-	1

The set **68 to 73** was made **without RITC**. The intention was to have a reference to point out the influence of the fluorescent dye on the process. The procedure remained the same, except for that the solution containing the RITC was not added to the reactor, and that no additional layer was added to the particles. This is easy to understand since the particles' stability is not affected by the RITC on the surface and therefore there would be no gain in doing so. All the concentrations are summarized in Table 2.9.

Table 2.9. Experimental conditions of samples without the fluorescent dye.

Run	[NH₃], mol/l	[H₂O], mol/l	[TEOS], mol/l
68	0.6	4	0.158
69	0.6	5	0.158
70	0.6	6	0.158
71	0.6	7	0.158
72	0.6	8	0.158
73	0.6	9	0.158

2.2.2 PBMA coating

The coating with the Poly-Butylmethacrylate (PBMA) is necessary to induce the eccentricity between the silica core and the polystyrene shell. When the polymerisation occurs in the reactor, the polystyrene oligomers behave as a sort of condensed state between a solid and a liquid. For this reason, they act almost as a drop of liquid when placed over a solid plane surface. The surface tension of the liquid and the interaction that this one has with the solid surface and the atmosphere will determine the shape of the drop as shown in Figure 2.2. The same considerations can refer to a curved surface, as it is the surface of the core particles, and a system composed of a solid particle, a polymer and a solvent. This gives us the three main morphologies that can be found in core-shell particles:

1. *Concentric particles*: The shell grows radially and isotropically. The centre of the core is coincident with the centre of the shell.
2. *Eccentric particles*: The particle is still spherical but the centre of the core and the centre of the shell are not coincident.
3. *Snowman particles*: The couple core-shell is no more spherical and the two parts are easily distinguishable.

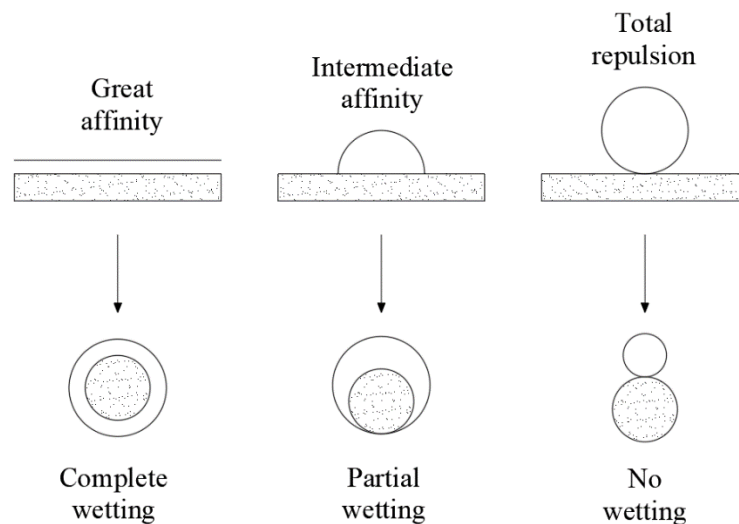


Figure 2.2. A schematic description of the process that leads to the eccentricity in the particles.

An example of concentric particles could be the coating of a polystyrene core with a polystyrene shell. The two parts have the same composition and, for this reason, the shell grows concentric to the core.

An example of snowman-shaped particles is the one given by Nagao *et al.*^[12]. They coated the silica core with poly-methylmethacrylate (PMMA) coupled with MPTMS and then grew a polystyrene shell on the particles. The polymer coating is necessary to have a polymer base over which grow the shell but, at the same time, the PMMA has a low affinity with polystyrene resulting in a good phase separation. The affinity between the PMMA and the polystyrene is relatively low because the functional group connected to the main hydrocarbon chain is, for polystyrene, a benzene group, that is a relatively big, aromatic and non-polar group while, for the PMMA it is a relatively short, polar and linear chain.

In this thesis, the objective was to produce eccentric particles with a spherical shape. For this reason, it was chosen to use and modify the process proposed by Nagao *et al.*^[12]. The main problem was to find a polymer for the first coating with a higher affinity with polystyrene than the PBMA but, still, repulsive enough to induce a partial phase separation.

For this reason, the poly-butylmethacrylate (PBMA) was chosen. The side group of the PBMA is still polar and linear, but it is longer than that of the PMMA. The increased length of the group decreases the polarity and, therefore, increases the affinity with the non-polar polystyrene's group.

The main problem of this first coating is the connection of the polymer to the solid surface of the silica particles. For this reason, a good choice is to use the coupling agent 3-methacryloxypropyltrimethoxysilane (MPTMS) which has three silane groups that can react with those on the silica surface and one double bond that, during the polymerisation, connects the PBMA chains to the particles.

To improve the stability of the system the co-monomer sodium *p*-styrenesulfonate (NaSS) is used. The NaSS has a principal polystyrene structure with a charged sulfonate group attached to each functional group. When it enters in the PBMA layer, it increases the surface charge, and consequently the absolute value of the ζ -potential, improving the colloidal stability of the system.

The process consists in:

1. *Change of the silica particles' solvent.* A series of centrifugations is necessary to change the solvent dispersing the silica particles from ethanol to water. Silica particles are very stable and, for this reason, they can be kept under ethanol for a long time even though its permittivity is very low. For polymeric particles, which have a lower ζ -potential, this is not possible and water, which have a very high permittivity, is required.
2. *Preparation of the reaction solution and reactor.* The solvent, water, is introduced in the reactor and then it is purged with nitrogen for 30 minutes to remove the oxygen that can interfere with the polymerisation. To avoid a further significant contamination during the injection of the other reactants, the cover is pierced with a drill and a micropipette's tip is placed in the hole and covered with laboratory film as shown in Figure 2.3. The particles' solution is then injected in the reactor and the reactor is placed in the isothermal water bath at room temperature and over the magnetic stirrer.
3. *MPTMS coupling.* The MPTMS is dissolved into 1 ml of ethanol and injected in the reactor. The MPTMS is not soluble in water so ethanol is used to improve the reproducibility of the system, but still the volume is small enough to keep the permittivity of the solvent almost unchanged. The MPTMS reacts for 30 minutes to modify the particles surface.
4. *Injection of the monomer and comonomer.* BMA and NaSS are injected in the reactor. The NaSS is previously dissolved in 1 ml of water. The system is stirred for 1 hour to guarantee the saturation of the solvent with the monomer and a good mixing.
5. *Reaction.* The temperature of the isothermal bath is raised to 65 °C and the solution containing the initiator, potassium persulfate (KPS), is injected in the reactor. The temperature raise is necessary for the KPS to dissociate and the reaction to start. The reaction is stopped after 2 hours and the solution is centrifuged.

The schematic process is described in Figure 2.4.

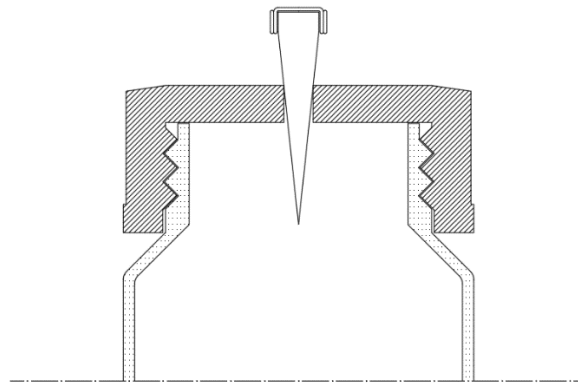


Figure 2.3. Reactor's cover modification. This solution guarantee an open access to inject the reactants without a substantial change of the reactor's atmosphere. When a component has to be injected, the micropipette tip is removed, the component is injected and then the tip is placed again.

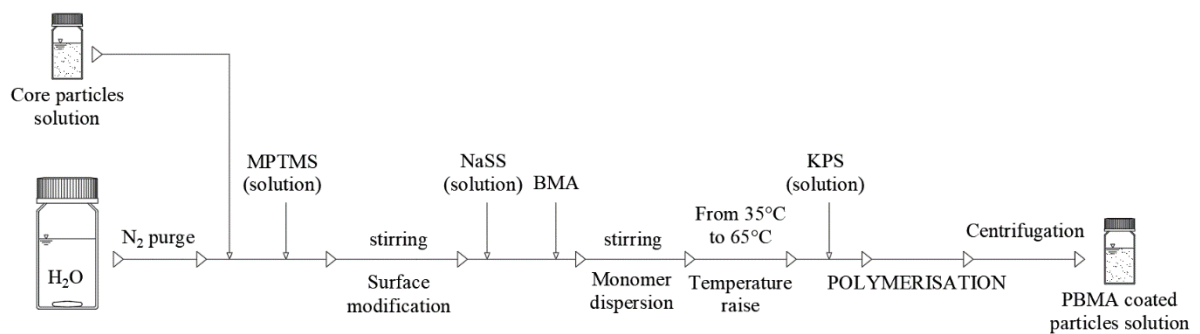


Figure 2.4. Scheme of reaction process.

The solvent is water and it is calculated so that the total volume sums up to the reaction volume of 30 ml. Before the injection in the reactor, the MPTMS is dissolved in 1 ml of ethanol, the NaSS in 1 ml of water and the KPS in 5 ml of water. The core particles solution is a solution of water containing the core particles in a concentration of 1.5 %_{vol} ($\text{vol}_{\text{part.}}/\text{vol}_{\text{solvent}}$). The main parameters of the reaction system and the composition in the reactor are described in Table 2.10, 2.11 and 2.12.

Table 2.10. Main reaction parameters.

Parameter	Value	Unit
Reaction volume	30	ml
Room temperature	35	°C
Polymerisation temperature	65	°C
Surface modification time	30	min
Monomer dispersion time	1	h
Polymerisation time	2	h

Table 2.11. Reactor composition. Concentrations refer to the reaction volume.

Component	Concentration, mol/l
Core particles	0.15(% _{vol})
MPTMS	0.002
BMA	0.20
NaSS	0.001
KPS	0.002

Table 2.12. A description of the solvents used to dissolve some components of the reaction system.

Component	Solvent	Volume, ml
Core particles	Water	3
MPTMS	Ethanol	1
NaSS	Water	1
KPS	Water	5

2.2.3 Shells

Once the core particles are coated with the PBMA/MPTMS layer, it is possible to perform a second polymerisation to produce the eccentric polystyrene shell.

The goal of this part was to study the interaction of the various reaction parameters with the polymerisation.

The reaction system is composed of only four components (five when the dye is added to the process):

1. *Solvent:* Water.
2. *Core particles:* PBMA/MPTMS coated silica particles.
3. *Monomer:* Styrene (insoluble in the solvent).
4. *Initiator:* KPS.
5. *(Dye:* Pyrene).

The process consists in:

1. *Preparation of the reaction solution and reactor.* This part is equal to the one described for the previous process. The solvent, water, is introduced in the reactor and then it is purged with nitrogen for 30 minutes to remove the oxygen that can interfere with the polymerisation. To avoid a further significant contamination during the injection of the other reactants, the cover is pierced with a drill and a micropipette's tip is placed in the hole and covered with laboratory film as shown in Figure 2.3. The particles solution is then injected in the reactor and the reactor is placed in the isothermal water bath at room temperature and over the magnetic stirrer.
2. *Injection of the monomer (and the dye).* The monomer, styrene, is injected in the reactor and the mixing proceeds for at least 1 h. This time is necessary for the system to reach its fluid dynamic equilibrium, for the monomer to saturate the solvent and for the polymeric layer that cover the core particles to absorb the monomer. The water bath is kept at room temperature, which is 35°C. When the process includes also the introduction of a fluorescent dye, the dye, pyrene (a powder), is dissolved in the liquid monomer and then everything follows in the same way as without the dye.
3. *Reaction.* The temperature of the isothermal bath is raised to 65 °C and the solution containing the initiator (KPS), is injected in the reactor. The temperature raise is necessary for the KPS to dissociate and the reaction to start.

The schematic process is described in Figure 2.5.

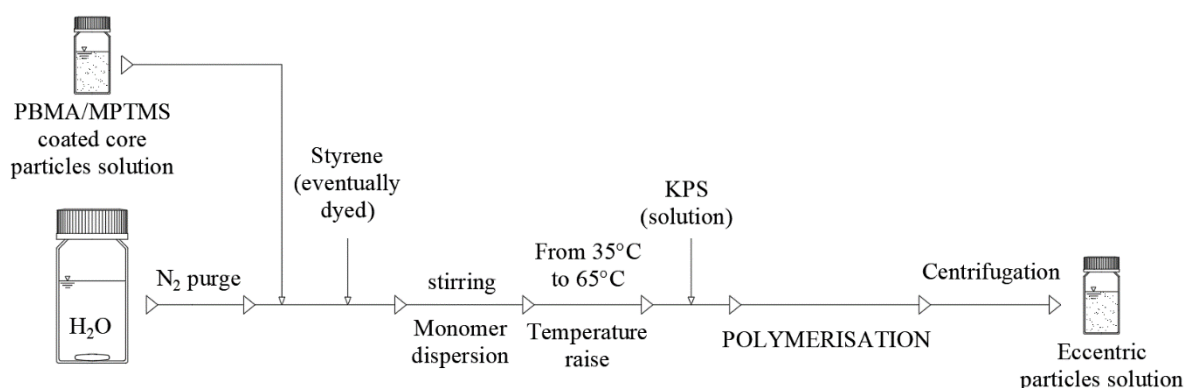


Figure 2.5. Scheme of reaction process.

The polymerisation is performed in small batch reactors with a reaction volume of 30 ml. Mixing is realized, as for the other steps, with a magnetic stir bar moved by a magnetic stirrer. This condition implies that the mixing power transferred to the solution is not strong enough to create the conditions of a typical emulsion polymerisation where the oil phase is finely dispersed in the solvent and the little

drops of monomer can be ideally described as micrometric batch reactors. On the contrary, in this particular case, it is more convenient to consider that the polymerisation occurs in solution and in the polymeric layer that cover the core particles as it would be in a CSTR reactor with a constant, low monomer concentration. When the monomer is injected in the reactor, a first transient condition in which the oil phase is dispersed occurs. After a while, the difference in density between the monomer and the solvent makes the monomer migrate to the surface of the water and the drops coalesce. When the system reaches its fluid dynamic equilibrium the styrene is present in three different state: in the oil phase floating above the water, dissolved in the solvent and absorbed in the thin PBMA/MPTMS layer on the particles. This condition is described in Figure 2.6. The oil phase, in this situation, acts as a “storage” of monomer and is slowly consumed during the reaction to compensate the amount of styrene that reacts. This assumption is confirmed by the fact that the solution in the reactor is not as turbid as it should be if the monomer was finely dispersed and the two phases are easily recognizable one over the other thanks to their different refractive index.

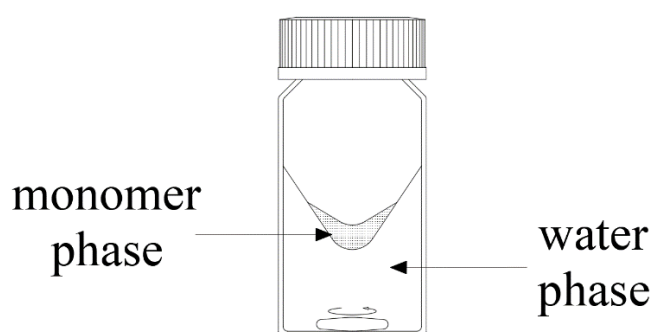


Figure 2.6. A scheme of the phase separation in the reactor.

For this reason, the injection of the initiator should follow a specific procedure. If it were injected directly from the hole in the reactor’s cover as all the other components, the oil phase would be mixed again breaking the equilibrium obtained previously and since the styrene is placed on top of the water, it would enter the system passing through the monomer and, consequently, interacting directly with it. If something like this happens there is the possibility that, locally, portions of solution at high initiator concentration interact with portions of solution at high monomer concentration. This situation will not create big problems most of the times and the equilibrium can be reached again shortly, but sometimes it can produce instability in the colloidal system with a consequent malfunctioning in the polymerisation. For this reason, the initiator is injected directly below the water surface using a Pasteur pipette. With this procedure, the fluid dynamic of the system is not disrupted and the process is more stable, which gives a significant increment in the reproducibility. The procedure is described in Figure 2.7.

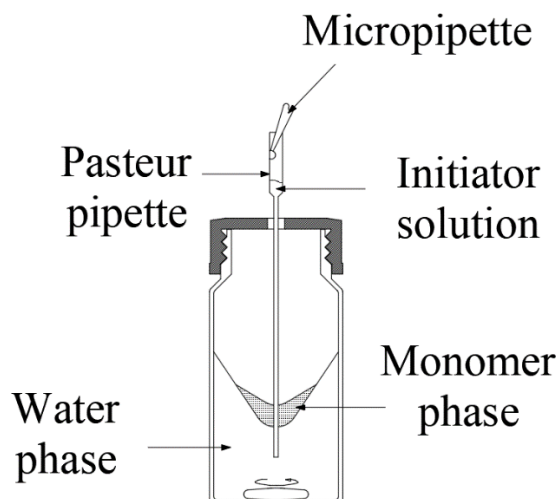


Figure 2.7. A scheme describing the procedure for the injection of the initiator solution under the oil phase.

The main parameters of the reaction process are summarized in Table 2.13. The core particles solution is a solution of water containing the PBMA-coated core particles in a concentration of 0.45 %_{vol} ($\text{vol}_{\text{part.}}/\text{vol}_{\text{solvent}}$). The amount of water used to dissolve the KPS is 5 ml.

Table 2.13. Main reaction parameters.

Parameter	Value	Unit
Reaction volume	30	ml
Room temperature	35	°C
Polymerisation temperature	65	°C
Monomer dispersion time	1	h
Polymerisation time	Variable	h

Many parameters were tested and analysed to determine their influence on the process:

- Presence of the **PBMA layer**.
- **Styrene** concentration.
- Reaction **time**.
- Presence of an **electrolyte**.
- **Mixing velocity**.
- **Core particles** concentration.

The experiments proceeded as follows:

In order to prove the effective necessity of a first **PBMA coating**, the experiment 112 was made without it. The process was modified to reduce the two steps into one. Starting from the procedure to coat the particles with the PBMA, the following changes were made:

1. The comonomer NaSS was not used.
2. The monomer was Styrene.
3. The polymerisation time was increased to 15 h.

The scheme of the modified process is shown in Figure 2.8 and the experimental conditions were as shown in Table 2.14.

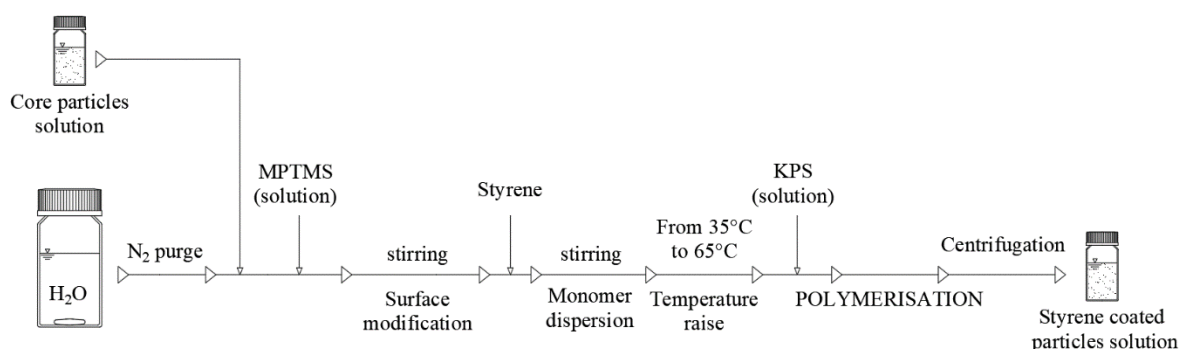


Figure 2.8. A scheme of reaction process for Run 112.

Table 2.14. Reactor composition of Run 112. Concentrations refer to the reaction volume. The core particles solution is the same as for the experiments for the PBMA coating. The solvent is water.

Component	Concentration, mol/l
Core particles	0.01 (%vol)
MPTMS (Coupling agent)	0.001
Styrene (Monomer)	0.10
KPS (Initiator)	0.002

Multiple samples were prepared to analyse the influence of the **styrene** concentration and the **polymerisation time** on the particles' diameter.

- *Runs from 84 to 88:* at low styrene concentration with 5 h reaction time.
- *Runs from 96 to 101:* at high styrene concentration with 5 h reaction time.
- *Runs from 104 to 109:* at high styrene concentration with 15 h reaction time.
- *Runs 119, 120 and 121:* at intermediate styrene concentration with 24h reaction time.

The solvent was water. The concentration of KPS was equal to 2 mM for all the samples. The particles concentration was equal to 0.01%_{vol} ($\text{vol}_{\text{part.}}/\text{vol}_{\text{solvent}}$). The other conditions are described in Table 2.15.

Table 2.15. Reaction conditions analysed to compare the effect of the styrene concentration and the reaction time.

Run	[St], mol/l	Reaction time, h
84	0.01	5
85	0.025	5
86	0.05	5
87	0.10	5
88	0.15	5
96	0.30	5
97	0.35	5
98	0.40	5
99	0.45	5
100	0.50	5
101	0.60	5
104	0.10	15
105	0.20	15
106	0.30	15
107	0.40	15
108	0.50	15
109	0.60	15
119	0.10	24
120	0.15	24
121	0.20	24

The introduction of an **electrolyte** in the reaction system lowers the permittivity of the water and should reduce the formation of the secondary particles (particles containing only polystyrene and not incorporating a silica core). During the nucleation phase the secondary particles, with the introduction of an electrolyte, should be less stable and, consequently, should aggregate to the particles containing the silica core, already big enough to be stable on their own. The production of secondary particles is a monomer-wasting process and, therefore, the diameter of the eccentric particle should be affected by it. Unfortunately, the introduction of an electrolyte in high concentrations can generate instability in the system. For this reason run 116 and 117 were made with the introduction of NaCl and compared with experiments in similar conditions without the electrolyte.

The concentration of KPS was equal to 2 mM for all the samples. The particles concentration was equal to 0.01%_{vol} ($\text{vol}_{\text{part.}}/\text{vol}_{\text{solvent}}$). The solvent was water. The reaction time was 15 h. The other conditions are listed in Table 2.16.

Table 2.16. Reaction conditions of runs 116 and 117.

Run	[St], mol/l	[NaCl], mol/l
116	0.10	0.01
117	0.20	0.01

The **fluid dynamic** of the system has a major relevance in the process because it controls the mass transport and, therefore, the reaction rate.

Even though with the magnetic stirrer available for the experiments it was not possible to control directly the number of rotations per minute of the magnetic stir bar, it was somewhat possible to modify its rotation speed.

With these considerations, three different fluid dynamic conditions were tested:

- *Run 124.* Minimum mixing velocity. The magnetic stirrer was set to its minimum. The magnetic bar was not rotating fast enough to induce a vortex in the reactive solution.
- *Run 125.* Medium mixing velocity. The velocity was increased until the vortex induced in the solution was significantly deep, but still not deep enough for its bottom to reach the moving magnetic bar. This is the maximum acceptable mixing velocity to keep the same fluid dynamic conditions described in Figure 2.6.
- *Run 126.* Maximum mixing velocity. The magnetic stirrer was set to its maximum. The bottom of the vortex reached the magnetic bar and the all the three phases in the reactor (hydrophilic, hydrophobic and the gas) were mixed together deeply.

A visual explanation of these conditions is shown in Figure 2.9 and the main concentrations are shown in Table 2.17.

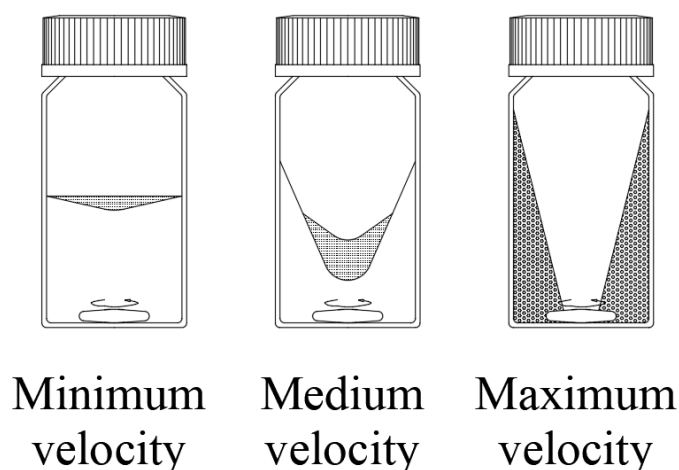


Figure 2.9. A visual description of the fluid dynamic conditions at different mixing velocity.

Table 2.17. Reaction conditions of runs 124, 125 and 126.

Run	[St], mol/l	[Py], mol/l	KPS, mol/l	Core particles, % _{vol}
124-125-126	0.10	0.002	0.002	0.01

One of the possible limiting factor in the polymerisation could have been the **core particles concentration**. Under the assumption of complete conversion of the monomer and negligible production of secondary particles, the cores concentration is an important factor to control the diameter of the shell. The same amount of polystyrene would split over a bigger or smaller quantity of cores and thus would generate a thinner or thicker shell respectively. However, this is just a prediction made under the ideal assumption of a negligible production of secondary particles, assumption that is way far from the real process. For this reason, a set of experiments was made to analyse if the cores concentration could affect the shell thickness even with the production of a big number of secondary particles.

The solvent was water, the KPS concentration was 2 mM and the pyrene concentration was 2 mM. The concentrations of the styrene and of the core particles are shown in Table 2.18.

Table 2.18. Styrene and cores concentration for runs 170 to 175.

Run	[St], mol/l	Core particles, % _{vol}
170	0.1	0.005
171	0.1	0.01
172	0.1	0.02
173	0.2	0.005
174	0.2	0.01
175	0.2	0.02

The fluorescent dye used to colour the shell in this work is pyrene. The first experiment in which it was used was the number 123. After the sample 123 all the other experiments were performed introducing the dye. Its concentration was chosen to be 2%_{mol} (respect to the styrene) as it was described by Tamai *et al.*^[13] for all the experiments. The dye was dissolved in the liquid monomer and injected in the reactor with no other specific procedures.

For run 123 the solvent was water and the other concentrations are described in Table 2.19.

Table 2.19. Reaction conditions of run 123.

Run	[St], mol/l	[Py], mol/l	KPS, mol/l	Core particles, % _{vol}
123	0.10	0.002	0.002	0.01

2.3 Characterisation and instrumentations

The particles were analysed using a transmission electron microscope (FE-STEM) model HD-2700 Type B from Hitachi, Japan.

Small quantities of the solutions obtained in the experiments were dropped on copper grids suitable for TEM observation and placed over blotting paper to let them dry before the observation.

The ζ -potential was measured using the machine for the Electrophoretic Light Scattering (ELS), model ELSZ-2 from Otsuka Electronics Co., Japan.

For the experiments concerning the production of the silica cores at least 200 particles were measured to determine the number-averaged diameter d_n , the volume-averaged diameter d_v , the standard deviation σ , and the polydispersity (Coefficient of variation) C_v , defined as follows:

$$d_n = (\sum n_i d_i / \sum n_i) \quad (2.1)$$

$$d_v = (\sum n_i d_i^3 / \sum n_i)^{1/3} \quad (2.2)$$

$$\sigma = (\sum (d_i - d_n)^2 / \sum n_i)^{1/2} \quad (2.3)$$

$$C_v = \frac{\sigma}{d_n} \cdot 100 \quad (2.4)$$

Where n_i is the number of particles with diameter d_i .

For the experiments concerning the PBMA coating no measurement of diameter was conducted because the polymeric layer is too thin and its thickness was not a parameter of valuable importance in this work. For the experiments on the production of the polystyrene shell only a rough measure of the diameter was given because no significant trend was detected that would require a more precise measure.

Some samples of the silica cores were observed under a confocal microscope model C2si from Nikon, Japan, to detect the fluorescence of the RITC. The excitation wavelength of the laser used for the observation was 561 nm.

The eccentric particles were not observed under the confocal microscope because the pyrene has an excitation wavelength of 350 nm and, in the confocal microscope, the minimum achievable wavelength is 405 nm.

However, the fluorescence of the pyrene was visually observed from Run 123 under a UV lamp Spectroline model ENF-240 C/J, U.S.A. with a wavelength of 365 nm and compared with other samples that did not incorporate the pyrene.

The effective incorporation of the pyrene inside of the shell was detected with a measurement of the fluorescence spectra of Run 123 using a fluorometer model F700 from Hitachi, Japan, using an excitation wavelength of 350 nm.

Pictures of the particles incorporating the two dyes were kindly provided by the researchers in the ETH of Zurich.

3 Results and discussions

3.1 Core particles

3.1.1 Injection delay

The first set of experiments, runs from I to V, was conducted to analyse the influence of an eventual delay between the injection of the dye solution and the TEOS solution, which corresponds to the beginning of the reaction. Figure 3.1 shows the particles after the coating with the first only-silica layer.

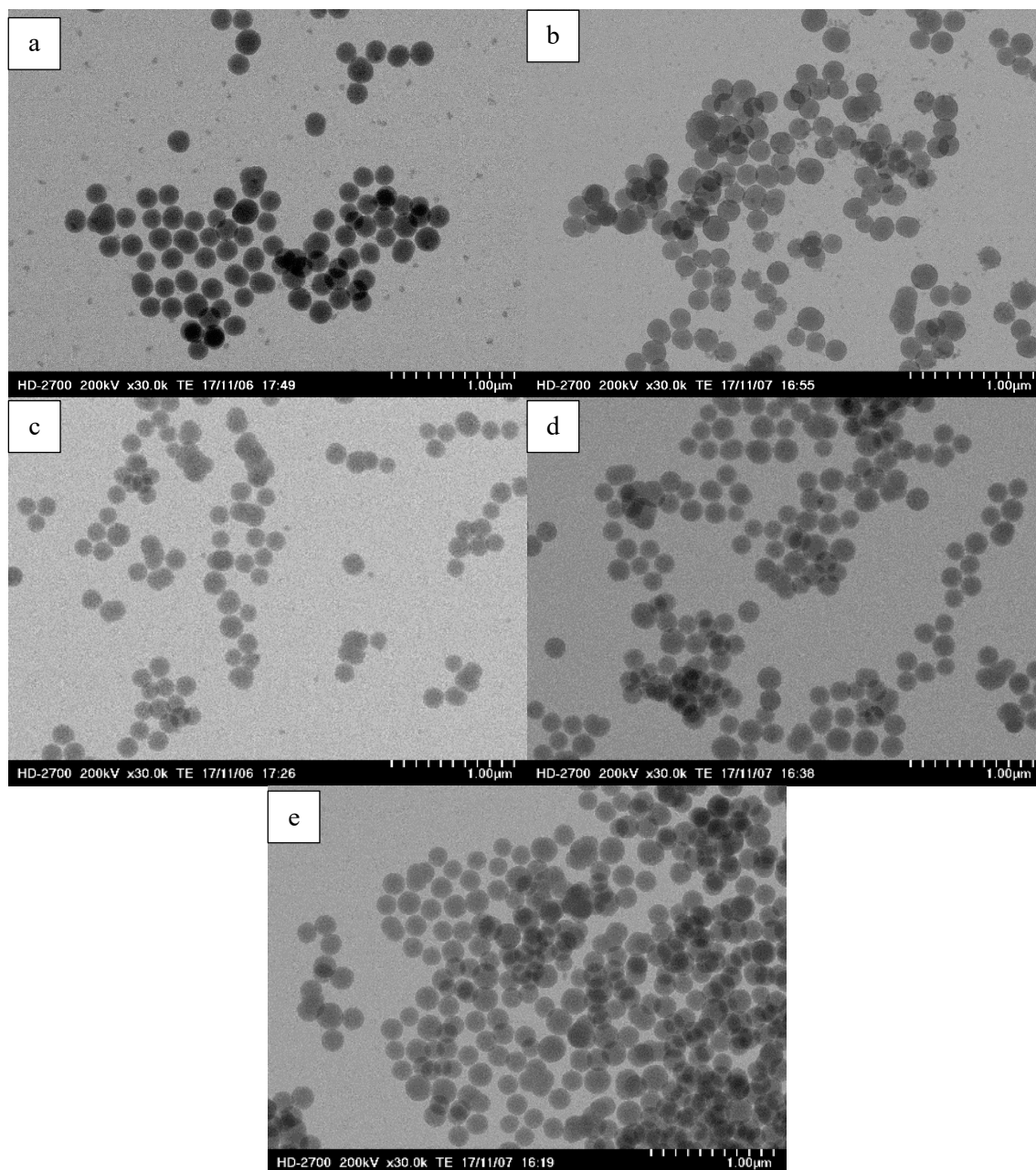


Figure 3.1. TEM images of particles after the first only-silica coating. The solution containing the RITC was injected, respect to the TEOS solution, with a delay of : (a) 6 min, (b) 7 min, (c) 8 min, (d) 9 min, (e) 10 min. All bars are 1 μm.

As it could be seen in Figure 3.2 and in Table 3.1, there is no significant change in the particles diameter when the injection delay increases from 6 min to 10 min. On the other hand, it is clear, from Figure 3.3 and Table 3.1, that the polydispersity of the system increases almost linearly.

This behaviour could be explained by the instability that the RITC brings into the colloidal system. The RITC is a non-charged molecule and when it enters into the silica lattice, the total charge of the surface decreases, reducing consequently also the absolute value of the ζ -potential. This will cause a lack in colloidal stability, which lead to severe aggregation between the particles already formed. If the concentrations of ammonia, water and TEOS remain the same for all the samples, it is plausible to assume that, statistically, there will be the same number of nucleation in each reactor and, in the same way, if the RITC concentration is the same, almost the same number of collision that will lead to an aggregation will occur. Considering these assumptions, one can make some considerations. The total number of particles remained the same (between different runs) even after the aggregation, and the total amount of silicon that could be converted into silica did not change too. Since the same volume of silica was divided into the same number of particles the final average diameter would be almost the same. On the other hand, a lower delay correspond to collisions between smaller, non-well developed particles, which means that the resultant particles distribution after the complete reaction will be more homogeneous.

Considering these results, it was chosen to inject the dye solution after one minute from the beginning of the reaction, and, later, they were injected consequently, with no delay, to reduce as much as possible the polydispersity of the system.

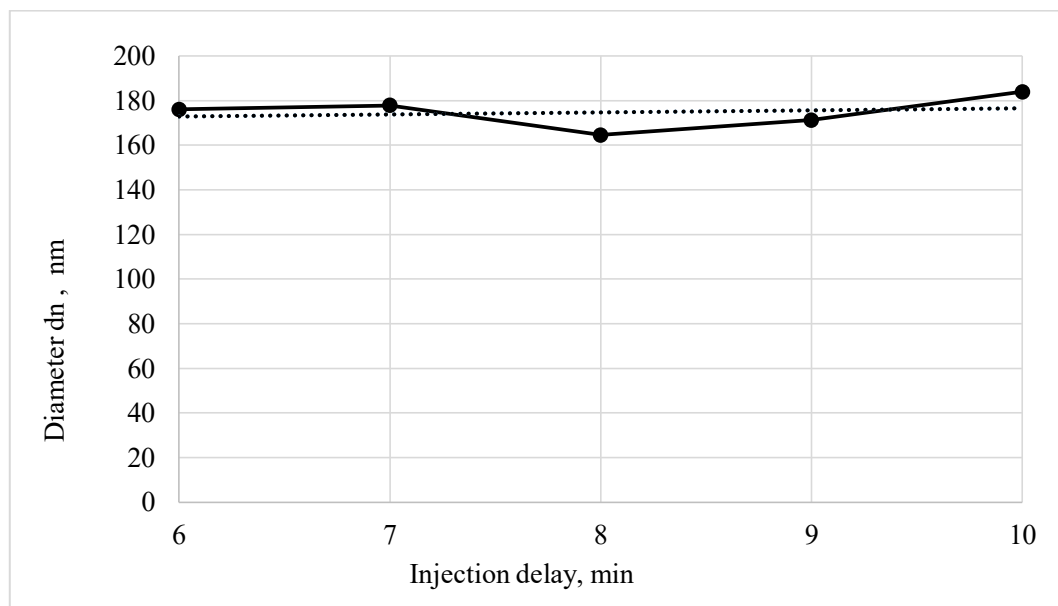


Figure 3.2. Relationship between the diameter d_n and the time elapsed between the injection of the TEOS solution and the RITC solution in the reactor.

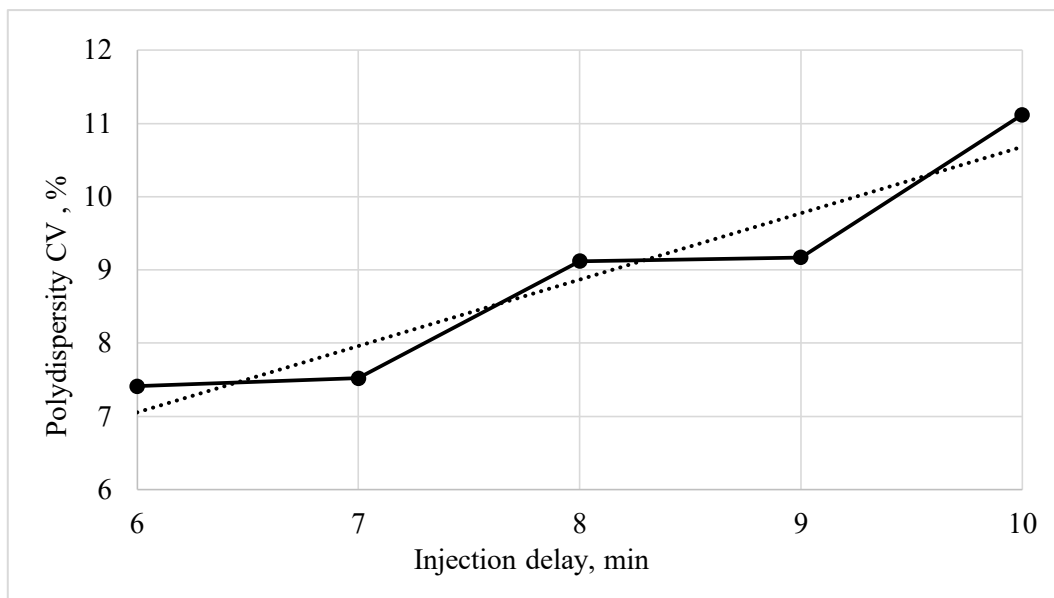


Figure 3.3. Relationship between the polydispersity, C_V , and the time elapsed between the injection of the TEOS solution and the RITC solution in the reactor.

Table 3.1. Calculated values of d_n and C_V of runs I, II, III, IV, V.

Run	Delay, min	d_n , nm	C_V , %
I	6	176.0	7.4
II	7	177.8	7.5
III	8	164.5	9.1
IV	9	171.2	9.2
V	10	183.9	11.1

3.1.2 Eventual silica coating

Data obtained from the ζ -potential measurements gave information on the effect of eventual only-silica additional coating. Samples VI to IX were analysed to determine the average value of the ζ -potential in the presence of one and two layers, samples 26, 27, 30 and 31 for particles not coated and the set of samples 68-73 gave the reference for pure silica particles. The values are summarised in Table 3.2. The ζ -potential was measured three times for each sample, then the average, ζ_{ave} , was calculated and then the overall average, describing the characteristic potential of a typology of particle, $\zeta_{ave,o}$, was calculated as the average of the averages.

As it can be seen in Table 3.2, the characteristic potential of pure silica is around -55 mV. When RITC is added to the particles and no coating is performed, it becomes less than half, and in some cases even one fourth (-13 mV and -14 mV for runs 27 and 31 respectively). In these conditions, the strength of the electric field is too weak to protect the particles from aggregation. On the other hand, values of the potential for particles coated with one and two layers (-51 mV in both cases) resembles quite perfectly those of the particles without RITC. First of all, this is a sign that an additional layer is effectively increasing the stability of the system and that the RITC that remain in the reactor during the coating process do not interfere with the reaction, as it was anticipated by Verhaegh and van Blaaderen^[9]. Furthermore, it is clear that one layer is sufficient to protect the particles and therefore the second layer is not needed.

Table 3.2. Measurements of ζ -potentials and relative averages.

Layers	Run	ζ_1 , mV	ζ_2 , mV	ζ_3 , mV	ζ_{ave} , mV	$\zeta_{ave,o}$, mV
-	68	-50.93	-54.06	-53.51	-52.83	-55.57
	69	-57.02	-57.51	-56.31	-56.95	
	70	-55.83	-54.69	-52.10	-54.21	
	71	-58.15	-58.96	-57.02	-58.04	
	72	-55.93	-56.74	-59.04	-57.24	
	73	-54.12	-56.21	-52.00	-54.13	
0	26	-30.19	-28.78	-30.77	-29.91	-24.46
	27	-10.97	-13.57	-15.14	-13.23	
	30	-42.17	-39.54	-39.11	-40.27	
	31	-16.13	-13.25	-13.85	-14.41	
1	VI	-51.28	-46.13	-47.72	-48.38	-51.59
	VII	-55.92	-54.30	-53.03	-54.42	
	VIII	-52.50	-46.01	-50.12	-49.54	
	IX	-57.93	-57.77	-57.90	-57.87	
2	VI	-53.80	-54.12	-52.61	-53.51	-51.49
	VII	-54.34	-57.30	-54.18	-55.27	
	VIII	-48.87	-46.14	-42.04	-45.68	

3.1.3 Ammonia concentration

Experiments VI, VII, VIII and IX determined the influence of the ammonia concentration on the diameter and the polydispersity of the particles. Pictures of the particles are shown in Figure 3.4 and results are summarised in Table 3.3, in Figure 3.5 and Figure 3.6.

The average diameter has, at least for the low concentrations in exams, a linear dependence over the concentration of ammonia and when the latter doubles, also d_n doubles as it was shown by Stöber *et al.*^[6] too, and it is actually a possible way to control the diameter. Unfortunately, as it can be seen in Figure 3.4 or in the diagram in Figure 3.6, the polydispersity of the system increases more than linearly with the ammonia and this is caused by the aggregation that occur at relative high concentrations. It is clear that particles are aggregated and were not the result of a different growing velocity because the bigger particles are not in spherical shape, but tend to look like the assembly of hemispheres.

For this reason, for all the subsequent experiments the concentration of ammonia was fixed to 0.6 M since, in this part of the study, a low polydispersity was more important than a bigger diameter.

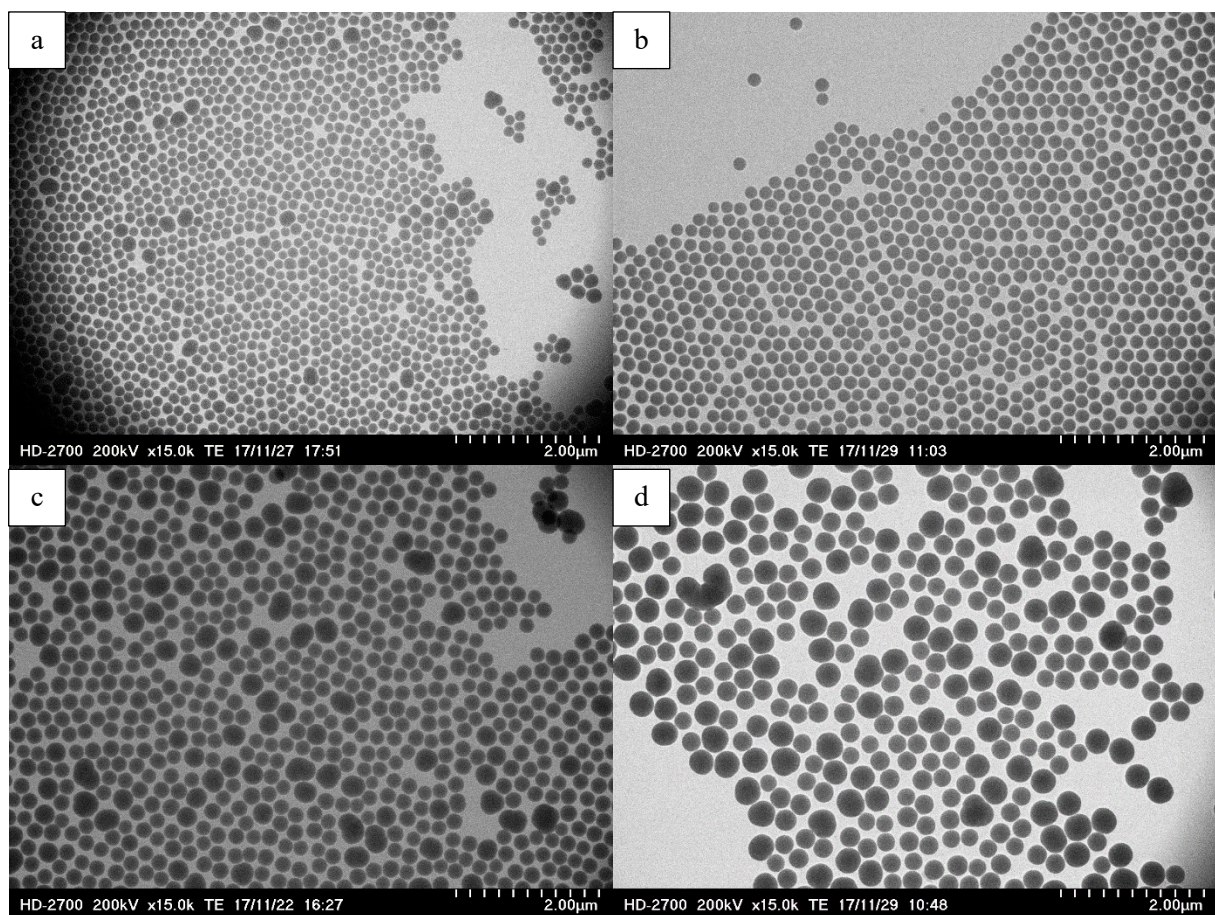


Figure 3.4. TEM images of particles grown in solutions with an ammonia concentration of: a) 0.6 M, b) 0.8 M, c) 1.0 M, d) 1.2 M. Pictures were taken after the first silica coating. All bars are 2 μm .

Table 3.3. Calculated values of d_n and C_v of samples VI, VII, VIII, IX.

Run	[NH ₃], mol/l	d_n , nm	C_v , %
VI	0.6	139.9	6.0
VII	0.8	173.1	6.4
VIII	1.0	214.8	7.8
IX	1.2	274.9	10.8

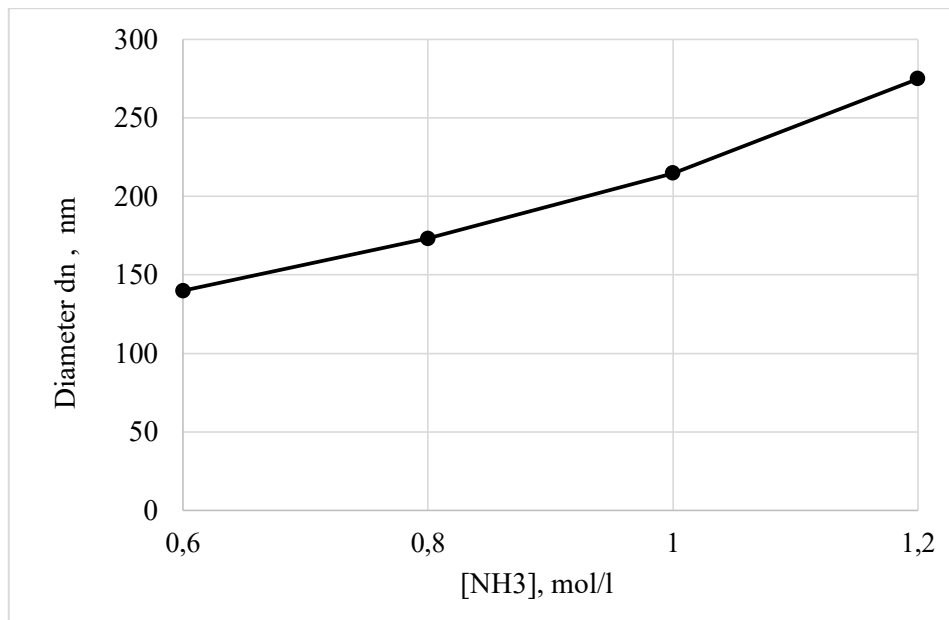


Figure 3.5. Relationship between the diameter d_n and the ammonia concentration in the reactor.

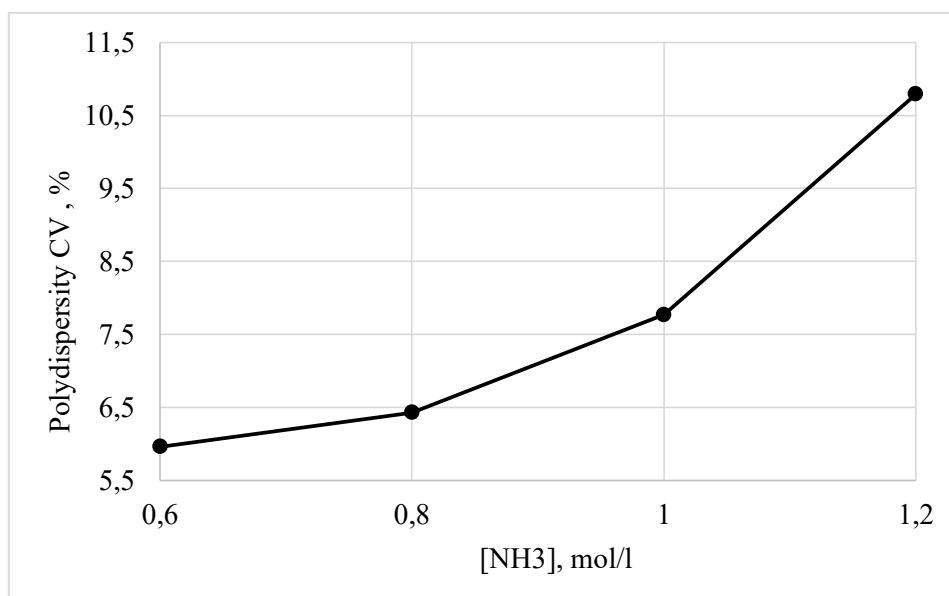


Figure 3.6. Relationship between the polydispersity, C_v and the ammonia concentration.

3.1.4 Water and TEOS concentrations

Experiments 1 to 8 and 18 to 25 gave information on the effect of the water and TEOS concentrations. Values shown in Tables 3.4 and 3.5 and in Figures 3.7 and 3.8, are in good accordance with the trends given by Stöber *et al.*^[6].

The TEOS concentration shows almost no influence in both the diameter and the polydispersity while the water concentration is the main factor over which it is possible to control the particles diameter. At low H₂O concentration the silicate cannot hydrolyse and therefore the silicic acid cannot condense forming the silica that builds the particles. Increasing the water content, the diameter increases until it reaches a maximum (around 500 nm) and then starts to decrease again, as it is shown in Figure 3.7. For values of [H₂O] between 3 M and 7 M, approximately, d_n over [H₂O] is linear enough to allow a good control of the diameter by simple interpolation.

TEM images of the particles are shown in Figures 3.9 and 3.10.

Table 3.4. Calculated values of d_n and C_V of samples 1 to 8.

Run	[H ₂ O], mol/l	[TEOS], mol/l	d_n , nm	C_V , %
1	1.7	0.32	35.9	12.2
2	1.7	0.24	32.2	13.7
3	1.7	0.16	44.5	12.0
4	2.55	0.32	77.1	18.6
5	2.55	0.24	79.0	14.6
6	2.55	0.16	85.1	8.2
7	3.4	0.32	120.9	9.3
8	3.4	0.24	123.7	12.0

Table 3.5. Calculated values of d_n and C_V of samples 18 to 25.

Run	[H ₂ O], mol/l	[TEOS], mol/l	d_n , nm	C_V , %
18	5.1	0.16	271.9	5.1
19	5.1	0.32	258.8	7.9
20	6.8	0.16	467.0	9.7
21	6.8	0.32	463.1	12.3
22	8.5	0.16	512.4	7.4
23	8.5	0.32	513.0	3.7
24	10.2	0.16	486.6	4.7
25	10.2	0.32	485.5	2.4

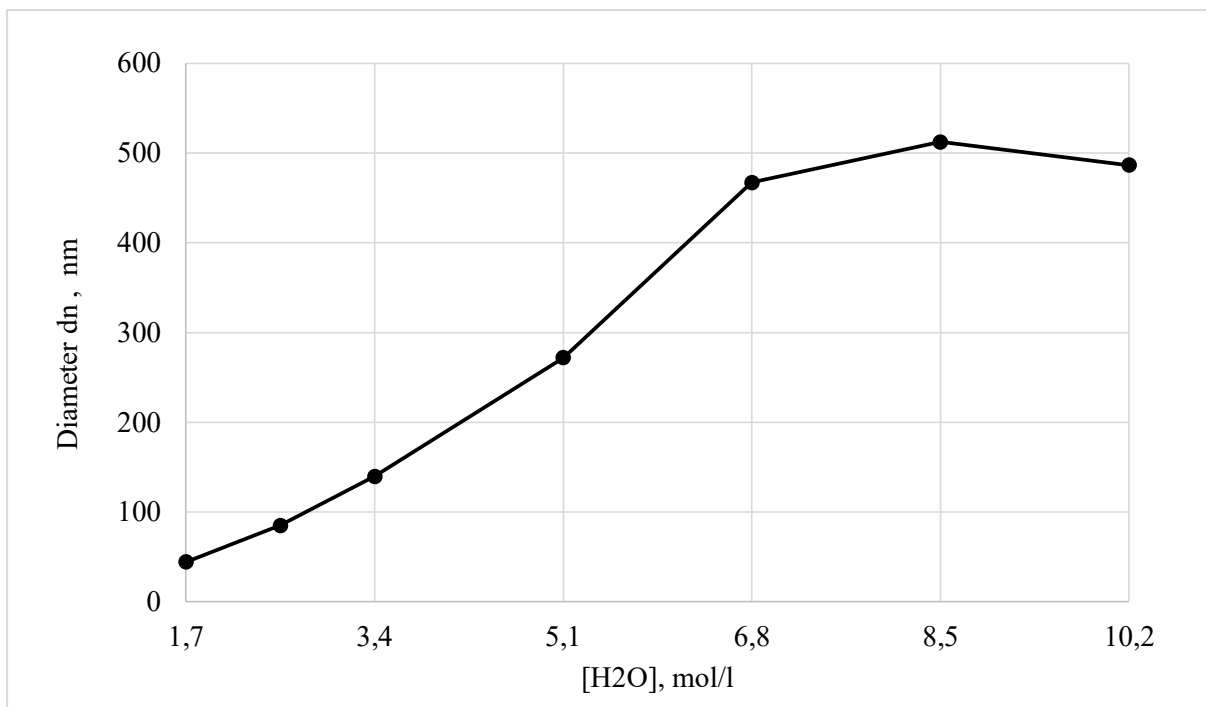


Figure 3.7. Relationship between the diameter d_n and the water concentration at the fixed TEOS concentration of 0.16 mol/l.

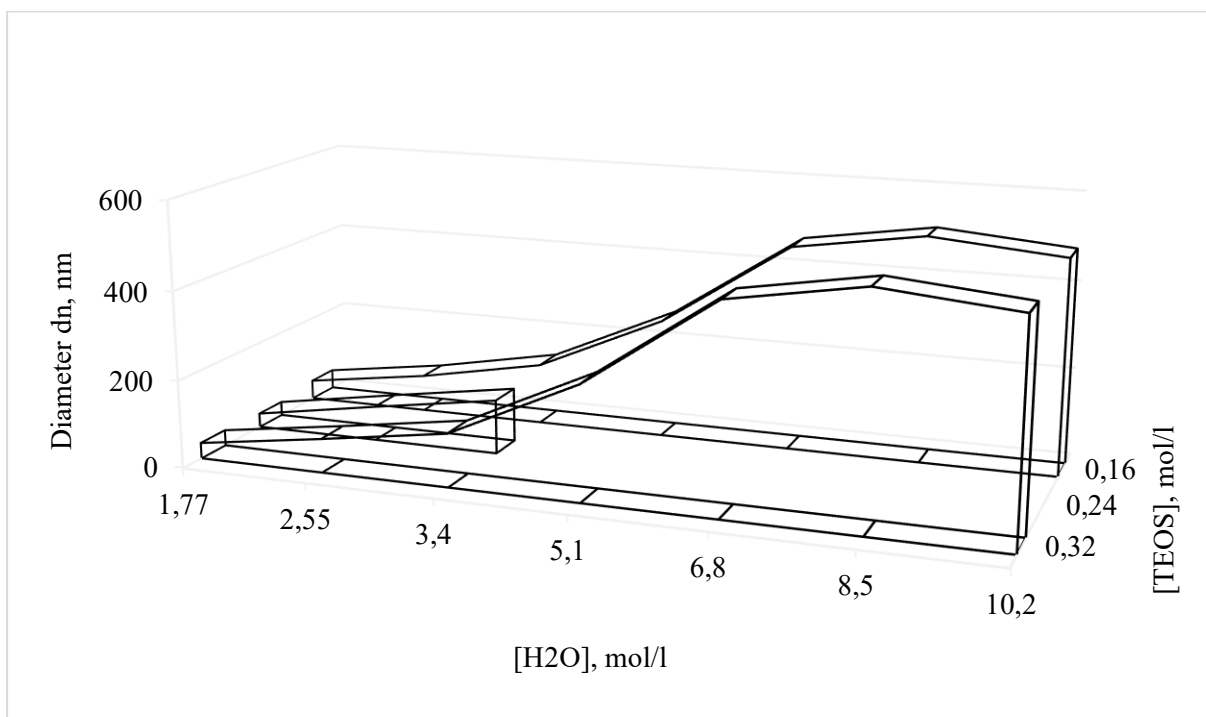


Figure 3.8. Three axis diagram showing the almost negligible influence of the TEOS concentration on the diameter d_n .

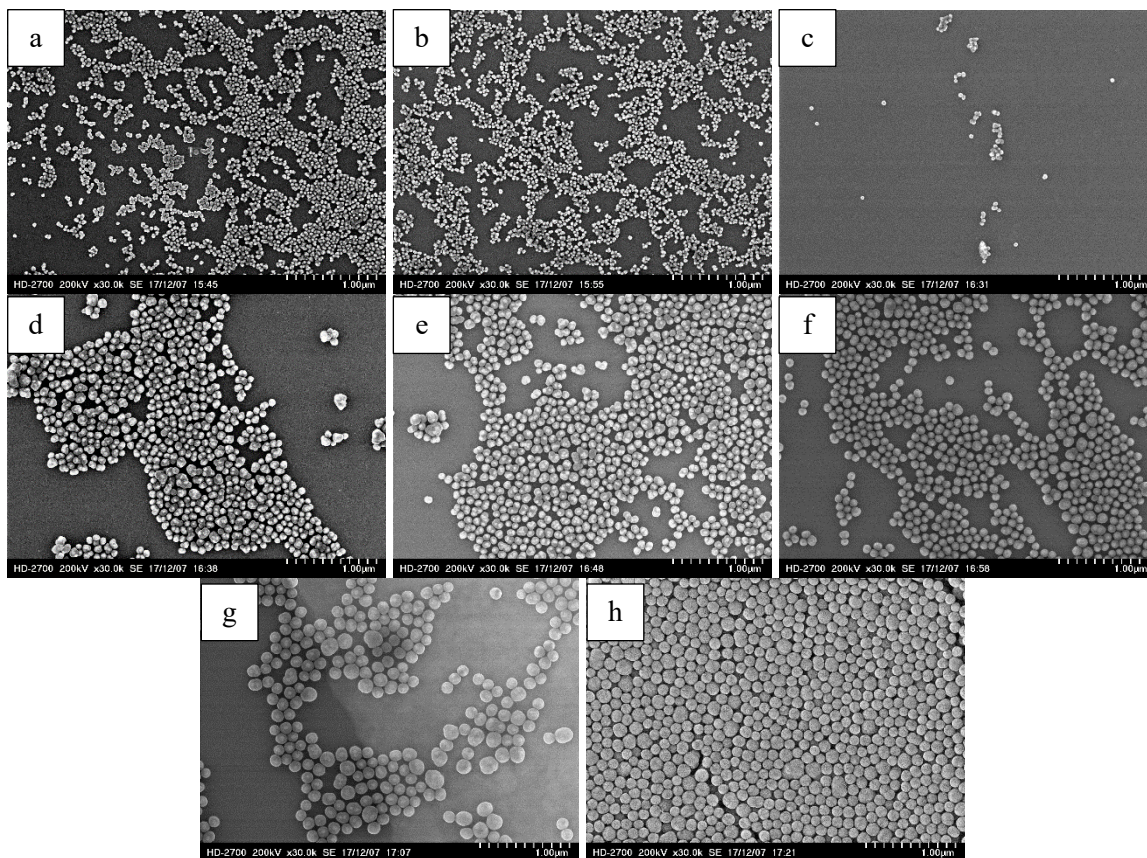


Figure 3.9. SEM images of runs from 1 to 8: $[\text{H}_2\text{O}] = 1.7 \text{ M}$ for a, b and c; $[\text{H}_2\text{O}] = 2.55 \text{ M}$ for d, e and f; $[\text{H}_2\text{O}] = 3.4 \text{ M}$ for g and h. $[\text{TEOS}] = 0.32 \text{ M}$ for a, d and g; $[\text{TEOS}] = 0.24 \text{ M}$ for b, e and h; $[\text{TEOS}] = 0.16 \text{ M}$ for c and f. All bars are $1 \mu\text{m}$.

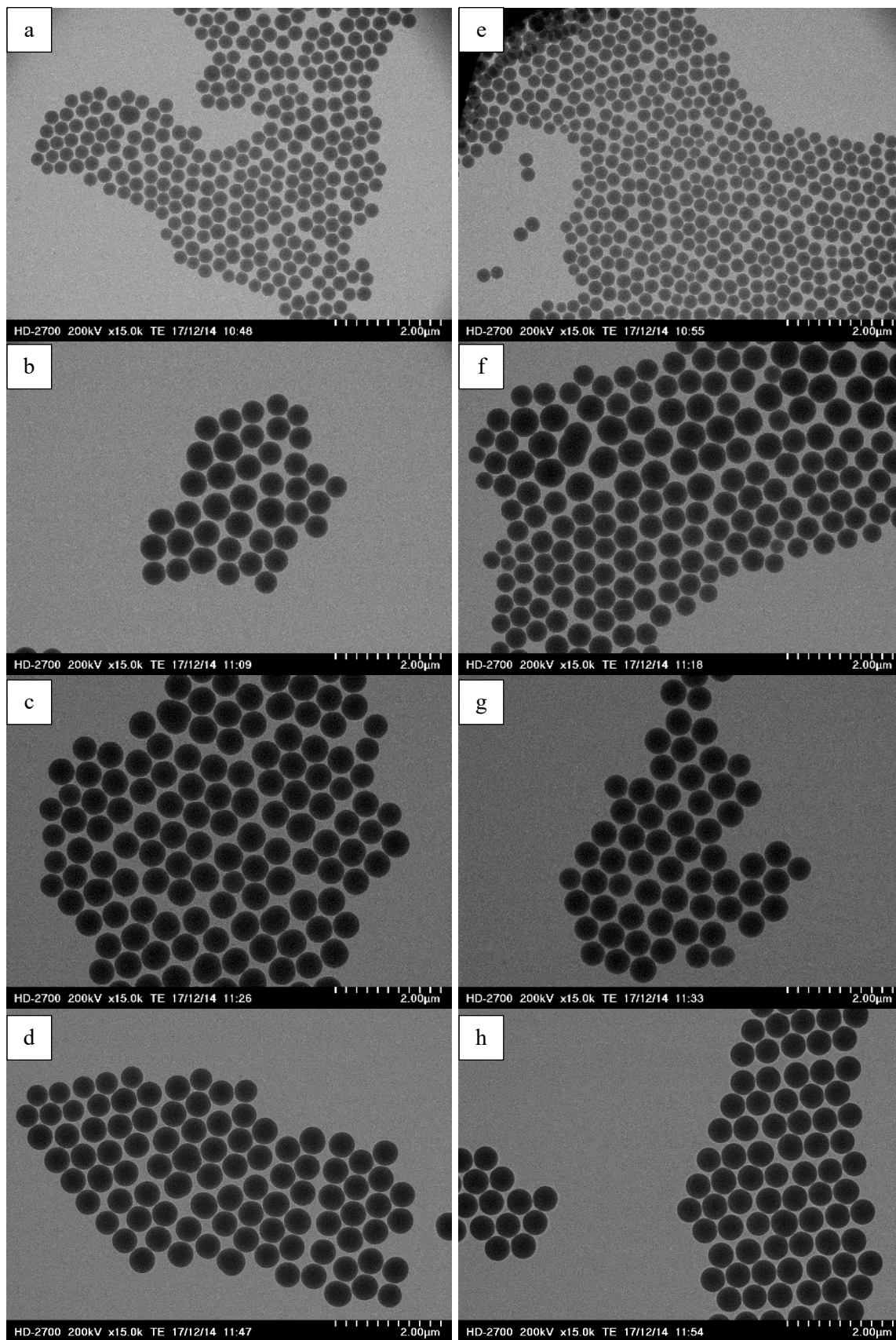


Figure 3.10. TEM images of runs from 18 to 25: [TEOS]=0.16 M for a, b, c and d; [TEOS]=0.32 M for e, f, g and h; [H₂O]=5.1 M for a and e; [H₂O]=6.8 M for b and f; [H₂O]=8.5 M for c and g; [H₂O]=10.2 M for d and h.

3.1.5 Reproducibility

To check the reproducibility of the process and to confirm the effective possibility to use the water concentration as a controlling parameter over the diameter, run 64 was made. The target diameter was 400 nm. From the interpolation between runs 18 ($d_n = 272$ nm, $[H_2O] = 5.1$ M) and 20 ($d_n = 467$ nm, $[H_2O] = 6.8$ M), the necessary water concentration was found to be 6.2 M, as shown below:

$$C_{target} = C_{18} + \frac{(C_{20} - C_{18})}{(d_{n,20} - d_{n,18})} \cdot (d_{n,target} - d_{n,18})$$

$$= 5.1 \frac{mol}{l} + \frac{(6.8 \frac{mol}{l} - 5.1 \frac{mol}{l})}{(467 nm - 272 nm)} \cdot (400 nm - 272 nm) \approx 6.2 \frac{mol}{l}$$

Ammonia concentration was 0.6 M and TEOS concentration was 0.18 M.

Figure 3.11 shows TEM images of the sample, Table 3.6 summarize values of d_n and C_v .

The obtained diameter is 401.4 nm and the polydispersity is close to 3%, which is the result of a very sharp particles distribution as seen in Figure 3.12. These results are not only a good indicator that the process has a high reproducibility, but confirm that water concentration is a good controlling parameter for the diameter and that in the linear region of the curve $d_n/[H_2O]$ a simple interpolation is enough to predict the final diameter.

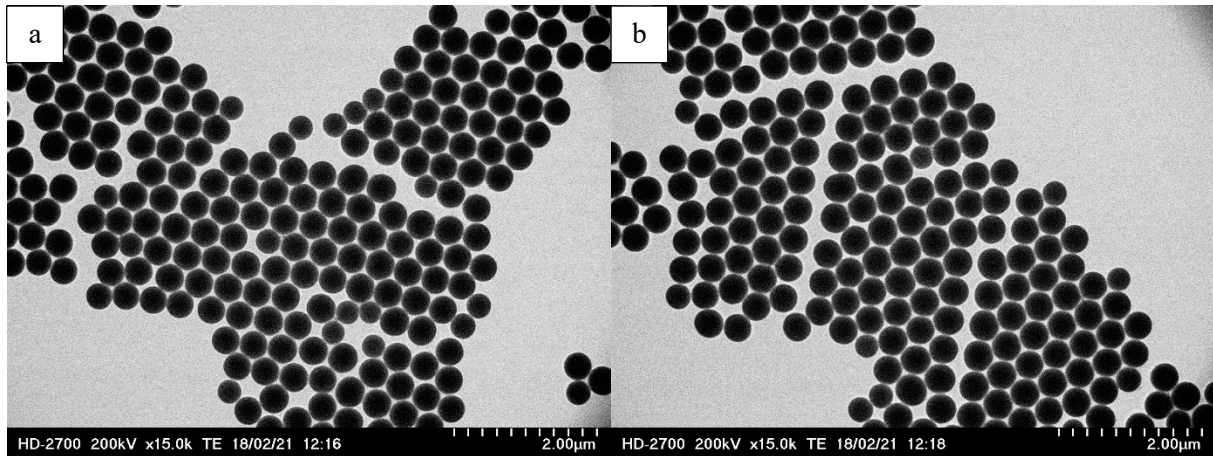


Figure 3.11. TEM images of run 64.

Table 3.6. Calculated values of d_n and C_v of samples 64.

Run	$[H_2O]$, mol/l	d_n , nm	C_v , %
64	6.2	401.4	3.2

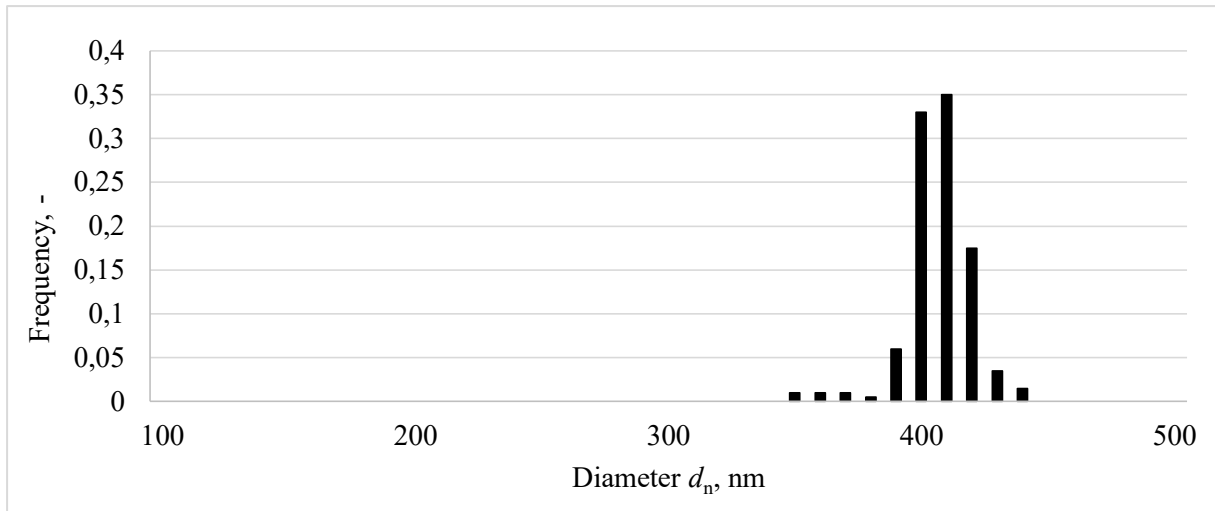


Figure 3.12. Particle size distribution of run 64, $d_n = 401.4$ nm and $C_V = 3.2\%$.

3.1.6 Reference with pure silica

The set of experiments 68 to 73 gave the reference with the process without the RITC. Results are summarized in Table 3.7 and Figure 3.13 while a comparison between fluorescent particles and pure-silica particles is shown in Figure 3.14.

The trend is in accordance with the one characteristic of the Stöber process^[6]. The diameter increases with water until it reaches a maximum and then decreases. The maximum is placed somewhere between $[\text{H}_2\text{O}] = 7 \text{ M}$ and $[\text{H}_2\text{O}] = 8 \text{ M}$ and correspond to a diameter around 320 nm.

It is interesting to notice in Figure 3.14 that the diameter of the fluorescent particles is always bigger than that of those without the dye. This means that the dye has an effective influence on the reactive system and that its introduction change significantly the process. The increment in the diameter can be explained quite well, again, by the instability that the RITC brings into the particles. In particular, if the particles are not stable during the nucleation process, aggregation will occur during the first part of the synthesis. If the nucleation is restricted to a limited, very short, time after the beginning of the reaction, and this is legit considering the narrow particle size distributions and the (relatively) low values of the polydispersity, then the total number of nuclei will be lower when the RITC is present in the reactor. In equal conditions of all the other parameters, a lower number of growing seed, with the same amount of silicon that converts to silica means a bigger volume per particles and therefore a bigger diameter.

Another factor that can explain the increment in the diameter is the volume occupied by the coupled RITC/APTES in the silica lattice. This compound has, obviously, its own volume that will add to the one of the silica and, therefore, the overall volume of the particles would be bigger even in the case in which the total number of the particles was the same.

Table 3.7. Calculated values of d_n and C_V of samples 68 to 73.

Run	$[\text{H}_2\text{O}]$, mol/l	d_n , nm	C_V , %
68	4	171.4	4.7
69	5	201.3	4.4
70	6	236.0	5.4
71	7	304.8	8.1
72	8	316.1	8.4
73	9	235.6	5.4

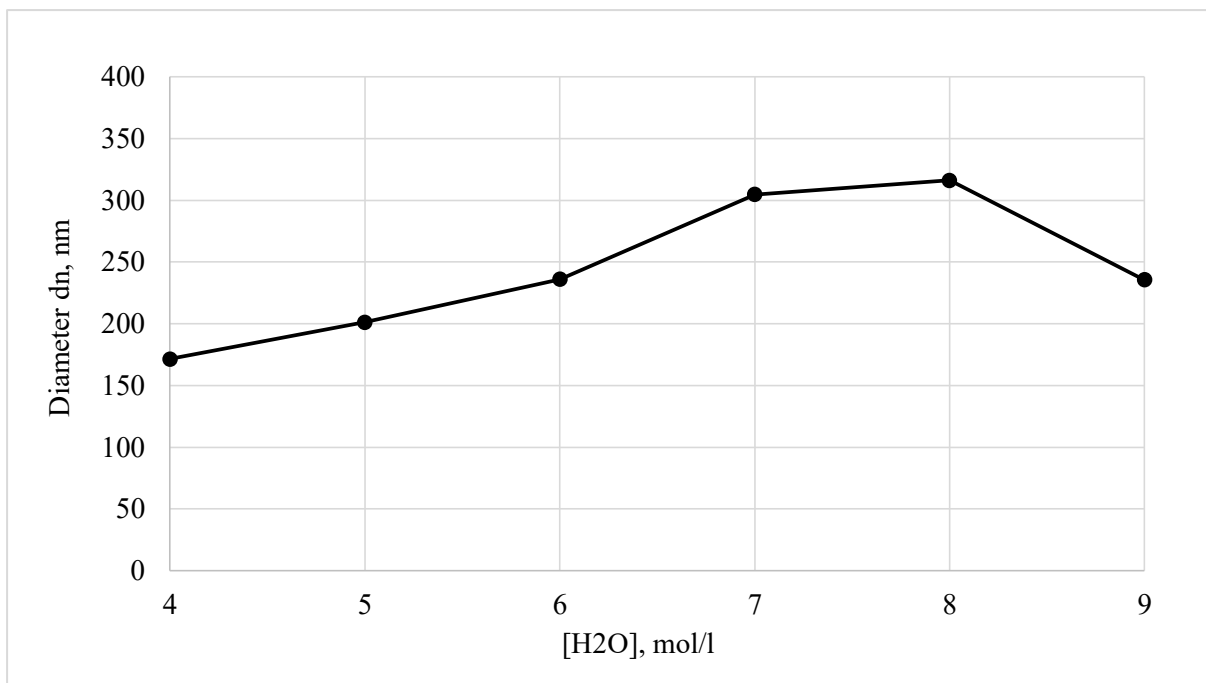


Figure 3.13. $d_n/[H_2O]$ curve for pure silica particles at fixed concentrations of ammonia and TEOS.

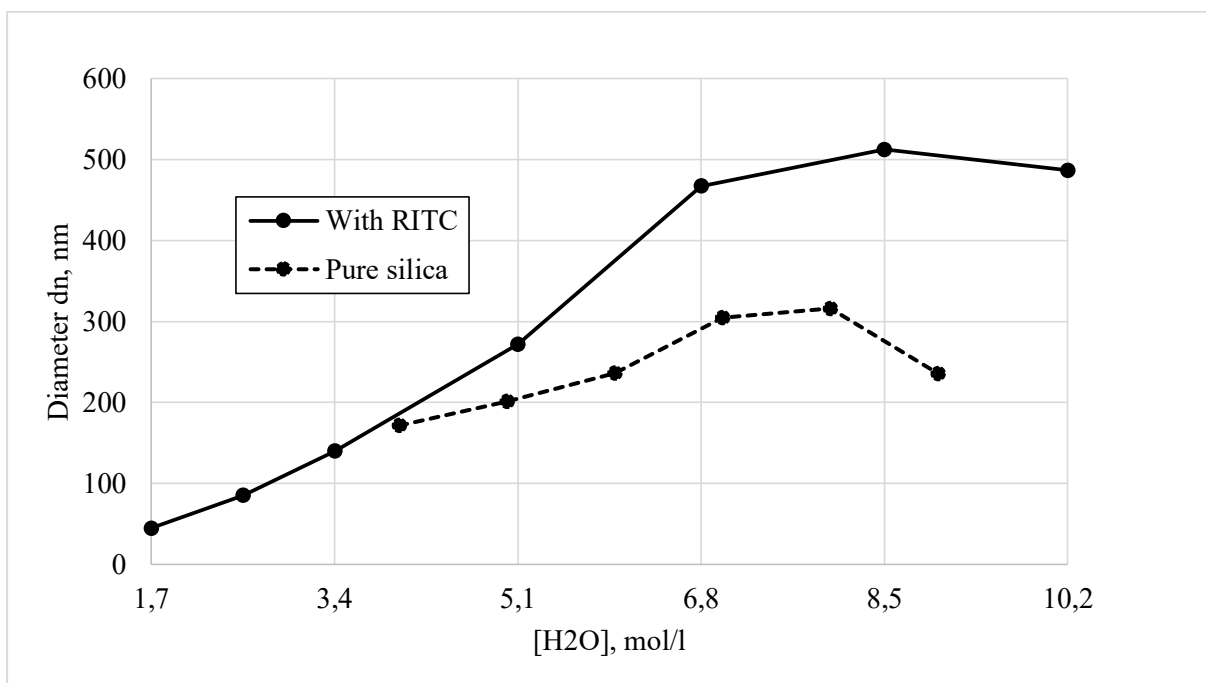


Figure 3.14. Comparison between results obtained from fluorescent particles and pure-silica particles. The continuous line refers to the fluorescent particles and the dashed one to the pure-silica particles.

3.1.7 Fluorescence of RITC

Once the particles are ready, it is possible to detect them in the confocal microscope thanks to the fluorescence of the RITC. The excitation wavelength is 561 nm. The observation is possible both with particles dispersed in the solvent and in the dried state. The only difference is that in the latter one it is easier to focus on them and to take pictures. As it is possible to see in Figure 3.15, taken in the dried state, the fluorescence is very strong and persistent.

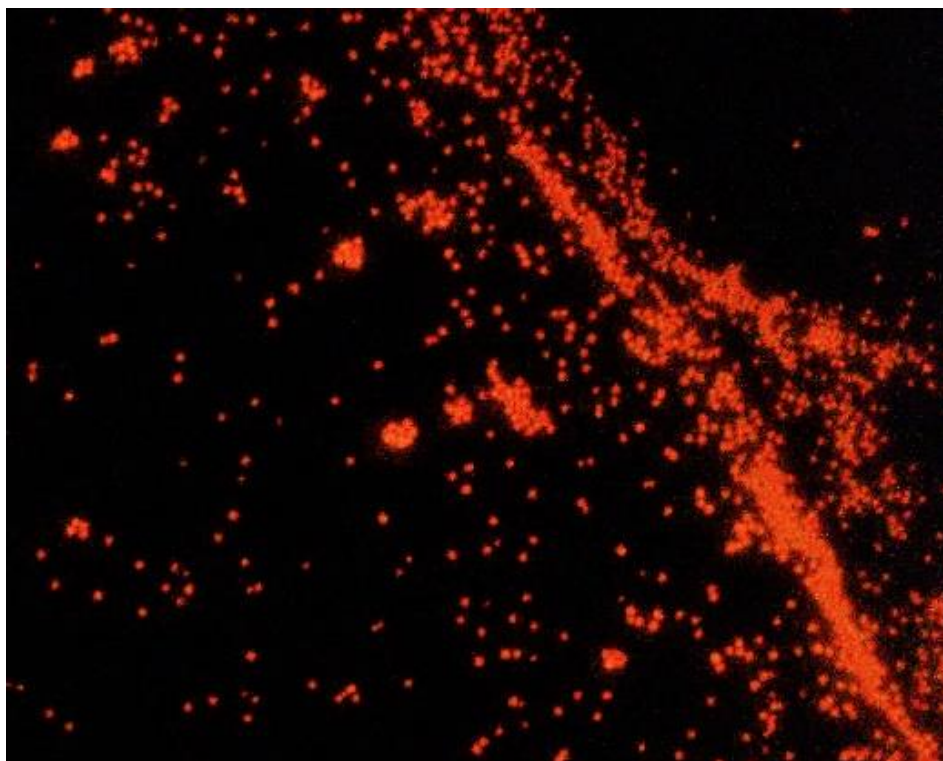


Figure 3.15. Image showing the fluorescence under the confocal microscope.

3.2 PBMA coating

In first instance, it should be noticed that the monomer is in large excess because, at the end of the reaction, a large amount of unreacted BMA is still present in the reactor. This means that probably the reaction time is too short to reach a significant conversion. Nevertheless, neither the reaction time nor the amount of BMA was changed. The reasons are:

- It is not important to achieve a complete conversion, but only to cover the particles with a homogeneous small layer of PBMA/MPTMS and this result was already reached.
- A longer reaction time means a longer process, which is inconvenient considering that two hours are enough to coat the particles with a thin layer.
- It was not of major importance the study of the influence of the thickness of the PBMA/MPTMS layer on the shell diameter.
- Reducing the volume of the monomer could have had the consequence of an incomplete covering of the core particles. Again, since the thickness of this layer was not a parameter to be analysed, it would have been too risky to change a condition that gave, anyway, a good result.

Some pictures of the thin PBMA layer are shown in Figure 3.16 and, in Figure 3.17, it is possible to distinguish the PBMA layer in particles with a very thin polystyrene shell.

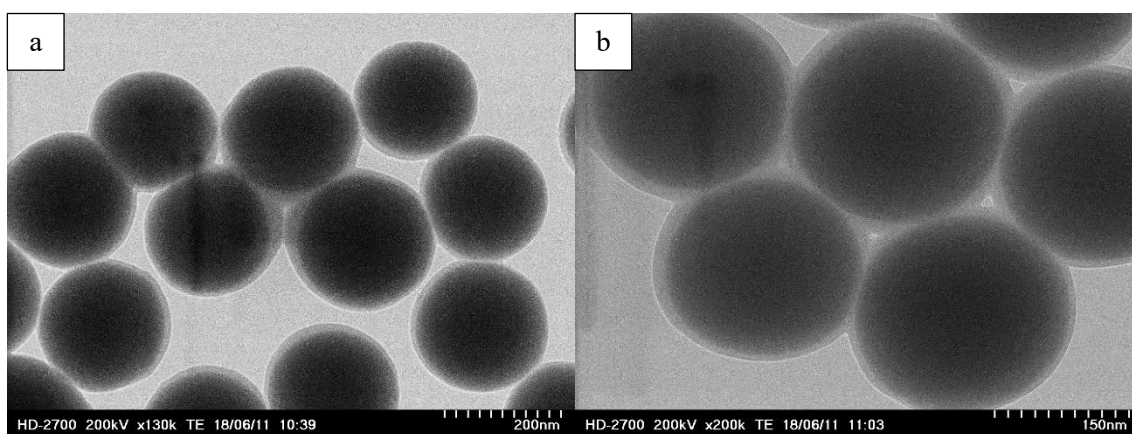


Figure 3.16. TEM images showing the thin PBMA layer.

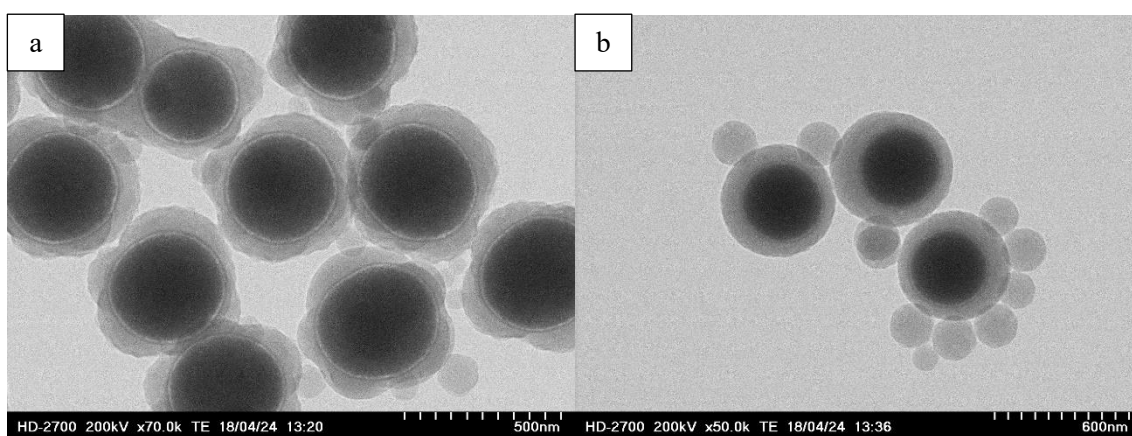


Figure 3.17. TEM images showing the thin PBMA layer between the silica core and the polystyrene shell.

3.3 Shells

3.3.1 PBMA coating

Experiment 112 was made to confirm the effective utility of the PBMA coating using only the MPTMS to link the polystyrene to the silica surface of the cores. The result can be seen in Figure 3.18 where it is compared to experiments made with the same experimental conditions but previously coated with the PBMA.

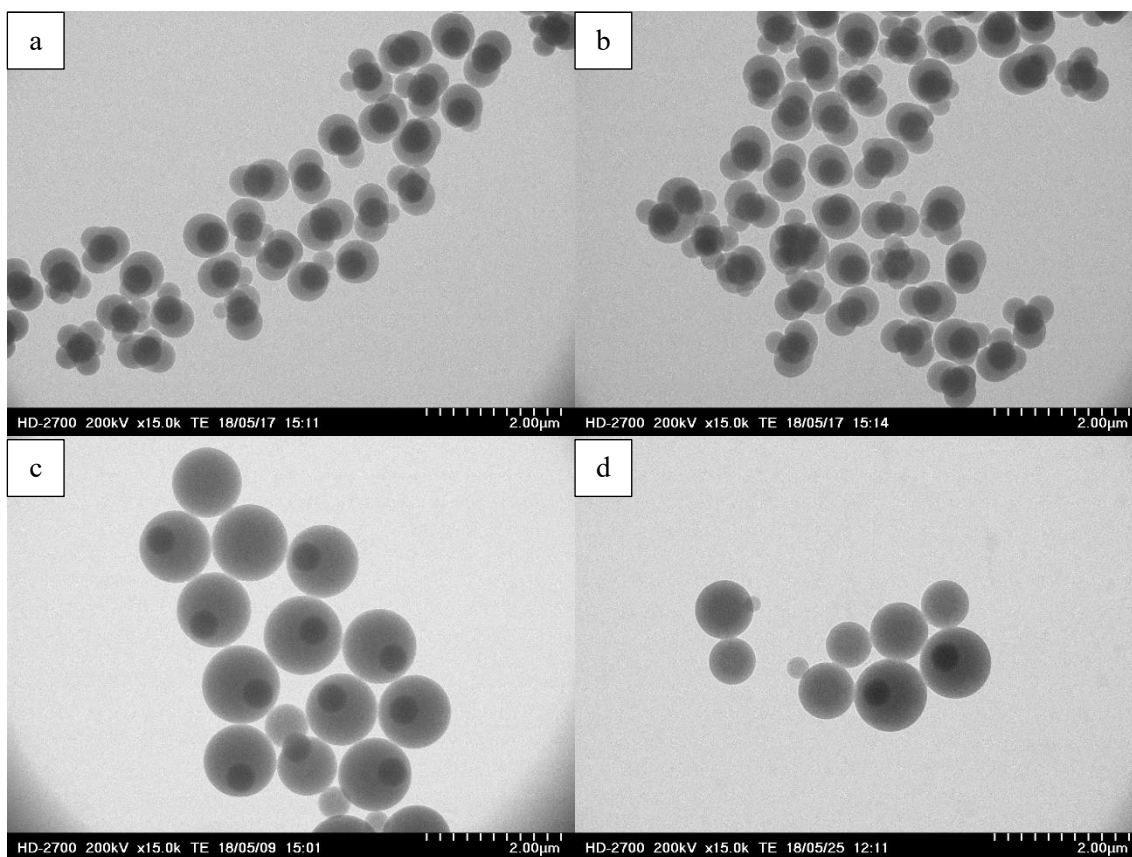


Figure 3.18. TEM images of particle with (c and d) and without (a and b) the PBMA coating.

It is possible to see that for the particles without the PBMA coating the polystyrene shell is not spherical and shows multiple lobes. However, even though the PBMA coating is very thin, coated particles show a perfect spherical morphology with the core eccentric to the shell. This result confirms the hypothesis made when the BMA was chosen as the monomer for the first coating. When BMA is not used the polystyrene reacts with the MPTMS on the surface. The MPTMS has a double bond that can react with the polystyrene to link the core to the shell, but the core particles are too hydrophilic compared to the polystyrene and the repulsion between the two phases tends to create irregular shapes to reduce the free energy of the system. On the contrary, when the PBMA cover the surface of the cores, the surface is hydrophobic enough to allow a homogeneous spherical shell, but also hydrophilic enough to guarantee the eccentricity of the shell. Under these circumstances, the thickness of the PBMA layer is not important for the process because its goal is to modify the surface characteristics and this can be achieved even with a very thin layer.

3.3.2 Reaction time and styrene concentration

Multiple experiments were compared to determine in which measure the reaction time and the monomer concentrations are limiting parameters in the production of the shells. Three reaction time were analysed with different monomer concentrations, 5 h, 15 h and 24 h.

From the set of experiments 84 to 88, with a reaction time of 5 h, it is possible to see that, at very low styrene concentrations the reaction time is not the limiting parameter in the process. This conclusion comes from the evidence that the shell thickness is increasing with an increment in monomer concentration. At very low monomer concentration, a reaction time of 5 h is long enough to consume all the monomer stored in the oil phase and the monomer concentration is the parameter that limits the dimension of the polystyrene shell. It can be seen that for very low concentrations of styrene, 0.01 M and 0.025 M, a thin, inhomogeneous shell starts to form around the silica particles (Figure 3.19 a and b). Under these conditions, the particles are not yet spherical and the reason is that there is not enough polymer to cover the surface uniformly so, locally, the surface tension will create bulges to reduce the free energy. When the volume of monomer increases enough, around 0.05M, for the polymer to cover completely the particles surface with a uniform layer, the free energy gets its minimum with the spherical structure and it is possible to obtain the core-shell geometry (Figure 3.19 c). It should be noticed that the increment in thickness of the shell is not proportional to the increment in monomer concentration because, already at very low styrene concentrations, around 0.025 M, a great number of secondary particles is formed. This is a monomer wasting process and will therefore limit the theoretical thickness of the shell when the monomer concentration will increase furtherly. Once the concentration of styrene reaches the value of 0.1 M or, better, 0.15 M (Figure 3.19 d, e.1 and e.2) it is possible to distinguish clearly the eccentricity between the core and the shell. It is important to notice that in this range of concentrations the number and the diameter of the secondary particles increase with an increment in monomer concentration almost proportionally.

When the styrene concentration increases over a limit value, placed around 0.15 M, keeping the reaction time unchanged at 5 h, the monomer concentration cease to be the limiting parameter and the reaction time takes its place. Runs from 96 to 101 were made with styrene concentrations in the range of 0.3 M to 0.6 M. Even though the quantity of monomer added to the reactor increased a lot, it is possible to see in Figure 3.20 that the diameter remained almost the same for all the experiments, never exceeding 900 nm, and the secondary particles did not grow anymore too. Moreover, the diameter is not only similar between these runs but it is also very close to the one obtained previously with a concentration of 0.15 M. From this comparison, it is possible to determine that, for a reaction time of 5 h, the maximum styrene concentration, below which the concentration is a controlling parameter is around 0.1 M or 0.15 M. Above this limit concentration, the reaction time is not long enough to guarantee a complete conversion of the monomer and thus the shell thickness do not change anymore. This conclusion comes also from the fact that for styrene concentrations higher than 0.3 M, at the end of the reaction, there remains a certain amount of unreacted monomer on the surface of the water and that this volume of unreacted monomer increases with the styrene concentration. A possible way to explain this behaviour is to consider the reactor as a CSTR in which the monomer reacts in the water phase and on the particles surface while the monomer floating above the water is a storage that provides the styrene continuously to replace the amount that reacts. As already said in the previous chapter, this assumption is confirmed by a visual examination of the reactor since the two phases floating one over the other are easily distinguishable. Now it is possible to add another confirmation to this hypothesis. In an ideal CSTR, the concentration of the reactants is always constant and very low, resulting in a constant and slow reaction rate. If, in the real process, it was not like this, an increment in the monomer concentration would have led to a consequent increment in the reaction rate and in the conversion. But this happens only for a very limited range of values and at very low concentrations. Considering, instead, the hypothesis of a CSTR reactor, the monomer reacts only in the water solution were it is present at a very low and constant concentration, the styrene solubility in water, and on the particles surface where the number of radicals that can react is limited by the limited surface of the particles. This explains why after a limit value of concentration the conversion do not increase but the unreacted monomer does and confirms that the hypothesis of considering the reactor as a CSTR is valid.

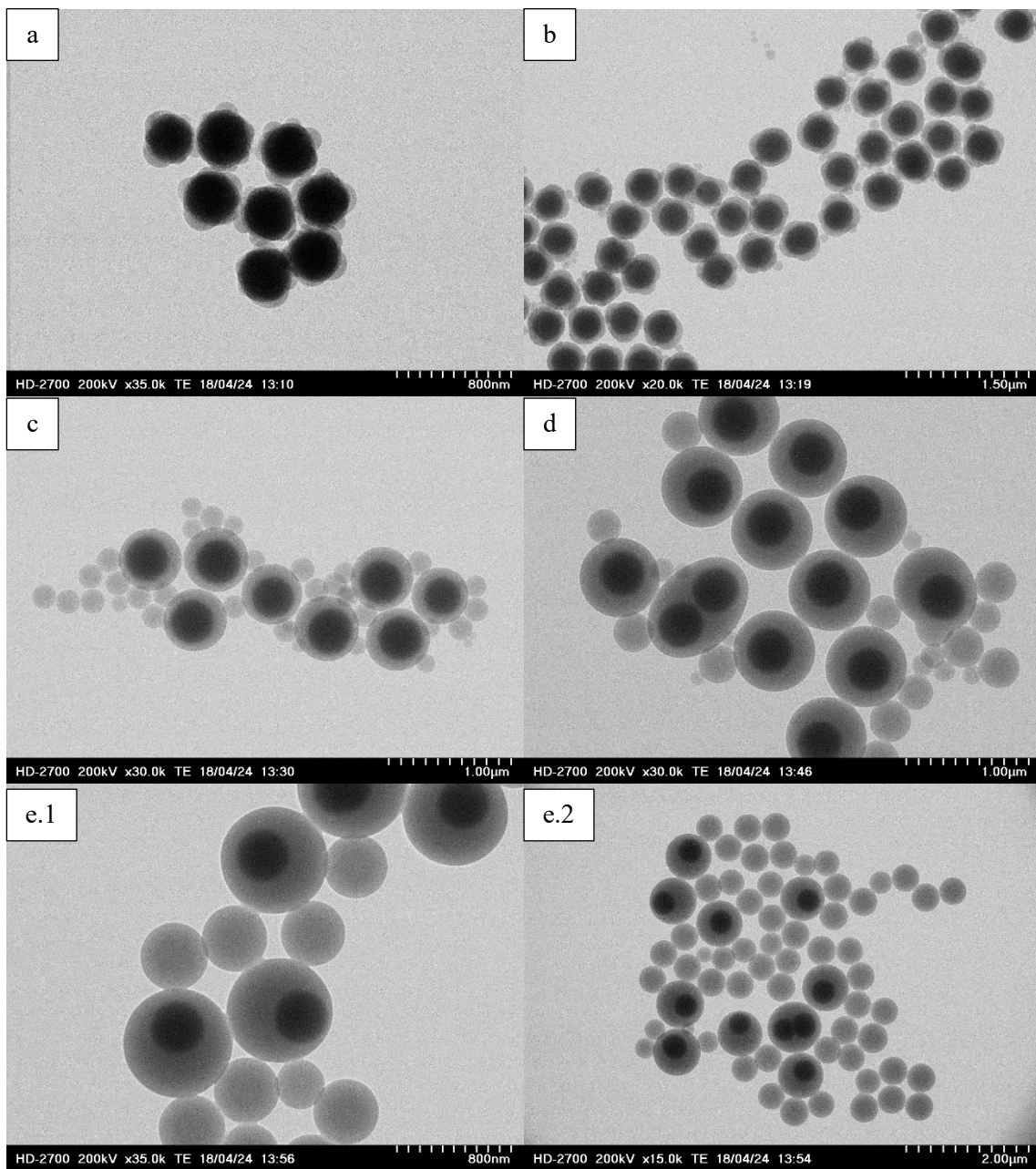


Figure 3.19. TEM images of runs 84 to 88 prepared with a reaction time of 5 h. The styrene concentration was: a) 0.01 M, b) 0.025 M, c) 0.05 M, d) 0.1 M, e) 0.15 M.

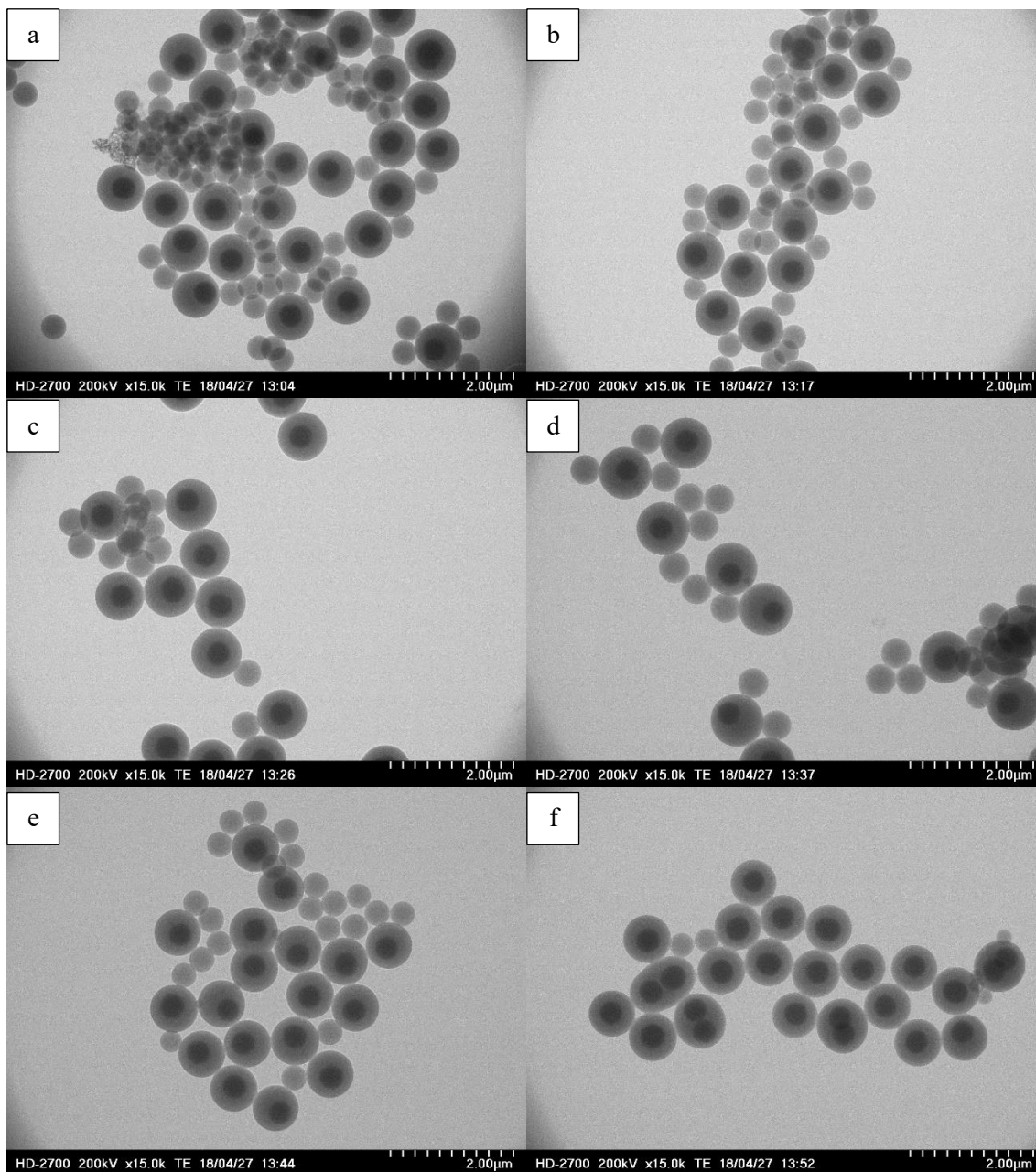


Figure 3.20. TEM images of runs 96 to 101 prepared with a reaction time of 5 h. The styrene concentration was: a) 0.3 M, b) 0.35 M, c) 0.4 M, d) 0.45 M, e) 0.50 M, f) 0.6 M.

In order to expand the concept of the limiting parameter in the process, the set of experiments 104 to 109 was prepared with a reaction time of 15 h and with concentrations from 0.1 M to 0.6 M, that is the range of concentrations for which the limiting parameter was the reaction time. As expected from the considerations made before, the thickness of the shell increased greatly if compared to the same concentrations conditions with a lower reaction time. The total diameter of the particles now can exceed 1200 nm and the conversion is complete even at high styrene concentrations. The results are shown in Figure 3.21.

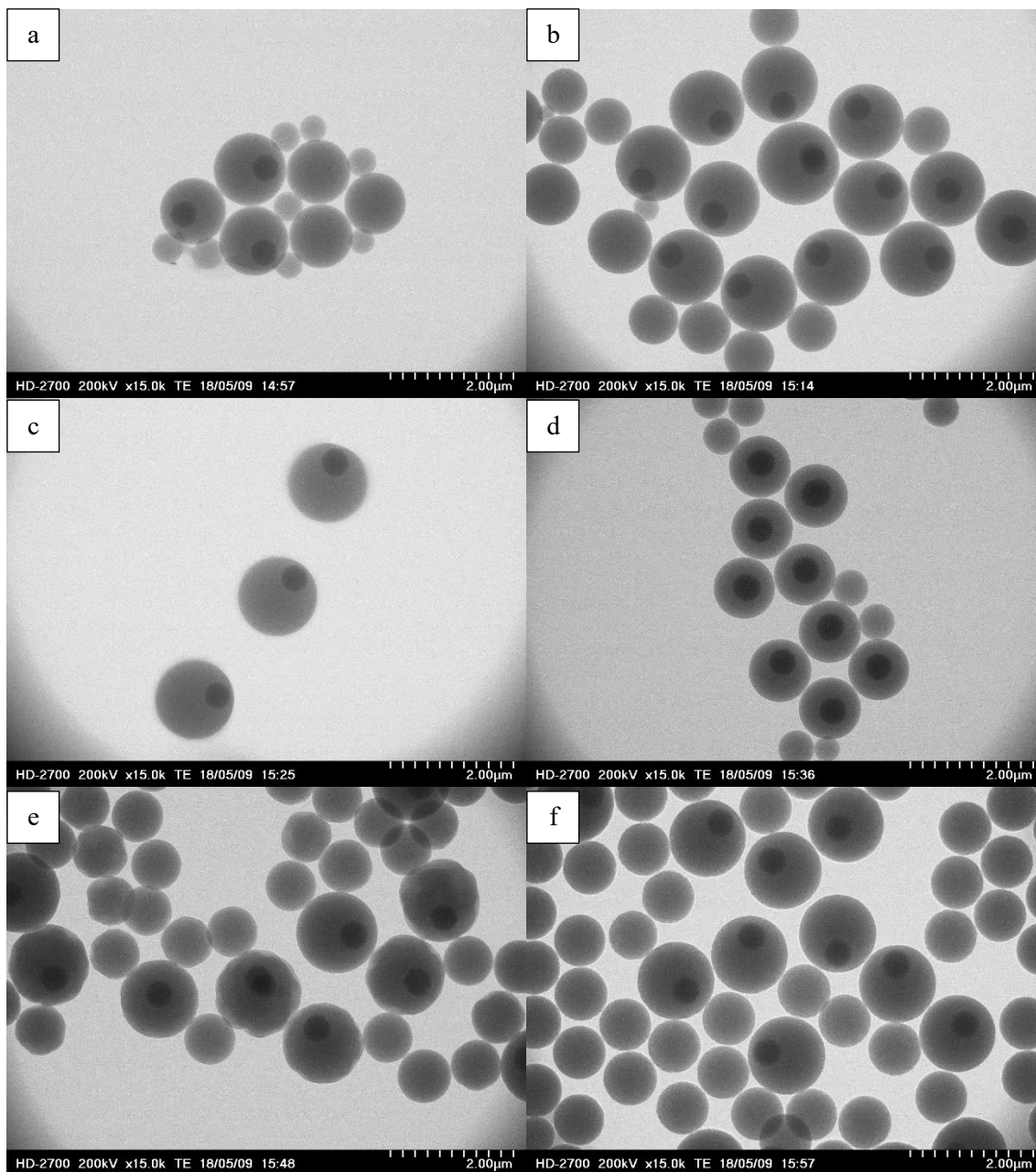


Figure 3.21. TEM images of runs 104 to 109 prepared with a reaction time of 15 h. The styrene concentration was: a) 0.1 M, b) 0.2 M, c) 0.3 M, d) 0.4 M, e) 0.5 M, f) 0.6 M.

Even though the results obtained from this set of experiments partially confirms the theory proposed before and the diameter almost reached the final target of roughly 1400 nm, some more questions need to be answered.

In first instance, it is possible to see that the diameter of the eccentric particles increased if compared to the previous set of experiments, but it did not increase with the styrene concentration. Moreover, the secondary particles increased in diameter too, but their diameters do not follow any kind of reasonable trend if related to the monomer concentration. The secondary particles show also some very different size distributions, sometimes very wide as in run 104 and sometimes very narrow as in run 109.

One possible explanation of these results could have been that the reaction time was still a limiting factor and the diameter had still the chance to increase if given enough time. Nevertheless after 15 h there was no unreacted styrene remained in the reactor and, therefore, the possibilities that the diameter could increase furtherly were limited.

Anyway, samples 119, 120 and 121 were prepared with a reaction time of 24 h with concentrations of 0.1 M, 0.15 M and 0.2 M, that are in the range in which the reaction time could have become sufficient for a complete conversion and for the concentration to become the limiting parameter again. In Figure 3.22 it is possible to see the results.

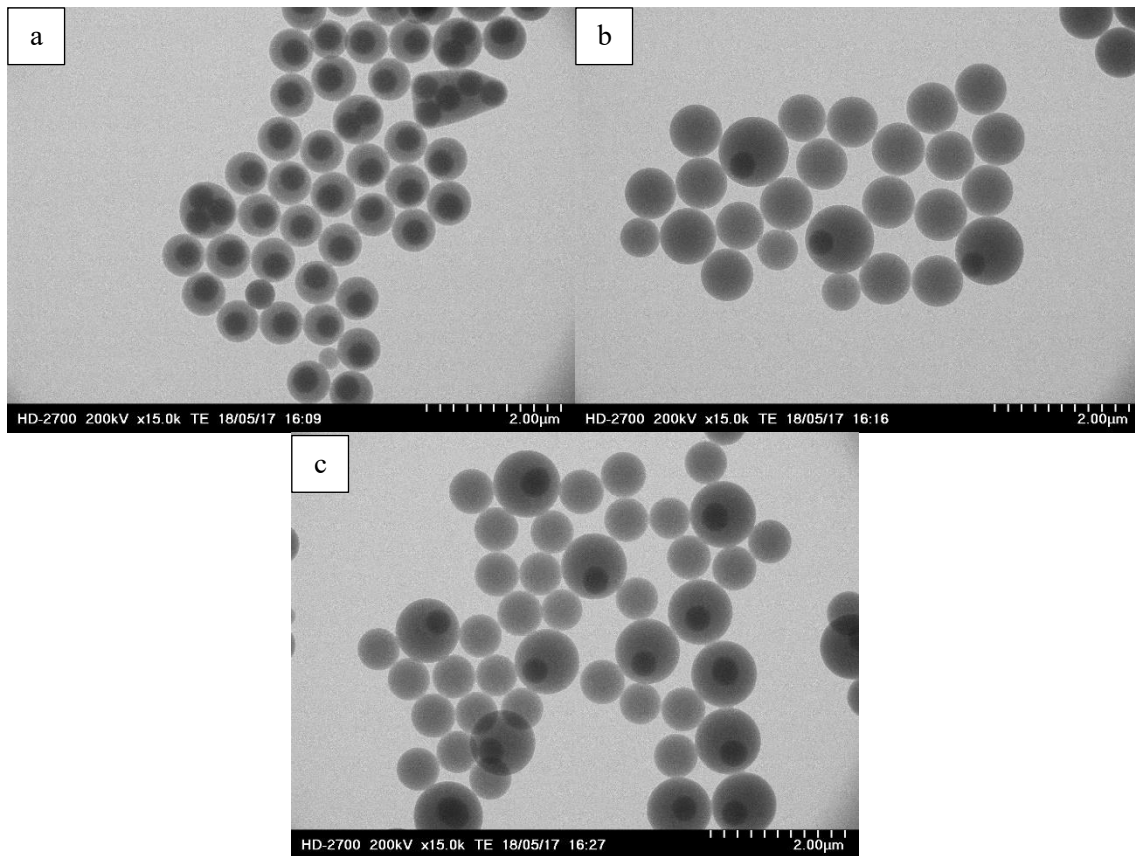


Figure 3.22. TEM images of runs 119, 120 and 121 prepared with a reaction time of 24 h. The styrene concentration was: a) 0.1 M, b) 0.15 M, c) 0.2 M.

Here the previous considerations lose their validity and some more have to be done.

First, the diameter of the particles in run 119 is way smaller than that of run 104 even though the reaction time increased by more than 50%. The thickness of the shell is now similar to that of run 87, which had a reaction time that was almost one fifth. From this comparison, it is possible to assume that neither the styrene concentration nor the reaction time are the limiting parameter in an absolute way.

Comparing runs 120 and 121 with the relative experiments at lower reaction time it can be seen that not only the diameter of the eccentric particles did not increase with an increment of the reaction time, but it did not increase even with an increment in the monomer concentration. From the first condition, it comes out that already at 15 h the reaction time was no more the limiting parameter, and from the second condition that after a certain concentration a further increment would not change the process in any significant way.

Making a quick recap, for systems at very low styrene concentration the concentration is a controlling parameter, the system is close to ideal and the production of the secondary particles do not interfere with the process in a significant way. For concentrations greater than 0.1 M the monomer concentration do not influence directly the diameter of the eccentric particles but, for a limited range of conditions, the reaction time does. After a certain reaction time, placed between 5 h and 15 h, both the parameters cease to be controlling factors and the system dissociates from the assumption of an ideal CSTR reactor.

It was important at this point to understand how and why the system cease to be controlled by those two parameters and if and how it is possible to modify the process to further increase the diameter of the particles.

The main factor that changed between the experiments at very low concentrations and all the others is the production of the secondary particles. As already said, the magnetic stirrer, under the conditions described in Chapter 2, do not transmit enough stirring power to the solution to generate a real emulsion and thus the secondary particles are probably generated by the condensation of the oligomers produced from the polymerisation in the aqueous solution. Once the secondary particles are formed, they will contribute to consume the monomer with two mechanisms, the first one is reacting with fresh styrene monomer and growing in size, and the second is absorbing the monomer present inside the solution. The styrene is hydrophobic and thus it will more likely absorb on the polystyrene particles than remaining in the aqueous solution. To explain why the diameter of both the eccentric and secondary particles is not directly related to the styrene concentration it is possible to assume that it is because the number of secondary particles increases almost proportionally with the volume of monomer. Therefore, the effective amount of styrene available for the eccentric particles is not proportional to the one added in the reactor. The number of secondary particles is greater than that of the core particles and therefore it is reasonable to assume that they will consume most of the monomer. Considering this, the dimension of the eccentric particles will depend only on the quantity of styrene that reacted and was absorbed on the shell before the secondary particles consumed all the remaining monomer.

If this assumption is true, the limiting parameters, under these conditions of monomer concentration and reaction time, will be the number of the secondary particles and the mass transfer rate in the solution.

3.3.3 Electrolyte

If the problem limiting the polymerisation is the production of the secondary particles, it is possible to solve it reducing their number. This way there would remain more monomer available for the eccentric particles and, therefore, their diameter should be bigger.

To reduce the number of the secondary particles there are two possibilities, to reduce the number of nucleation or to reduce the total number of nucleated particles. Even though it is difficult to control the nucleating process and therefore the number of nucleation, it is possible to control the total number of nuclei that will be stable enough to grow. The introduction of an electrolyte in the reactor should decrease the permittivity of the solution resulting in a lower stability of the particles. Under this condition, the secondary particles will more likely aggregate than grow. This process has two advantages, the first one is that if a secondary particles aggregates with an eccentric particle it will contribute in the formation of the shell, and the second is that if this happens, there will be one particle less that will consume monomer.

Unfortunately, there is also the possibility that the core particles aggregates between each other and this is inconvenient for the final product because only one core should be incorporated in each particle.

In Figure 3.23 it is possible to see the particles produced in run 116 and 117 and in Figure 3.24 and 3.25 it is possible to see a comparison with particles produced without the electrolyte but in similar monomer concentration.

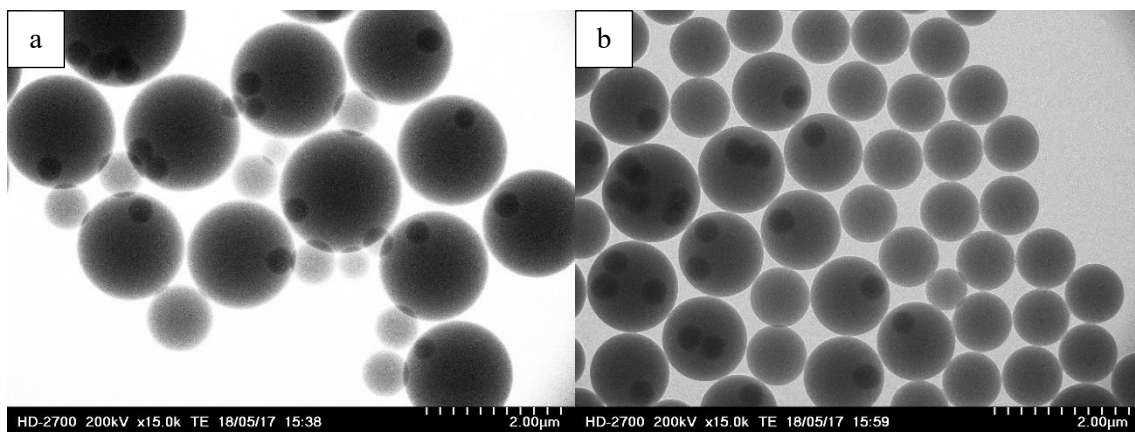


Figure 3.23. TEM images of runs 116 and 117 prepared with a concentration of NaCl of 10 mM. The styrene concentration was: a) 0.1 M, b) 0.2 M.

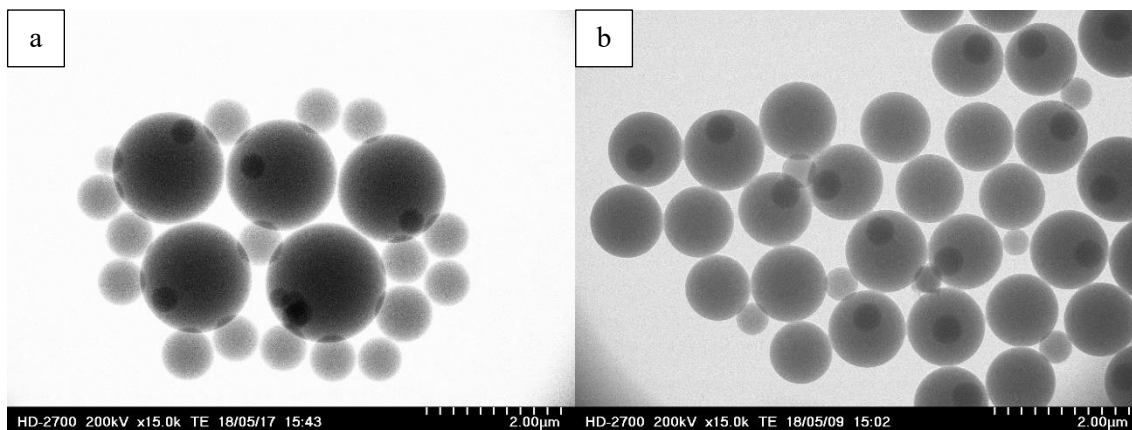


Figure 3.24. A comparison between TEM images of runs 116 (a) and 104 (b) prepared with a styrene concentration of 0.1 M. The NaCl was used only for a).

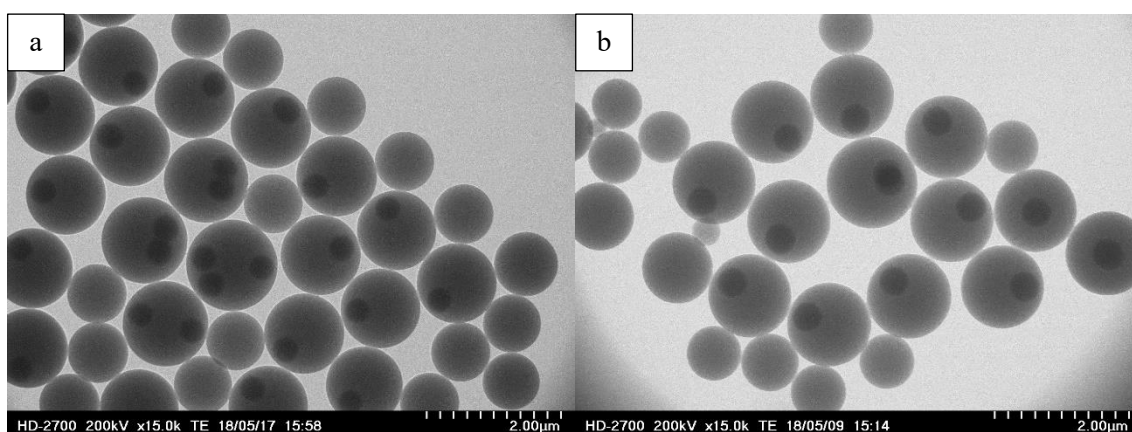


Figure 3.25. A comparison between TEM images of runs 117 (a) and 105 (b) prepared with a styrene concentration of 0.2 M. The NaCl was used only for a).

From Figure 3.23 and 3.24 it is possible to see that the electrolyte has effectively increased the dimension of the eccentric particles with the diameter reaching 1700 nm in run 116.

Unfortunately, from Figure 3.23 it is also possible to see how the introduction of the electrolyte caused sometimes the aggregations between core particles or between eccentric particles since the eccentric particles often incorporate multiple cores.

This is, as already said, inconvenient because each eccentric particle should have only one core to allow an easy definition of an optical axis and to track a rotational movement.

Furthermore, from Figure 3.25 it is possible to notice that the electrolyte do not always succeed in creating bigger particles because from run 117 and 105 both the eccentric and the secondary particles have about the same diameter. The only difference between the two samples is that, when the NaCl is added to the reactor, the eccentric particles incorporate multiples cores.

The introduction of an electrolyte is effectively a possible way to increase the particles diameter during the polymerisation, but, for this process in particular, it is not the best way to proceed because the product lose its main characteristic that is the single, eccentric core.

3.3.4 Mixing rate

In every reaction, the mass transfer and the fluid dynamic are fundamental parameters that should be considered. In this study, the only way to have a control over these two aspects was the rotation speed of the magnetic stir bar placed inside the reactor.

In Figure 3.26 it is possible to see the particles produced in the different fluid dynamic conditions generated when the magnetic stirrer was set to its minimum, medium and maximum rate, respectively Figure 3.26 a, b and c.

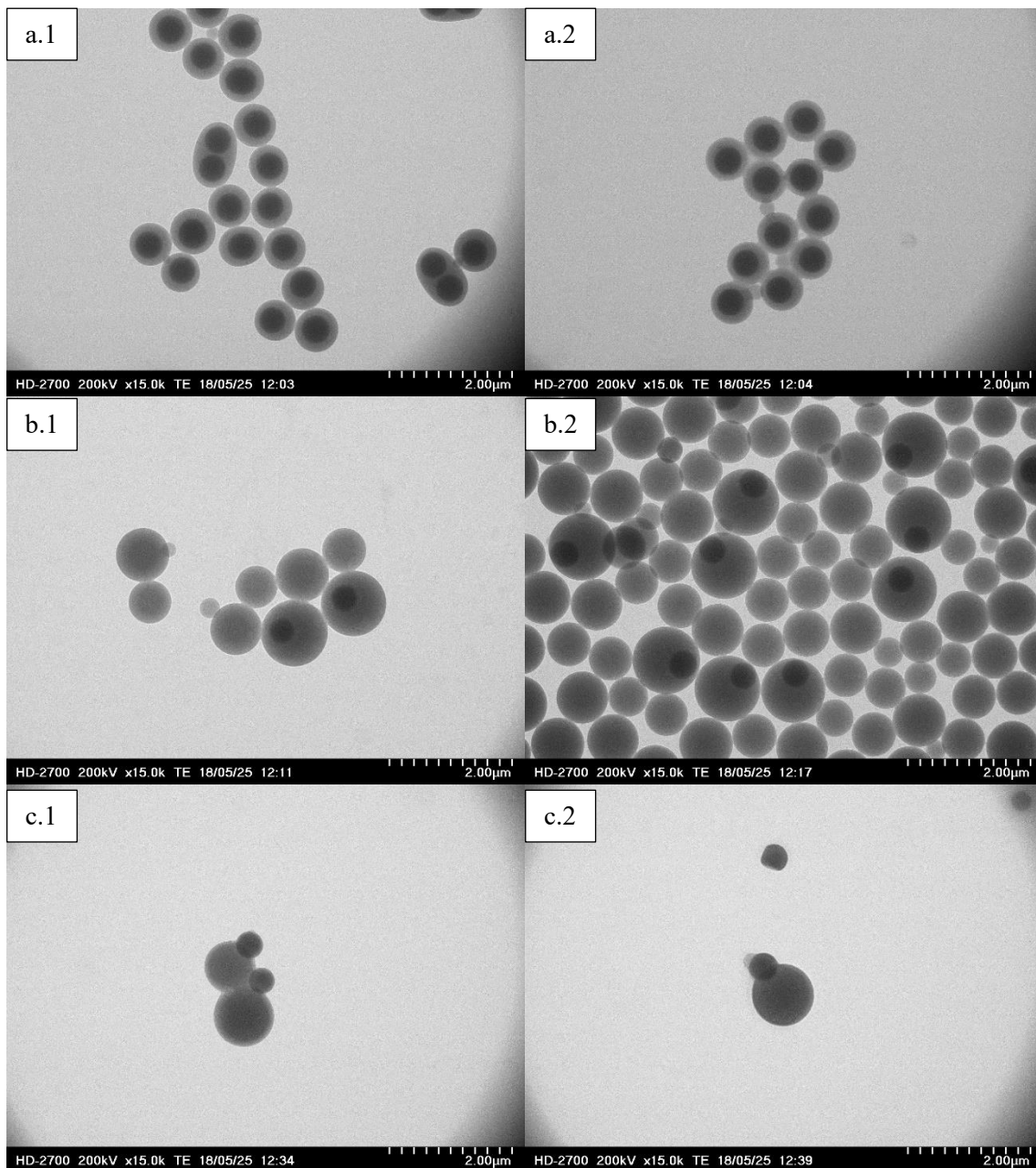


Figure 3.26. A comparison between TEM images of runs 124 (a), 125 (b) and 126 (c) prepared at different mixing velocity. All the samples have the same styrene concentration and reaction time.

At very low mixing velocity, as in run 124 (Figure 3.26 a1 and a2), the thickness of the shell is very small and the result is similar to the one obtained in experiments with a short reaction time. Increasing

the mixing velocity, the diameter of the particles, both the eccentric and the secondary, increases considerably but, when increased too much, the morphology of the particles changes from eccentric and spherical to the snowman shape with the core that is no more incorporated completely in the shell as it can be seen in Figure 3.27.

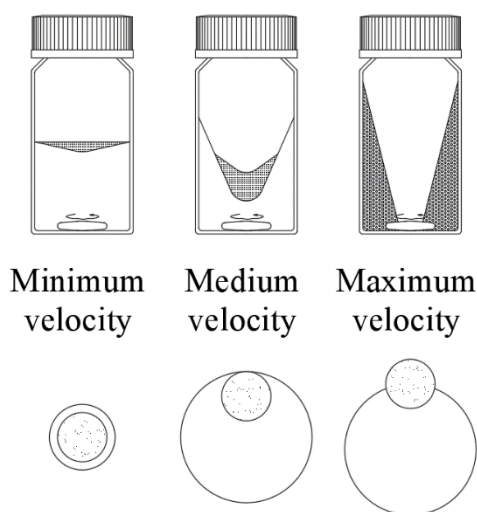


Figure 3.27. A comparison between the mixing velocity and the morphology of the particles.

At the minimum mixing velocity, the mass transfer in the reactor is not fast enough to dissolve the styrene in the water phase at a rate sufficient to replace the monomer that reacts and to keep the styrene concentration constant and equal to its maximum value, which is represented by the solubility of styrene in water. The reaction rate is therefore slower than the maximum and the mass transfer will be the controlling parameter. The conversion of the monomer is incomplete and the shell thickness is limited by the amount of styrene that succeed to diffuse from the oil phase to the aqueous phase and react.

When the mixing velocity is increased, the mass transfer increases and more monomer dissolves in the water phase increasing the reaction rate and the conversion. The thickness of the shell, therefore, increases proportionally to the increment in mixing velocity. When the mass transfer is fast enough to supply enough monomer to the solution for the monomer concentration to remain constant at its maximum value, the shell thickness do not increase anymore because, at that point, the reaction rate is limited by the monomer concentration in the water phase.

Even though the mixing velocity at which this ideal condition is reached is not known because there is no possibility to control precisely the rotation rate of the magnetic stir bar, the rate cannot increase over an upper limit.

When the mixing velocity increases to the point at which the bottom of the vortex induced in the solution reaches the stir bar, the three phases in the reactor, water phase, oil phase and the gas, will be mixed deeply. The core particles that have characteristics in between hydrophilic and hydrophobic, will position along the interface between the phases and the shell will therefore grows outside of the core. Since the particles must be spherical, this condition determines the limit in rotation speed over which it is not possible to work to keep the right morphology in the particles.

It should be noticed that the use of a magnetic stir bar is not the best way to guarantee a good mixing in a reactor and that there are other engineering solutions that can solve the problem caused by the vortex. Unfortunately, with the small scale of these experiments it is not possible to apply those technologies because they require larger reaction volumes that would be difficult to obtain without a proper scale up of the entire process.

3.3.5 Core particles concentration

The core particles concentration could be an important parameter only if there is no production of secondary particles. Since this process do not work under this ideal condition, the result is that, at least for very low concentrations of core particles, their concentration has no effect on the size of the eccentric particles as it can be seen in Figure 3.28.

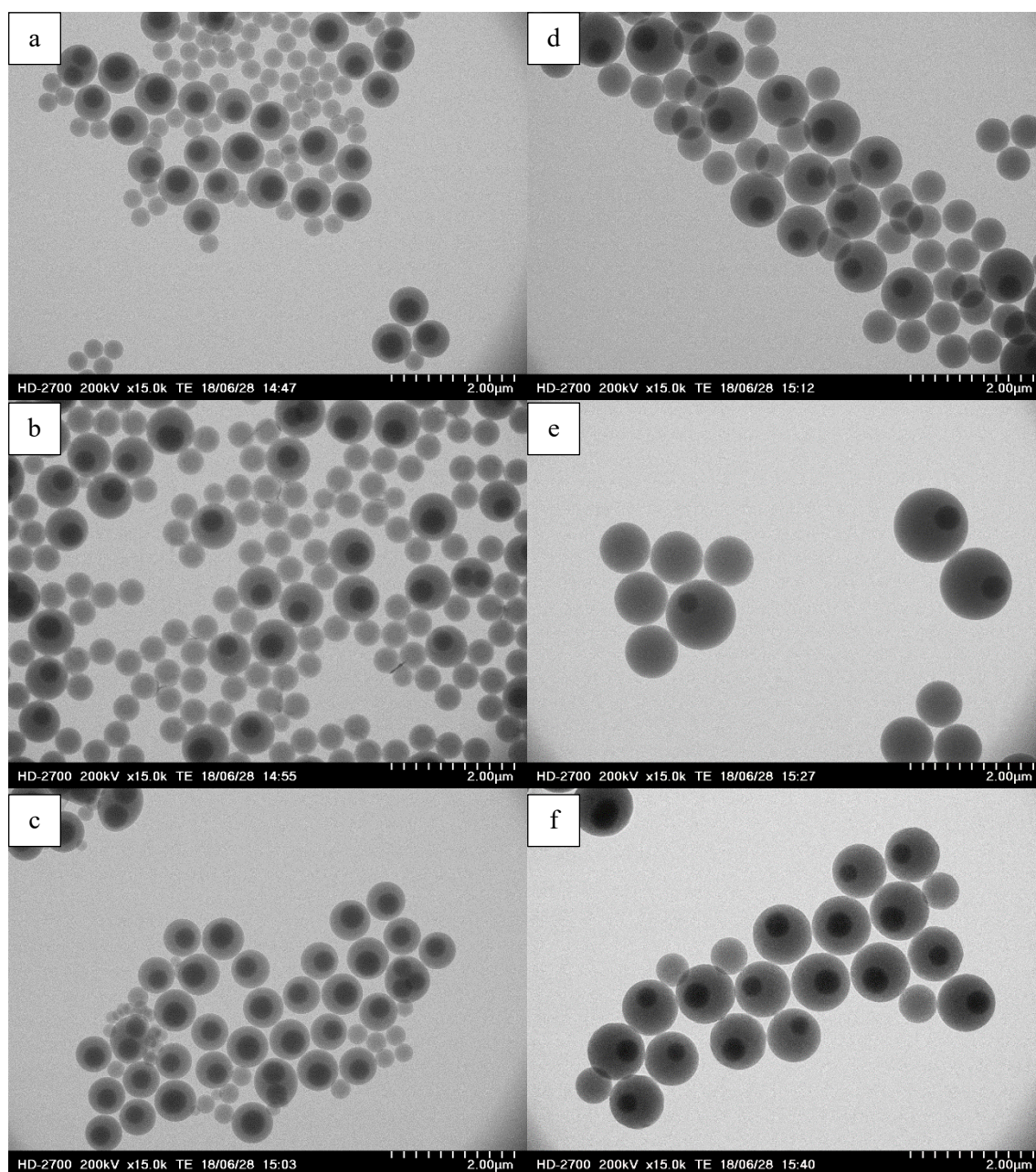


Figure 3.28. A comparison between TEM images of particles prepared at different cores concentrations and different monomer concentrations. Particles from a, b and c were prepared at $[St]=0.1$ M while d, e and f at $[St]=0.2$ M. Core particles concentration was: 0.005 %_{vol} for a and d, 0.01 %_{vol} for b and e, 0.02 %_{vol} for c and f.

As it is possible to see from Figure 3.28, there is no clear correlation between the core particles concentration and the diameter of the eccentric particles. Furthermore it should be noticed that some experiments had the same cores/monomer ratio as it happens for the couples of runs 170-174

(respectively (a) and (e) in Figure 3.28) and 171-175 (respectively (b) and (f) in Figure 3.28) but the particles obtained from those experiments are completely different one from the other.

The diameter changes only when the concentration of monomer is changed and it grows with it as it was already seen when the styrene concentration was tested, but has no significant variation when the core particles concentration is changed. These results confirm the hypothesis that the number of secondary particles generated during the polymerisation is much larger than the number of core particles and that a change in their concentration is almost negligible compared to the total amount of particles in the reactor. Therefore, the polymerisation will be controlled by other parameters as the monomer concentration, the reaction time or the fluid dynamic of the system, parameters that can actually control the number of secondary particles produced.

From samples 171 and 174 (respectively (b) and (e) in Figure 3.28) it is possible to notice that there is actually a slight increment in the diameter of the particles when the concentration of the cores is equal to 0.1 %_{vol} but, for both higher and lower concentrations the diameter is smaller. One possible explanation could be that the cores concentrations has a parabolic effect on the particles diameter and that its maximum is placed exactly on the concentration equal to 0.01 %_{vol}, but this would be hard to explain and it was already seen how other parameters affect the diameter more and with an easier explanation. It is possible, for example, that the mixing velocity for those two runs was slightly higher than it was in the others, since it is not possible to choose it precisely, and that this difference is the reason for a different shell thickness.

3.3.6 Fluorescence of pyrene

Even though it has not been possible to detect the fluorescence of the pyrene in the shell directly with the confocal microscope used for the cores, in our laboratory its presence in the polystyrene matrix was detected indirectly and then some samples were observed with the confocal microscope owned by the ETH of Zurich.

Firstly, a small amount of the solution containing the particles of run 123 was diluted and observed under a UV lamp operating at a wavelength of 365 nm, very close to the excitation maximum of pyrene, which is roughly 350 nm. The solution was compared to other two solutions containing eccentric particles, one with the fluorescent dye RITC incorporated in the core only and one with no fluorescent dye at all. This test was made to exclude the possibility that the colour reacting with the UV light was, somehow, the RITC and that the visual effect of luminescence was actually fluorescence and not just light scattering. From Figure 3.29 it is possible to see that there is no difference between the sample containing the particles with the RITC in the core and the one containing particles with no dyes. As it was expected, since the excitation wavelength of the RITC is much higher than the one generated with the UV lamp, the RITC does not contribute to the fluorescence of the particles in this specific test. On the contrary, the sample containing the particles incorporating the pyrene shows clearly some kind of fluorescence.

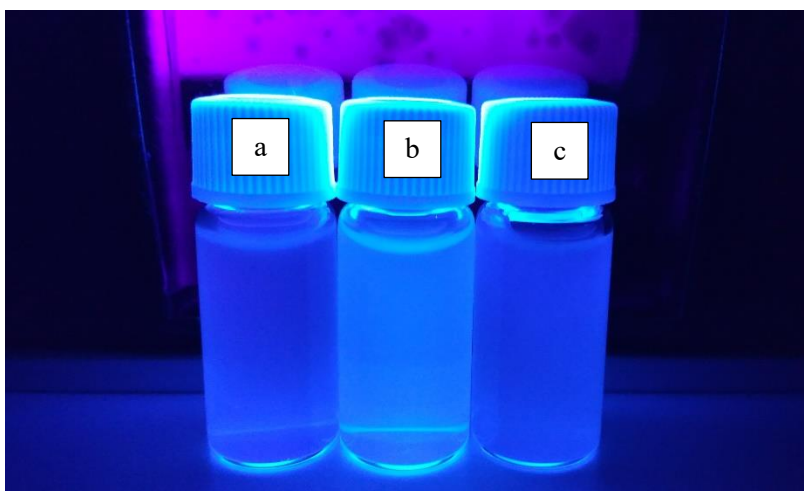


Figure 3.29. A comparison under a UV lamp between solution of particles containing: a) no dye, b) RITC in the core and pyrene in the shell, c) RITC in the core but no dye in the shell.

After this inspection, it was sure that the pyrene was inside the solution, but it was not sure yet that the dye was incorporated in the polystyrene shell and not just dissolved in the water. The probability that the pyrene was dissolved in the water was very low because pyrene is almost not soluble in water, but the inspection with the fluorometer gave a numerical proof that the dye is effectively incorporated in the shells.

As described by Kalyanasundaram and Thomas^[14], the emission spectra of the pyrene undergoes a significant modification when the dye is dissolved in different solvents and measuring particular peaks of the spectra it is possible to determine somewhat precisely the solvent. In particular, the intensity ratio between the peaks called I_1 and I_3 . The intensity ratio I_1/I_3 ranges from 1.87 when pyrene is dissolved in water to 0.6 when dissolved in aliphatic hydrocarbon solvents. The emission spectra of sample 123 is shown in Figure 3.30 at an excitation wavelength of 350 nm.

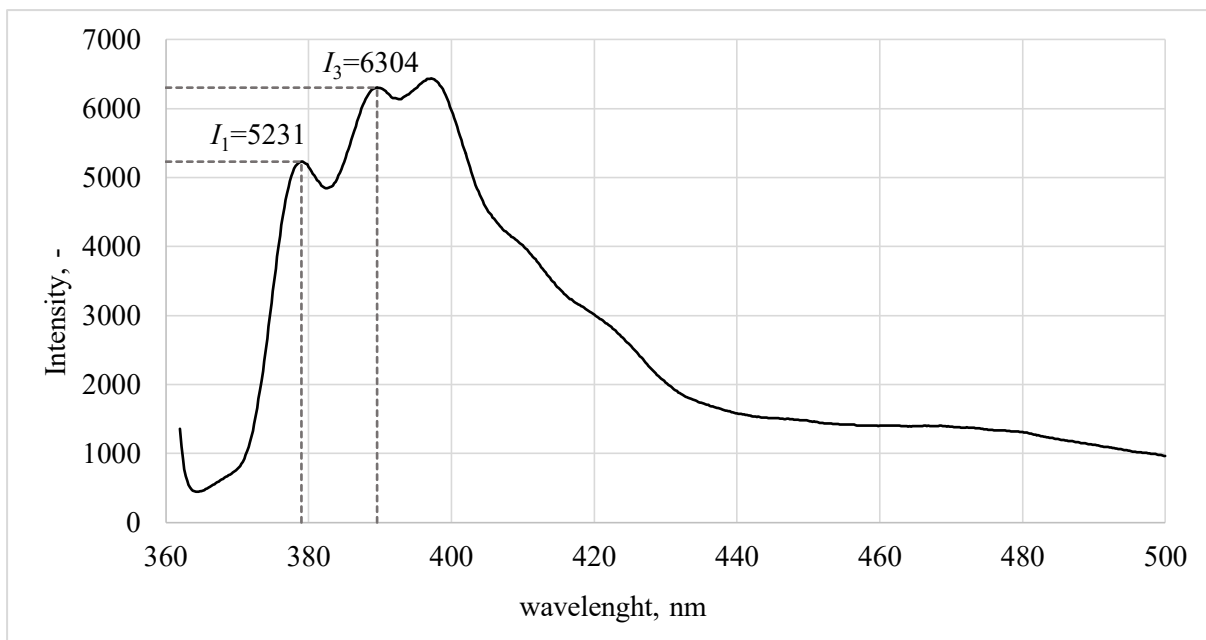


Figure 3.30. Emission spectra of sample 123 with an excitation wavelength of 350 nm. The two peaks I_1 and I_3 are highlighted.

Comparing data showed by Kalyanasundaram and Thomas^[14] with the emission spectra of sample 123 it is possible to locate the peaks I_1 and I_3 respectively at 379.0 nm and 389.6 nm. The emission intensity at those two peaks are equal to 5231 and 6304 as it can be seen in Figure 3.30 and Table 3.8. The intensity ratio I_1/I_3 is equal to 0.83, which is really close to the ideal 0.9 related to polystyrene and very far from 1.87 that refers to water. With this value, it is possible to confirm that the fluorescent dye was successfully incorporated in the polystyrene shell and that the procedure is consistent in the production of eccentric core-shell particles with two different dyes.

Table 3.8. An analysis of the peaks in the emission spectra of sample 123.

Peak	Peak wavelength, nm	Emission intensity, -	I_1/I_3
I_1	379.0	5231	0.83
I_3	389.6	6304	

Even though it was not possible to observe directly the two colours in the confocal microscope available in our laboratory, some samples were sent to the researchers in the ETH of Zurich who commissioned the particles and they had the opportunity to observe them and to send us some pictures, as shown in Figure 3.31. From these it is finally possible to see that particles are visible and that it is possible to detect the eccentricity between the core and the shell and to follow their relative movement.

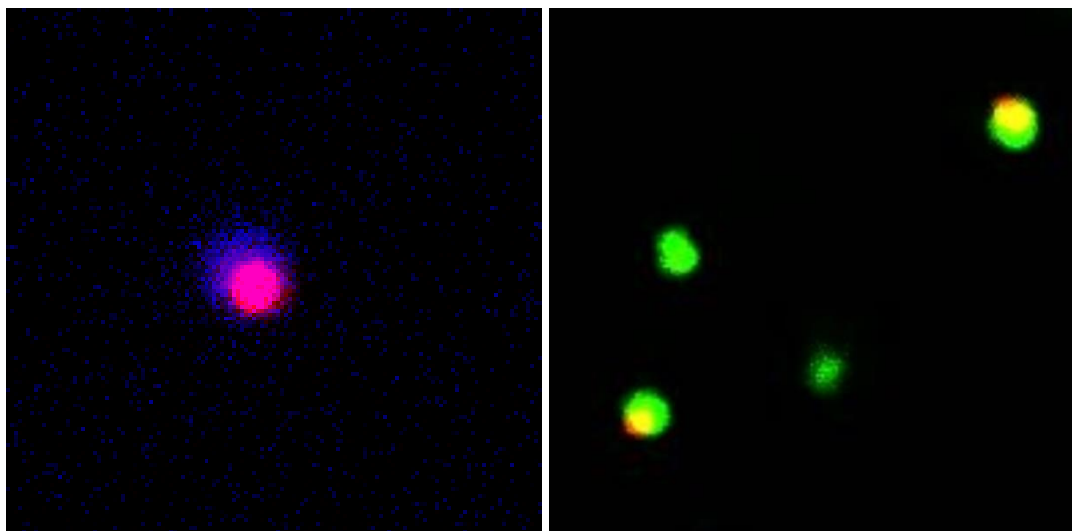


Figure 3.31. Pictures showing the eccentric morphology of the particles thanks to the fluorescence of the core and the shell.

4 Conclusions

This thesis focused on the development of a procedure to produce dual fluorescent eccentric core-shell particles to be used as probes in the study of colloidal science.

The procedure was divided into three steps, the production of the silica cores and the relative incorporation of the fluorescent dye RITC, the coating with the PBMA, a polymer layer that is needed to guarantee the eccentricity between the core and the shell and, finally, the production of the polystyrene shell and the incorporation of the fluorescent dye pyrene.

During the first step, the production of the cores, multiple parameters of the process were examined to understand how the incorporation of the RITC influences the synthesis and how it is possible to control the average diameter of the particles.

Firstly, it was determined that the solution containing the fluorescent dye should be introduced in the reactor possibly with no delay respect to the beginning of the reaction because, even though an eventual delay do not change significantly the diameter of the cores, it will increase the polydispersity of the system, an highly undesired aspect in this work.

It has been shown, later, that the introduction of the fluorescent dye in the particles increases their average diameter, probably because of the destabilization of nuclei in an early stage of polymerization due to specific adsorption of RITC molecules onto the nuclei. Moreover it was shown that the particles requires a single layer only-silica coating to improve their stability as the ζ -potential drop to one third or even one fourth of the average value of pure silica particles when the cores are produced in a single step reaction.

For what concerns the possibility to control the diameter of the particles the concentrations of the main three reactants were examined: TEOS, the silicon source, ammonia, the basic catalyst and water, the initiator. It has been shown that the concentration of TEOS does not affect in any way the dimension of the particles, while the concentration of ammonia is proportional to the diameter. Unfortunately, an increment in ammonia concentration increases also the polydispersity of the system. On the other hand, the water concentration showed to be a perfect parameter to control the diameter of the particles, at least in a certain range of values. For values of $[H_2O]$ between 3 M and 7 M it is possible to predict the diameter of the particles with high precision with a simple linear interpolation of the curve obtained by the experiments showed in this work.

In the end, the core particles were successfully observed under the confocal microscope and they showed a strong, long lasting fluorescence.

During the second step, it has been shown the importance of the PBMA coating. The silica surface of the cores is too hydrophilic compared to the polystyrene and therefore, if the coating with the PBMA is not applied, the shell does not grow as a homogeneous thick layer, but in the form of multiple lobes. The thickness of the PBMA layer is not important since a thin layer of a few nm is enough to guarantee the homogeneity of the shell and its eccentricity to the core, but anyhow its presence is essential.

The third step was the production of the eccentric polystyrene shell and the incorporation of the second dye, the pyrene. Both long polymerization times and high monomer concentrations produced thick polymer shell, but the diameter reaches a plateau after certain values. When the polymerisation time and the monomer concentration grows more than 15 h and 0.2 M respectively, no increment in the shell

thickness is expected. This is probably due to the massive production of secondary particles that strongly affects the process.

The addition of an electrolyte in the reactive solution showed to be effective in increasing the particles diameter but, unfortunately, the system becomes too unstable to be reproducible and, most of the times, each shell incorporates more than one core, characteristic that is in contrast to the objective to create a clear optical axis in the particles. The stirring rate of the impeller in the reactor exhibited a strong impact on the morphology of the particles since it controls directly the mass transport in the reactor. When the stirring rate increase, the monomer dissolve faster in the aqueous solution and the reaction proceed faster resulting in a thicker shell. Unfortunately, when the stirring rate increases too much the morphology of the particles changes and they lose their spherical shape, result that is in contrast with the goal of this thesis. Finally, it has been shown that the concentration of the seed particles does not affect in any way the thickness of the shell, probably because they are just a small fraction compared to the great number of secondary particles produced during the polymerisation.

Once the pyrene was incorporated in the shell, the solution containing the eccentric particles was analysed with the fluorometer. The fluorescence spectra of pyrene undergo a strong modification when placed in different solvents and the spectra detected for these particles was in perfect accordance with the one that pyrene should have when placed in polystyrene, confirming the incorporation of the dye.

To complete the study, some sample were sent to the ETH of Zurich where it has been possible to observe directly the fluorescence of the particles under the confocal microscope, confirming that this procedure is suitable for the production of good probes in the study of colloidal science.

Even though with this study a new procedure to create dually coloured eccentric particles was found, there are still many efforts to be done to improve the technique. The procedure to produce the RITC/silica cores is quite well defined and precise, but still it is limited to the production of particles smaller than 550 nm. For this reason, it is important to determine other solutions to increase furtherly the diameter like seeded growth polymerisations or the utilisation of different reactants like higher alcohols as solvents or higher silicates as the source of silicon, which showed to be effective for this purpose in the study conducted by Stöber *et al.*^[6]. For what concerns the coating of the PBMA layer, it would be interesting to analyse if and how the thickness of the PBMA layer influence the production of the polystyrene shell and if different polymers with similar characteristics could lead to better results. In the process involving the production of the polystyrene shell many efforts should be done to improve the reproducibility of the system and to control more precisely the diameter of the particles. For example, it should be studied in detail how the stirring rate can affect the diameter of the particles and if better results can be achieved with different impellers or different reactor morphologies. Moreover, other parameters like the polymerisation temperature, the concentration of initiator and the introduction of new reactants to improve the stability of the system should be studied.

The direct applications of these particles is, as mentioned when the research was introduced, the study of the rotational dynamic of colloidal spheres in different states, but, basically, they are good probes in the study of any kind of subject concerning the colloids. Moreover, the possibility to dispose of monodispersed probes that emit a fluorescence, as in the case of the silica cores, is of great value in the production of functionalized materials.

Bibliography

- [1] Shaw, D.J., *Introduction to Colloids and Surface Chemistry*, Fourth Edition, Butterworth-Heinemann, Oxford, 1992.
- [2] Hunter, R.J., *Foundations of Colloidal Science*, Second Edition, Oxford University Press, Oxford, 2009.
- [3] Dhont, J.K.G., *An Introduction to Dynamics of Colloids*, Elsevier, Amsterdam, 1996.
- [4] Terentjev, E.M and Weitz, D.A., *The Oxford Handbook of Soft Condensed Matter*, Oxford University Press, Oxford, 2015.
- [5] Liu, B. and Böker, A., Measuring rotational diffusion of colloidal spheres with confocal microscopy. *Soft Matter*, 2016, **12**(28): 6033-6037.
- [6] Stöber, W., Fink, A., Bohn, E., Controlled growth of monodisperse silica spheres in the micron size range, *Journal of Colloid and Interface Science*, 1968, **26**(1): 62-68.
- [7] Chen, S.L., Dong, P., Yang, G., Yang, J., Kinetics of formation of monodisperse colloidal silica particles through the hydrolysis and condensation of tetraethylorthosilicate, *Industrial and Engineering Chemical Research*, **48**(12): 4487-4493.
- [8] van Blaaderen, A., Vrij, A., Synthesis and characterisation of colloidal dispersions of fluorescent, monodisperse silica spheres, *Langmuir*, 1992, **8**(12): 2921-2931.
- [9] Verhaegh, N.A.M. and van Blaaderen, A., Dispersions of rhodamine-labeled silica spheres: synthesis, characterisazion, and fluorescence confocal scanning laser microscopy, *Langmuir*, 1994, **10**(5): 1427-1438.
- [10] Sheu, H.R., El-Aasser, M. S., Vanderhoff, J. W., Phase separation in polystyrene latex interpenetrating polymer networks, *Journal of Polymer Science: Part A: Polymer Chemistry*, 1990, **28**(3): 629-651.
- [11] Sheu, H.R., El-Aasser, M. S., Vanderhoff, J. W., Uniform nonspherical latex particles as model interpenetrating polymer networks, *Journal of Polymer Science: Part A: Polymer Chemistry*, 1990, **28**(3): 653-667.
- [12] Nagao, D., Hashimoto, M., Hayasaka, K., Konno, M., Synthesis of Anisotropic Polymer Particles with Soap-Free Emulsion Polymerisation in the Presence of a Reactive Silane Coupling Agent, *Macromolecular Rapid Communications*, 2008, **29**(17): 1484-1488.
- [13] Tamai, T., Watanabe, M., Maeda, H., Mizuno, K., Fluorescent Polymer Particles Incorporating Pyrene Derivatives, *Journal of Polymer Science: Part A: Polymer Chemistry*, 2008, **46**(4):1470-1475.
- [14] Kalyanasundaram, K. and Thomas, J. K., Environmental effects on vibronic band intensities in pyrene monomer fluorescence and their application in studies of micellar systems, *Journal of American Chemical Society*, 1977, **99**(7):2039-2044.